Universidade Federal de Minas Gerais

Instituto de Ciências Biológicas

Departamento de Morfologia

Programa de Pós-graduação em Biologia Celular

Matheus de Castro Fonseca

Efeito Dos Anestésicos Gerais Inalatórios Sevoflurano E Isoflurano Na Exocitose De Vesículas Sinápticas Em Junção Neuromuscular De Diafragma de Camundongo

Belo Horizonte

Maio de 2014

Matheus de Castro Fonseca

Efeito Dos Anestésicos Gerais Inalatórios Sevoflurano E Isoflurano Na Exocitose De Vesículas Sinápticas Em Junção Neuromuscular De Diafragma de Camundongo

Dissertação submetida ao Programa de Pós-graduação em Biologia Celular do Instituto de Ciências Biológicas da Universidade Federal de Minas Gerais, como requisito parcial para obtenção do grau de Mestre em Ciências Biológicas: Biologia Celular.

Área de concentração: Biologia Celular

Orientador: Profa.Cristina Guatimosim Fonseca
Co-Orientador: Prof. Renato Santiago Gomez

Belo Horizonte
Maio de 2014

APOIO INSTITUCIONAL

Este trabalho foi realizado no Laboratório de Biologia da Neurotransmissão do Departamento de Morfologia do Instituto de Ciências Biológicas da Universidade Federal de Minas Gerais, com colaboração da Dra. Vany Perpétua Ferraz do Laboratório de Química da Separação do Departamento de Química do Instituto de Ciências Exatas da UFMG e do Dr. Renato Santiago Gomez do Departamento de Cirurgia da Faculdade de Medicina da UFMG. Todo o estudo foi orientado pela Profa. Dra. Cristina Guatimosim Fonseca e com apoio financeiro das seguintes instituições:

- Fundação de Amparo à Pesquisa do Estado de Minas Gerais (FAPEMIG);
- Conselho Nacional de Desenvolvimento Científico e Tecnológico (CNPq);
- Coordenação de Aperfeiçoamento de Pessoal de Nível Superior (CAPES).

"Não há fatos eternos, como não há verdades absolutas".
Friedrich Nietzsche

AGRADECIMENTOS

Agradeço, primeiramente, a Deus pela força e refúgio concedido.

À minha mãe Jaqueline (*in memoriam*) por ser a razão pela qual dei continuidade aos meus estudos. Pela constante presença em minha memória, em meus passos e em minhas decisões. Obrigado por continuar sorrindo e por me dar forças, mãe.

Ao meu pai Sérgio por ser mais que um pai e por sempre me oferecer todo suporte para que eu pudesse chegar até aqui.

À minha irmã Thaís pela amizade e companheirismo.

Aos meus avós Zizinha e Fonseca por fazer da casa deles minha segunda casa. Obrigado por todo apoio e carinho sempre disponível.

À minha Tia Imaculada pelos conselhos, amizade, companheirismo e carinho, que mesmo a distância na maior parte das vezes, nunca me faltaram.

Às minhas primas Luísa e Débora por me fazerem rir quando nem sempre a vontade era essa.

Às minhas queridas "Tias" pelo carinho, orações, prosas de domingo, viagens pelo mundo e constante presença, sempre empolgadas em me ajudar para o alcance de novas conquistas. Agradeço em especial à Tia Helena e Tia Neném, por tudo, muito obrigado!!

Ao Rodrigo pela amizade, companheirismo, carinho e por me ajudar a finalizar e dividir comigo esta importante etapa da minha vida, me dando apoio e força para continuar.

À minha querida amiga/irmã de alma/colega de trabalho/anjo da guarda Priscila por toda amizade ao longo desses anos, amizade essa que se iniciou no ambiente de trabalho, mas que cruzou essa fronteira e com certeza se estenderá por toda vida. Muito obrigado por todo carinho, amor e apoio constante Priquitita. Com você ao meu lado foi mais fácil chegar aqui.

A todos os meus amigos pelos momentos de descontração oferecidos quando eu já estava prestes a surtar. Agradeço em especial ao Victor, Juci, Lino e Hiuri Metaxas por todo carinho e por me oferecerem o ombro sempre que eu precisei.

À Patrícia Campos-Christo por ser responsável por grande parte do que sou hoje. Por ser mais do que uma terapeuta e por ter me ajudado de uma forma imensurável ao longo de todos esses anos.

À Janice pela amizade, força, carinho e conselhos. Por dividir longas horas de conversa comigo, em especial nas escadarias do Depto de Química enquanto aguardávamos para o uso do cromatógrafo. Muito obrigado por tudo Janice, principalmente por ser um exemplo de profissional que pretendo ser.

À minha orientadora Cristina por ter aberto as portas do laboratório pra mim em 2008 e por ter me dado grandes oportunidades de construir minha carreira acadêmica até hoje.

Ao meu co-orientador Renato Santiago por me receber várias vezes na porta do bloco cirúrgico para solucionar dúvidas e por contribuir para o desenvolvimento desta dissertação.

À Vany Ferraz do Depto. de Química do ICEx pela grande contribuição para a realização dos experimentos de cromatografia e por sempre tão solícita.

A todos os amigos do LabNeuro (egressos e atuais) por fazerem os momentos de trabalho pesado mais divertidos: Hermann, Matheus, Priscila, Isadora, Fernanda, Debora, Luana, Luciana, Marina, agradeço demais a vocês.

Aos meus amigos da graduação em Ciências Biológicas pela parceria ao longo de todos esses anos, em especial à Mary, Arthur, Cristiano e ao Bruno Repolês.

A todos os amigos e professores do programa de Pós-Graduação em Biologia Celular em especial à professora Fernanda Almeida por todos os conselhos e por ter me dado grande exemplo de como ser um professor.

Ao Programa de Pós-Graduação em Biologia Celular, à Universidade Federal de Minas Gerais e às agências financiadoras que proporcionaram o desenvolvimento deste trabalho.

Enfim, a todos que tiveram algum tipo de participação em minha vida e que me auxiliaram de alguma forma, me dando força, suporte, apoio emocional ou profissional, fundamentais para o desenvolvimento desta dissertação, muito obrigado!

PARTE DOS RESULTADOS DESTA DISSERTAÇÃO FOI APRESENTADA NOS SEGUINTES EVENTOS:

- II Simpósio de Integração dos Programas de Pós-Graduação em Biologia Celular e VI Simpósio de Biologia Celular da Universidade Federal de Minas Gerais – Prof. Hugo Pereira Godinho. Belo Horizonte, Brasil, 2013.

- 10th International Congress on Cell Biology and 16th Meeting of the Brazilian Society for Cell Biology. Rio de Janeiro, Brasil, 2012.

- I Simpósio de Integração dos Programas de Pós-Graduação em Biologia Celular e V Simpósio de Biologia Celular da UFMG. Belo Horizonte, Brasil, 2012.

- IV Simpósio de Biologia Celular. Belo Horizonte, Brasil, 2011.

- XX Semana de Iniciação Científica da UFMG, Belo horizonte, Brasil, 2011.

PREMIAÇÕES OBTIDAS:

- Este trabalho recebeu menção honrosa, ao nível de mestrado, no II Simpósio de Integração dos Programas de Pós-Graduação em Biologia Celular e VI Simpósio de Biologia Celular da Universidade Federal de Minas Gerais – Prof. Hugo Pereira Godinho, 2013.

SUMÁRIO

LISTA DE ABREVIATURAS

µm	Micrômetro
µM	Micromolar
ACh	Acetilcolina
$CaCl_2$	Cloreto de cálcio
Ca^{2+}	Íons cálcio
CSSV	Canais para sódio sensíveis à voltagem
CCSV	Canais para cálcio sensíveis à voltagem
CO_2	Dióxido de carbono
FM1-43	N-(3-triethylammonium-propyl)-4-(4(dibutylamino) styryl)pyridinium dibromide
JNM	Junção Neuromuscular
KCl	Cloreto de potássio
K^+	Íons Potássio
$MgCl_2$	Cloreto de magnésio
mM	Milimolar
mm	Milimetro
Munc13	*Mammalian uncoordinated-13*
Munc18/nSec	*Mammalian uncoordinated-18*
nm	Nanometros
Na^+	Íons Sódio
NaCl	Cloreto de sódio
nAChR	Receptor nicotínico para acetilcolina
$NaHCO_3$	Bicarbonato de sódio
NaH_2PO_4	Fosfato de sódio monobásico
NSF	*N-ethylmaleimide sensitive fusion*
O_2	Oxigênio
Rab3	*Ras-related in brain - 3*
RIM	*Rab-interacting molecule*
SCSV	Canais para sódio sensíveis a voltagem
SNARE	Soluble NSF attachment protein receptor
SNAP-25	Proteína de 25 kDa associada ao sinaptosoma
t-SNARE	*Target SNARE*
TTX	Tetrodotoxina
VAChT	Transportador vesicular da acetilcolina
VAMP	Proteína de membrana associada à vesícula
v-SNARE	*Vesicular SNARE*

LISTA DE FIGURAS

RESUMO

Sevoflurano e isoflurano são anestésicos inalatórios utilizados tanto para a indução quanto para a manutenção da anestesia. Apesar de serem amplamente utilizados na prática clínica, seus mecanismos sinápticos de ação não são completamente elucidados. Além disso, esses fármacos também causam relaxamento muscular esquelético durante sua utilização em procedimentos cirúrgicos. Este efeito pode estar relacionado a um efeito inibitório destes agentes na liberação de acetilcolina na região da junção neuromuscular. Desta forma, o objetivo deste trabalho foi investigar e comparar os efeitos pré-sinápticos dos anestésicos sevoflurano e isoflurano na junção neuromuscular de camundongos, utilizando técnicas de microscopia óptica para visualizar a reciclagem de vesículas sinápticas. No presente trabalho, preparações neuromusculares de diafragma de camundongos foram isoladas e os aglomerados de vesículas sinápticas marcados com a sonda fluorescente FM1-43 com o objetivo de avaliar a interferência do sevoflurano e isoflurano no ciclo espontâneo ou evocado das mesmas. Sevoflurano e isoflurano (0,45, 0,6 e 0,9 mM) não alteraram a exocitose espontânea de vesículas sinápticas. Além disso, sevoflurano e isoflurano não apresentaram efeito inibitório sob o estímulo despolarizante gerado por solução concentrada de KCl, um estímulo Na^+-independente. Por outro lado, sevoflurano e isoflurano mostraram significativo efeito inibitório sob os estímulos despolarizantes Na^+-dependente evocados por 4AP (1mM) e veratridina (100 µM), sugerindo uma ação destes anestésicos em canais para Na^+. Além disso, o efeito inibitório de sevoflurano sob a desmarcação do FM1-43 induzida por 4AP foi maior do que o observado com isoflurano. A exocitose evocada por veratridina (100 µM) foi inibida por tetrodotoxina (1 µM TTX), porém nenhuma inibição adicional foi observada quando TTX foi usada conjuntamente com os anestésicos testados. Contudo, TTX 0,5 µM concentração esta que reduz em 50% a exocitose induzida pela veratridina, com 0,45 mM de sevoflurano ou de isoflurano inibiu o estímulo despolarizante da veratridina de forma similar a inibição causada por 1µM TTX, indicando que estes anestésicos podem ter como alvo canais para Na^+ voltagem-dependente. Nossos resultados mostram que os anestésicos voláteis sevoflurano e isoflurano inibem a exocitose evocada por estímulos dependentes de Na^+ provavelmente por atuarem em canais para Na^+ sensíveis a TTX. Estes achados podem contribuir para um melhor entendimento dos efeitos neuromusculares observados durante a administração destes fármacos na anestesia geral.

Palavras-chave: sevoflurano; isoflurano; exocitose; junção neuromuscular; FM1-43.

ABSTRACT

Sevoflurane and isoflurane are halogenated anesthetics used for induction and maintenance of anesthesia. Despite being routinely used in clinical practice, their synaptic mechanisms of action are not clearly understood. In addition, these drugs also cause skeletal muscle relaxation during their administration in clinical procedures. This effect might be correlated with an inhibitory effect on the release of acetylcholine at the neuromuscular junction. Thereby, the aim of this work was to investigate and compare the presynaptic effects of sevoflurane and isoflurane at the mouse neuromuscular junction using optical techniques to visualize the recycling of synaptic vesicles. In the present study, diaphragm nerve-muscles preparations of mice were isolated and clusters of synaptic vesicles were labeled using the fluorescent vital dye FM1-43 to examine whether these volatiles anesthetics might interfere with the spontaneous and/or evoked exocytosis. Our data showed that both sevoflurane and isoflurane (0.45, 0.6 and 0.9 mM) did not evoke spontaneous exocytosis of synaptic vesicles. In addition, sevoflurane and isoflurane had no effect in inhibiting depolarization evoked by KCl (60 mM), a Na+-independent stimulus. However, sevoflurane and isoflurane significantly inhibited the depolarization evoked by 4AP (1mM) and veratridine (100 µM), suggesting a putative action on sodium channels. Furthermore, the inhibition of FM1-43 destaining evoked by 4AP was greater under sevoflurane treatment compared to isoflurane. Exocytosis evoked by veratridine was inhibited by tetrodotoxin (1 µM TTX) but no further inhibition was observed when TTX (1 µM) was associated with either anesthetic. Nevertheless, a reduced TTX concentration (0.5 µM) used together with 0.45 mM sevoflurane or isoflurane showed an inhibition similar to TTX (1 µM) alone, indicating that both agents may target in voltage gated sodium channels. Thus, our data suggest that the volatile anesthetics sevoflurane and isoflurane inhibit exocytosis evoked by sodium dependent depolarization and it might act on sodium channels that are sensitive to TTX. These findings contribute to a better understanding of some clinical muscular aspects observed during administration of these halogenated volatile agents.

Key words: sevoflurane; isoflurane; exocytosis; neuromuscular junction; FM1-43.

1. INTRODUÇÂO

1.1 A Junção Neuromuscular

Sinapses são regiões especializadas que permitem a comunicação entre uma célula pré-sináptica com uma célula alvo pós-sináptica. Até o presente momento, dois tipos de sinapses foram descritos: a sinapse elétrica e a sinapse química (ZHAI & BELLEN, 2004). A sinapse elétrica é um mecanismo de comunicação e transmissão de impulsos através da condução de íons por proteínas de membrana de uma célula para outra, em regiões especializadas (*gap junctions*) (revisado por HORMUZDI et. al., 2004). Já nas sinapses químicas, mais lentas do que a sinapse elétrica, um sinal elétrico resultante da propagação de correntes iônicas é convertido em um sinal químico, representado pela liberação de neurotransmissores que irão atuar sobre a célula alvo (KATZ, 1966; revisado por ZHAI & BELLEN, 2004).

A junção neuromuscular (JNM) da classe dos mamíferos (FIGURA 1) é um dos modelos atuais de sinapses mais utilizados para estudos neuroquímicos e neurofisiológicos e de melhor compreendimento, dada sua simplicidade estrutural, tamanho e acessibilidade (KUMMER *et.al.*, 2006). Esta estrutura consiste em uma sinapse química composta por uma célula pré-sináptica (terminal axonal de um neurônio motor) contendo abundantes vesículas sinápticas preenchidas com o neurotransmissor acetilcolina (ACh), uma fenda sináptica e um aparato de recepção na membrana da célula pós-sináptica (célula muscular). Em determinadas regiões da terminação, é possível observar, no plano ultraestrutural, regiões eletrondensas denominadas zonas ativas que marcam os sítios subcelulares da transmissão sináptica. Cada zona ativa pode ser identificada pela sua associação com aglomerados de vesículas sinápticas pequenas, de aproximadamente 50nm de diâmetro, preenchidas com ACh em. Nestas regiões, vesículas sinápticas se ancoram, fusionam-se com a membrana e liberam neurotransmissores na fenda sináptica. O aparato de recepção pós-sináptico, justaposto a zonas ativas, contém aglomerados de receptores de neurotransmissores e canais iônicos e é referido como densidade pós-sináptica, dada sua aparência quando observado sob microscópio eletrônico de transmissão (GARNER *et.al.*, 2000). Na JNM de camundongos este aparato é formado por receptores nicotínicos para a ACh. Esses receptores não estão uniformemente distribuídos pelo aparato pós-sináptico, mas sim formando agrupamentos nas dobras da membrana pós-sinaptica, atingindo nesses locais

densidades que podem chegar a mais de 10000 por mm^2. Esse arranjo permite aos receptores detectar de forma rápida e eficiente a ACh liberada durante a exocitose (revisado por HALL, 1992 E HALL & SANES, 1993).

A exocitose de vesículas ocorre na zona ativa e a subseqüente recuperação endocítica dos componentes vesiculares pode ocorrer tanto na zona ativa quanto na área da zona peri-ativa (ROOS & KELLY, 1999).

Todo este arranjo demonstrado anteriormente garante a integração entre células nervosas e as células musculares e constitui um modelo para o estudo do ciclo de vesículas sinápticas e possíveis interferências farmacológicas neste processo.

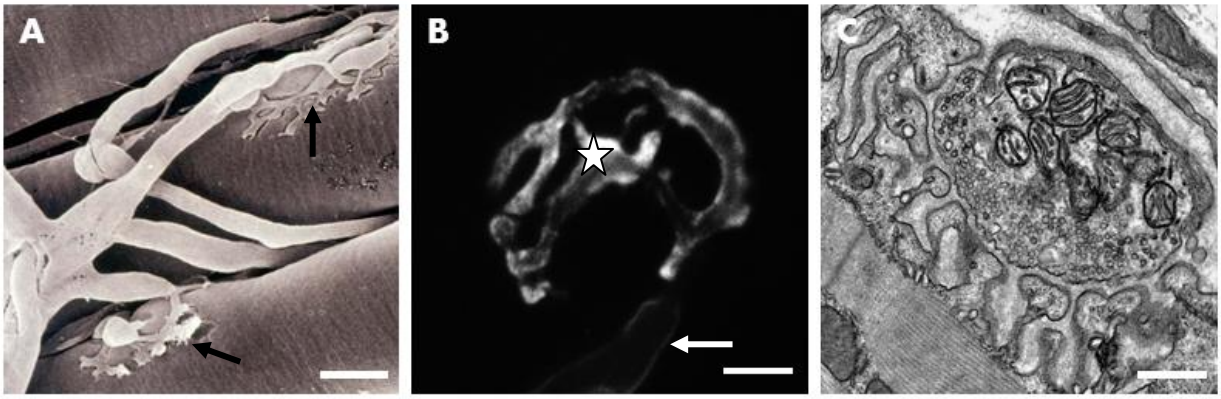

Figura 1: Junção Neuromuscular de camundongo. (A) Micrografia eletrônica de varredura de JNM de camundongo. Nota-se a presença de terminais axonais (setas) disposto de forma circular sobre uma célula muscular estriada esquelética, que apresenta na membrana pós-sináptica diversas dobras juncionais, nas cristas das quais se concentram aglomerados de receptores para ACh (TORREJAIS *et al*, 2002) (Barra de escala: 10 µm). (B) Imagem de microscopia de fluorescência de JNM de camundongo (Matheus de C. Fonseca). Observa-se o axônio mielinizado (seta) e o terminal pré-sináptico de aspecto circunscrito (estrela) (Barra de escala: 10 µm). (C) Micrografia eletrônica de transmissão de uma JNM de camundongo (Hermann A. Rodrigues). O componente pré-sináptico apresenta diversas vesículas sinápticas e algumas mitocôndrias. A célula muscular, pós-sináptica, apresenta em sua membrana dobras juncionais. Os elementos pré e pós-sinápticos são separados por uma estreita fenda sináptica (Barra de escala: 1 µm).

1.2 A comunicação neuronal e o ciclo de vesículas sinápticas

A comunicação neuronal química é um fenômeno regulado e de grande importância para a realização das atividades vitais do organismo. Para que esta comunicação ocorra de forma adequada e precisa, uma série de eventos precisa ocorrer: a despolarização de uma célula pré-sináptica devido à dinâmica dos canais iônicos; a exocitose de vesículas sinápticas mediada por proteínas específicas; e a liberação de neurotransmissores que se ligarão a seus receptores específicos e desencadearão resposta típica. As regiões especializadas de comunicação entre o terminal axonal de um neurônio e uma célula pós-sináptica onde os neurotransmissores são liberados da célula pré-sináptica e ativam seus receptores pós-sinápticos são denominadas sinapses (SHERINGTON, 1906, WU *et.al*., 2010).

O ciclo de vesículas sinápticas envolve um tráfego cíclico destas organelas, o qual pode ser descrito em dois grandes eventos gerais: (1) Exocitose: (a) os neurotransmissores são sintetizados e ativamente transportados para dentro das vesículas sinápticas; (b) as vesículas agrupam-se em na região da zona ativa; (c) ancoram-se nela; (d) amadurecem e então; (e) tornam-se aptas para a fusão e consequente exocitose disparada pelo influxo de Ca^{2+} para o interior do terminal (SÜDHOF, 2004) (FIGURA 2). (2) Endocitose: após a exocitose, as vesículas sinápticas são endocitadas e recicladas por uma de três vias alternativas: (a) endocitose chamada "*Kiss and Run*" - neste modelo, após as vesículas liberarem os neurotransmissores via um poro de fusão transiente, elas são recapturadas, podendo permanecer no local, ser novamente preenchidas com neurotransmissor e submeter-se a um novo ciclo de exocitose ou, alternativamente, podendo não ancorar e permitir que outras vesículas ocupem seu lugar (CECCARELLI *et al.*, 1973; SÜDHOF, 2004); (b) endocitose mediada pela formação da cobertura de clatrina (FIGURA 3) - após a completa fusão da membrana da vesícula com a membrana plasmática do terminal, forma-se uma cobertura de clatrina, que ailiada por proteínas acessórias, fornece a força necessária para a invaginação da membrana. Em seguida, a vesícula é reacidificada e repreenchida diretamente ou após passar por um endossoma intermediário (HEUSER & REESE, 1973; MURTHY & DE CAMILLI, 2003); (c) endocitose via grandes invaginação de membrana e formação de cisternas, das quais brotam novas vesículas cobertas por clatrina (TAKEI et al., 1995; RICHARDS *et al*., 2000) (FIGURA 3).

Os eventos que culminam com a exocitose de vesículas sinápticas se iniciam com a chegada de um potencial de ação no terminal pré-sináptico, que levará à modificação estrutural em proteínas especializadas de membranas, responsáveis pelo influxo/efluxo de íons, denominadas canais iônicos (SÜDHOF, 2004). A abertura de canais para Na^+ (íons sódio) sensíveis à voltagem (CSSV) leva ao influxo deste íon no terminal axonal aumentando o potencial de membrana desta região (SÜDHOF, 2004). Consequentemente, ocorre a abertura de canais para Ca^{2+} (íons cálcio) sensíveis à voltagem (CCSV) que permitem o influxo de Ca^{2+} para o interior do terminal, desencadeando assim a exocitose de vesículas sinápticas e subsequente liberação do neurotransmissor na fenda sináptica. (FIGURA 2). Para que a membrana retorne a seu potencial de repouso, existe a participação dos canais vazantes para K^+ (íons potássio) e ativo trabalho da bomba ATPásica de Na^+ e K^+.

A exocitose de vesículas sinápticas compartilha muitos princípios básicos e proteínas homólogas com outros eventos de fusão de membrana (LI & CHIN, 2003). Os componentes conservados da maquinaria geral de fusão vesicular incluem as chamadas proteínas SNARE [soluble NSF attachment receptor – vesiculares (v-SNARE) e membranares (t-SNARE)], ATPase NSF, Munc18/nSec 1,GTPase Rab3 e proteínas exocíticas (LI & CHIN, 2003; SUDHOF, 2013) Além destes elementos conservados, a exocitose de vesículas sinápticas usa um conjunto de proteínas únicas como a sinaptotagmina, complexina, Munc 13 e RIM, responsáveis pela rápida resposta a alterações no transiente de Ca^{2+} intracelular (LI & CHIN, 2003). A maquinaria mínima essencial para a fusão de vesículas sinápticas é composta pelas proteínas do complexo SNARE: 1) a sinaptobrevina/VAMP, localizada na membrana da vesícula e também chamada de v-SNARE (*vesicular SNARE*); 2) sintaxina e SNAP-25, situadas na membrana plasmática do terminal pré-sináptico e por esta razão chamadas de t-SNARE (*target SNARE*) (SÖLLNER *et al.*, 1993). A fusão de membranas que possibilita a liberação dos neurotransmissores é regida pela progressiva interação entre SNAREs de vesícula sináptica com as da membrana do terminal. A sinaptotagmina I é uma proteína integral presente na membrana da vesícula sináptica que funciona como um sensor para Ca^{2+}, ligando-se a este íon, o que permitirá a interação das v-SNAREs com as proteínas t- SNAREs e desencadeará a exocitose da vesícula (MURTHY & DE CAMILLI, 2003; CHAPMAN, 2006).

Como mencionado, a transferência de impulsos nervosos para a célula-alvo pós-sináptica ocorre através da liberação de neurotransmissores a partir de vesículas

sinápticas previamente maturadas. A maturação das vesículas compreende a acidificação do lúmem da organela, preenchimento com neurotransmissores, associação com proteínas de membrana e agrupamento em um dos três possíveis *pools* ou aglomerados de vesículas conhecidos: o aglomerado prontamente liberável, o aglomerado de reciclagem ou o aglomerado de reserva (RIZZOLI & BETZ, 2005; ALABI & TSIEN, 2012). Com isso, pode-se dizer que a manutenção da transmissão sináptica relaciona-se diretamente com a disponibilidade de vesículas sinápticas preenchidas com uma alta concentração de neurotransmissores e passíveis de serem exocitadas. (SCHWEIZER & RYAN, 2006).

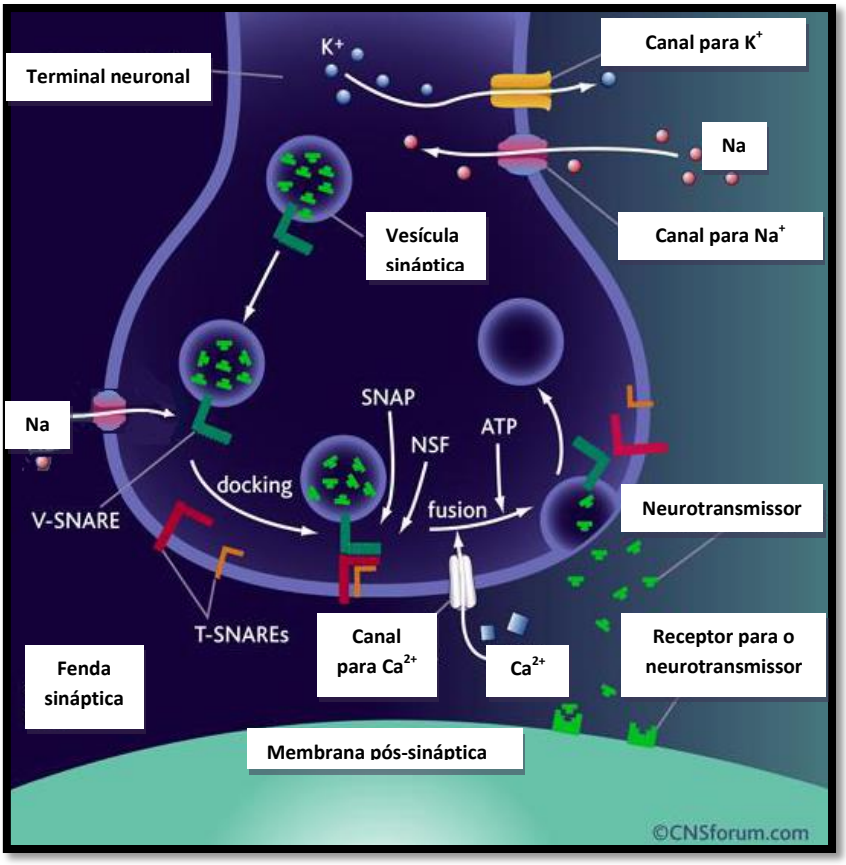

Figura 2: A exocitose de vesículas sinápticas. O influxo de Na^+ no terminal gera uma mudança no potencial de membrana da célula, fazendo com que o interior do terminal fique carregado positivamente. Esta mudança de potencial leva a abertura de canais para K^+ e Ca^{2+} sensíveis a voltagem. O influxo de K^+ leva ao restabelecimento do potencial de membrana, enquanto que o influxo de Ca^{2+}é responsável por desencadear o evento de exocitose vesicular. A exocitose de vesículas ocorre graças a um conjunto de proteínas, dentre elas, proteínas SNARE. Após a exocitose, porções de membrana são endocitados para o interior do terminal pré-sináptico para a formação de novas vesículas passíveis de serem novamente preenchidas com neurotransmissores e, assim, iniciar um novo ciclo.
FONTE: www.cnsforum.com/content/pictures/imagebank/hirespng/vesicle_fusion.png

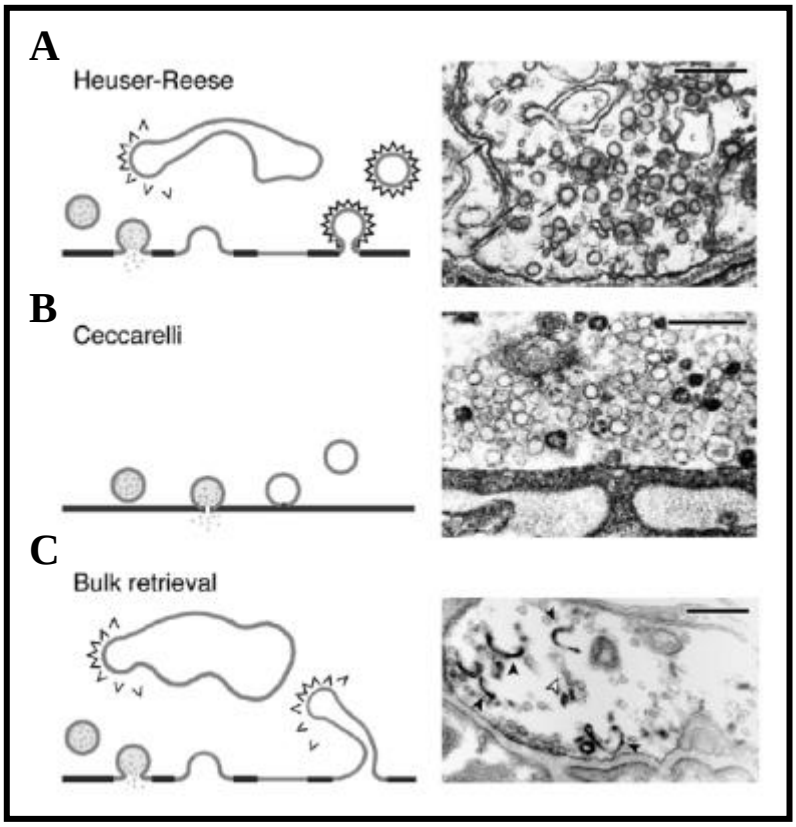

Figura 3: Modelos propostos de endocitose de vesículas sinápticas. (A) Endocitose mediada por capa de clatrina. Modelo proposto por Heuser & Reese no qual as vesículas sinápticas são completamente integradas à membrana da zona ativa durante a exocitose e são recicladas por meio de endocitose mediada por capa de clatrina. Micrografia eletrônica (à direita) demonstrando a presença de depressões de membrana e vesículas cobertas por capa de clatrina (setas) em terminação motora submetida a estímulo elétrico. É possível observar também a presença de cisternas "c". (B) Modelo de *kiss and run* (à esquerda) proposto por Ceccarelli no qual, durante a liberação de neurotransmissores, as vesículas abrem um poro de fusão transitório, mas não se fundem completamente a membrana pré-sináptica, sendo recicladas localmente. Micrografia eletrônica (à direita) de terminação motora submetida a estímulo elétrico de baixa frequência por duas horas. Destaca-se a ausência de vesículas cobertas por capa de clatrina e de cisternas. (C) Diagrama representando endocitose via grandes invaginações de membrana (à esquerda) após liberação vesicular. Micrografia eletrônica (à direita) indicando invaginações de membrana contendo FM1-43 fotoconvertido (setas negras) ou desprovidas do marcador (seta clara) (TAKEI *et al.*, 1996, RICHARDS *et al*., 2001) (*revisado por ROYLE & LAGNADO, 2003).*

1.3 Os anestésicos inalatórios

De todos os marcos e conquistas na história da medicina, o controle da dor aguda durante procedimentos cirúrgicos pode ser considerado como um dos poucos que potencialmente afetou a todos os seres humanos. A demonstração das propriedades anestésicas do volátil éter por Willian Morton em 1846 foi uma das descobertas mais significantes na ciência médica e desde então diversos outros compostos têm sido desenvolvidos, sempre buscando alternativas mais efetivas e com menores efeitos colaterais para produção da anestesia (VANDAM, 1994).

Os anestésicos inalatórios são substâncias de grande importância e utilização na medicina moderna (HEMMINGS *et.al*., 2005), com o intuito de promover os seguintes principais efeitos: imobilidade, inconsciência, analgesia e supressão de reflexos do sistema nervoso autônomo. Apesar de existirem relatos de uso destas substâncias por mais de 150 anos e serem amplamente utilizadas na prática clínica, os mecanismos moleculares e celulares de ação destas drogas ainda não estão completamente elucidados. Logo, um grande esforço tem sido feito para elucidar seus alvos moleculares e consequentemente seus efeitos nas terminações nervosas.

Os anestésicos já foram considerados como drogas sem receptores, produtoras de um mesmo efeito neurobiológico, agindo, portanto nos mesmos alvos. Porém, atualmente, esta hipótese tem sido contestada (SOLT & FORMAN, 2007) já que estudos recentes demonstraram que diferentes classes de anestésicos gerais atuam por vias diferentes em distintos alvos, enfatizando assim a existência de múltiplos sítios e mecanismos de ação. Além disso, estudos têm demonstrado que os anestésicos atuam tanto em alvos pré-sinápticos, quanto em alvos pós-sinápticos (FRANKS, 2006).

A depressão da neurotransmissão excitatória e/ou facilitação da neurotransmissão inibitória são os principais efeitos neurobiológicos dos anestésicos gerais na neurotransmissão sináptica central e também, salvo algumas exceções, na periférica (OUYANG *et.al*., 2003; PEROUANSKY, 2008).

Didaticamente, os anestésicos gerais podem ser divididos em duas classes, conforme sua via de administração: anestésicos inalatórios e anestésicos intravenosos. Os anestésicos inalatórios geralmente são utilizados para a manutenção da anestesia. Os anestésicos intravenosos são empregados para induzir a anestesia, fornecer anestesia complementar ou permitir anestesia nos procedimentos operatórios curtos. Dentre os anestésicos inalatórios mais utilizados atualmente, podemos destacar: halogenados em

geral (halotano, enflurano, isoflurano, sevoflurano e desflurano) e óxido nítroso. Já entre os anestésicos gerais intravenosos destaca-se o etomidato, alguns barbitúricos e o propofol (HEMMINGS, 2005).

Apesar do grande interesse em se descobrir os exatos mecanismos de ação destas drogas, é desejável que um anestésico ideal, não importando qual seja seu mecanismo de ação, apresente um efeito indutor rápido (mas também suave), ofereça ótimas condições para a realização de uma cirurgia e permita rápida recuperação do paciente quando a administração da droga for cessada. Até o presente momento, quase todos os anestésicos gerais utilizados apresentam vantagens e desvantagens terapêuticas (FIGURA 4) e nenhum é capaz de realizar todos os efeitos mencionados por si mesmo (HEMMINGS *et.al*., 2005), porém alguns, como os inalatórios sevoflurano e isoflurano, estão mais próximo em atender os requisitos mencionados anteriormente.

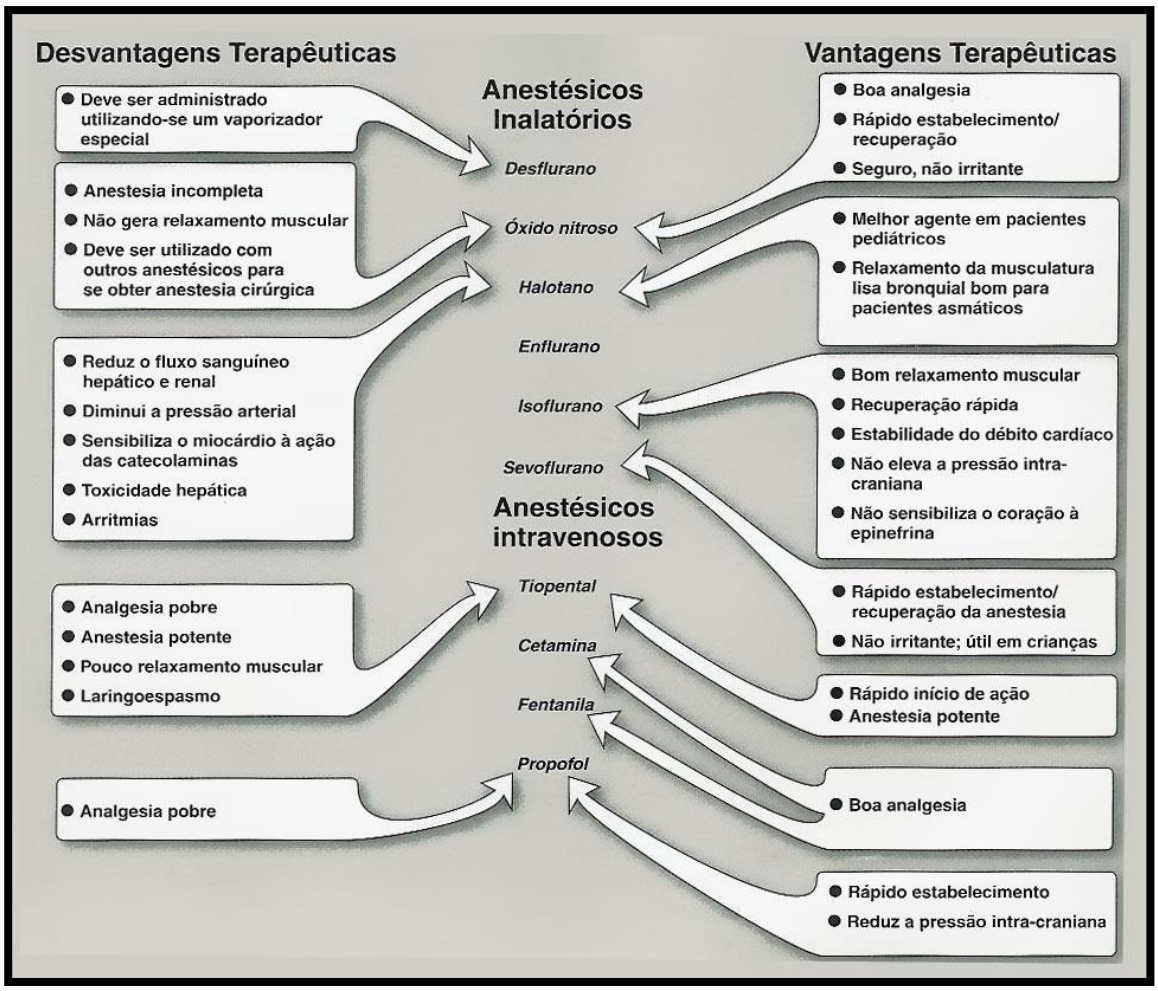

Figura 4: Vantagens e desvantagens terapêuticas dos anestésicos gerais intravenenosos e inalatórios. Dentre os anestésicos inalatórios, os halogenados sevoflurano e isoflurano se destacam por apresentarem poucos efeitos adversos conhecidos.

Fonte: Howland, D., , Mycek, M. J. Farmacologia Ilustrada. Tradução da 3ª edição. Porto Alegre: Artmed Editora S.A.; 2007. p. 125-138.

1.4 Sevoflurano, Isoflurano e os anestésicos inalatórios.

Os anestésicos inalatórios são substâncias voláteis utilizadas para indução e/ou manutenção da anestesia, que apresentam vantagens farmacocinéticas expressivas sobre os anestésicos intravenosos. Aumentando ou diminuindo a concentração da substância que é inspirada pelo paciente, é possível aumentar ou diminuir a concentração deste agente no sangue e nos tecidos corporais, o que permite mudanças rápidas na profundidade da anestesia e oferece um método simples para induzir, manter ou cessar a anestesia geral. (TORRI, 2010).

Desde a década de trinta, novos anestésicos inalatórios vêm sendo produzidos. Os primeiros eram inflamáveis, porém este problema veio a ser resolvido com a introdução de um átomo de flúor na estrutura da molécula. Além disso, esta alteração trouxe benefícios como aumento da estabilidade e menor efeito na camada de ozônio (JONES, 1990; MERRET & JONES, 1994)

Em 1972, o sevoflurano foi descrito pela primeira vez (WALLIN *et.al.*, 1975), porém com uso aprovado apenas em 1990 no Japão. Dentre as propriedades deste fármaco, incluem-se os pequenos efeitos sobre o sistema cardiorrespiratório, efeitos reversíveis no sistema nervoso central, ausência de efeito tóxico cumulativo com as exposições repetidas, dentre outras. Como apresenta um baixo coeficiente de partição sangue:gás, a indução e a recuperação anestésicas são mais rápidas e previsíveis. Apresenta ainda odor adocicado, sem provocar irritação do trato respiratório e um potente efeito broncodilatador, tornando-o um excelente candidato para indução de anestesia sob máscara tanto em adultos quanto em crianças (JACOB *et.al.*, 2009). Atualmente é o anestésico inalatório mais usado em humanos no mundo (CESAROVIC *et.al.*, 2010), porém, seus mecanismos de ação ainda não foram completamente esclarecidos.

O anestésico isoflurano, também uma substância volátil do grupo dos halogenados, é o anestésico inalatório mais utilizado na clínica veterinária desde 1988. Por possuir um coeficiente de partição sangue:gás maior do que sevoflurano, a recuperação dos pacientes após o procedimento anestésico é um pouco mais lenta, quando comparado com pacientes submetidos à anestesia com sevoflurano (MATTHEWS, 2003). Em cães adultos, a indução com máscara anestésica e a recuperação é mais rápida, e de melhor qualidade com o sevoflurano, comparativamente com o isoflurano (HOFMEISTER, *et.al.*, 2008).

Diferentes alvos moleculares em várias regiões do sistema nervoso estão envolvidos nos vários componentes da anestesia geral mediada por anestésicos inalatórios ou venosos e estes alvos podem variar entre os anestésicos. Além disso, os anestésicos necessários durante muitos procedimentos cirúrgicos afetam tanto a transmissão sináptica excitatória e inibitória no sistema nervoso central (RICHARDS *et.al.,* 2002). Experimentações eletrofisiológicas mostram que as ações sinápticas dos anestésicos gerais inalatórios envolvem alvos tanto pré e / ou pós-sinápticos (HEMMINGS, 2009).

DINIZ e colaboradores (2013) mostraram que os anestésicos voláteis, como halotano e sevoflurano induzem a liberação de [^{3}H] GABA, em fatias de córtex cerebral de rato por induzir o transporte reverso deste neurotransmissor. Outros estudos realizados pelo nosso grupo também mostraram que o anestésico inalatório sevoflurano induz a liberação de serotonina e dopamina em fatias de cérebro de rato, agindo pré-sinapticamente (DINIZ, 2007; SILVA, 2008). Além disso, VALADÃO e colaboradores (2013) mostraram que o anestésico intravenoso etomidato, estimula a exocitose de vesículas sinápticas e também pode interferir com os receptores nicotínicos para acetilcolina (nAChRs) pós-sinápticos, indicando que esta droga pode exercer um efeito pré e pós-sináptico. Sevoflurano, interagindo diretamente com nAChR , também potencializa o efeito de drogas não despolarizantes geradoras de bloqueio neuromuscular e leva a respostas mais intensas do que outros anestésicos voláteis, como halotano e isoflurano (PAUL, 2002; NITAHARA, 2010) .

Portanto, estes fármacos alteram a liberação de neurotransmissores e/ou modulam as respostas pós-sinápticas (PASHKOV & HEMMINGS, 2002). No entanto, as contribuições de cada um desses alvos não foram ainda claramente definidas.

Desde os anos 1980, os canais iônicos têm sido considerados como o alvo molecular mais promissor para os anestésicos gerais (HEMMINGS, 2005), mas uma investigação mais profunda ainda é necessária. Grandes esforços têm sido feitos a fim de obter uma melhor compreensão de como os anestésicos voláteis interferem com a transmissão neuromuscular. Por exemplo, KENNEDY & GALINDO (1975) mostraram que o enflurano é capaz de provocar um relaxamento muscular atuando diretamente sobre a placa motora. HEDENSTIERNA & EDMARK (2005) também mostraram os efeitos da anestesia geral com anestésicos inalatórios e paralisia muscular gerada por eles sobre o sistema respiratório. Outros trabalhos anteriores mostraram os efeitos pós-sinápticos de anestésicos inalatórios sobre a liberação de neurotransmissores no plano

da JNM. VIOLET (1997), por exemplo, mostrou que nAChRs neuronais e musculares são sensíveis aos anestésicos gerais, incluindo o sevoflurano , com graus diferentes de sensibilidade. TASSONYI (2002) e colaboradores mostraram que os anestésicos voláteis e cetamina são os inibidores mais potentes do subtipo neuronal dos receptores nACh e também produzem excelente efeito inibidor sobre o subtipo muscular.

No entanto, os mecanismos pré-sinápticos, mais especificamente, os passos básicos para a liberação de neurotransmissores envolvidos nos efeitos causados pelo sevoflurano nas junções neuromusculares, permanecem obscuros.

2. OBJETIVOS

2.1 Objetivo Geral

- Investigar o provável efeito dos anestésicos inalatórios sevoflurano e isoflurano na exocitose espontânea e evocada de vesículas sinápticas na JNM de diafragma de camundongo.

2.2 Objetivos Específicos

- Realizar curva dose-resposta dos anestésicos sevoflurano e isoflurano na exocitose espontânea de vesículas sinápticas em JNMs de diafragma;

- Investigar se sevoflurano e isoflurano são capazes de bloquear a exocitose de vesículas sinápticas evocada por estímulo independente de íons Na^+ nas JNMs de diafragma de camundongos;

- Investigar se sevoflurano e isoflurano são capazes de bloquear a exocitose de vesículas sinápticas evocada por estímulos dependentes do influxo de íons Na^+ nas JNMs de diafragma de camundongos.

- Comparar o efeito bloqueador dos anestésicos sevoflurano e isoflurano na exocitose com o efeito de um bloqueador de ação conhecida em JNMs de diafragma de camundongos.

3. MATERIAL E MÉTODOS

3.1 Animais utilizados

Neste estudo, utilizamos camundongos fêmeas da linhagem *Swiss* com idade média de 7-8 semanas. Todos os animais foram fornecidos pelo Centro de Bioterismo (CEBio) da Universidade Federal de Minas Gerais. Todos os procedimentos foram aprovados pelo Comitê de Ética em Experimentação Animal (CETEA) e Comissão de Ética no Uso de Animais (CEUA) com o protocolo CETEA-UFMG 82/2008.

3.2 Soluções

-Solução Ringer

- NaCl 135 mM, KCl 5 mM, $CaCl_2$ 2 mM, $MgCl_2$ 1 mM, $NaHCO_3$ 12 mM, NaH_2PO_4 1 mM, D-glicose 11 mM, pH ajustado para 7.4.

- Solução Ringer Alto Potássio (60 mM):

- NaCl 80 mM, KCl 60 mM, $MgCl_2$ 2 mM, $NaHCO_3$ 12 mM, NaH_2PO_4 1 mM, D-glicose 11 mM, pH ajustado para 7.4.

- Solução aquosa de sevoflurano e isoflurano

Os anestésicos foram gentilmente doados pelo Prof. Renato Santiago Gomez do Departamento de Cirurgia da Faculdade de Medicina da UFMG e armazenado em temperatura ambiente (25 °C).

Dada à sua baixa solubilidade, para cada experimento foi preparada uma solução estoque concentrada do anestésico sevoflurano (15 – 16mM) ou isoflurano (11 – 13 mM) e deixada em agitação em um rotador vertical por no mínimo 6 horas. Isto foi feito com o objetivo de se produzir uma solução homogênea do anestésico em questão.

Em parceria com o Departamento de Química do Instituto de Ciências Exatas da UFMG (ICEX-UFMG), após a produção da solução homogênea dos anestésicos, estas foram avaliadas através da extração com heptano (MILLER & GANDOLFI, 1979) em um aparelho de cromatografia gasosa Hewlett Packard Series II-5890. Esse aparelho era equipado com uma coluna capilar (DB-WAX, 30 metros de comprimento; diâmetro interno 25 mm; espessura de filme de 0,33 μm; temperatura máxima: 325ºC), onde dois microlitros da solução estoque eram introduzidos diretamente através de um septo

(elastômero). As condições de separação incluíam uma análise cromatográfica à temperatura constante da coluna (80ºC) e uma mistura de hidrogênio (fluxo: 35, 350 e 30 ml /min, respectivamente) como gás carreador. A leitura da solução injetada era feita através de um detector FID (100ºC) e as curvas eram plotadas em um computador equipado com o programa Varian Star 5.5. Este procedimento foi realizado com o objetivo de avaliar a homogeneidade da solução produzida. Posteriormente, utilizando a mesma técnica, avaliamos a porcentagem de perdas do anestésico no decorrer do experimento, dado a volatilidade do fármaco. Desta maneira, a concentração exata testada em cada experimento foi conhecida e as correções de concentração necessárias para a produção das soluções anestésicas foram feitas. Posteriormente, em nosso protocolo experimental, uma amostra da solução estoque produzida era retirada com o auxílio de uma seringa e diluída em mouse Ringer presente em um frasco vedado, com o objetivo de se obter a concentração desejada a ser testada nos experimentos subsequentes de microscopia de fluorescência.

3.3 Reagentes e toxinas

- Toxina d-tubocurarina (Sigma-Aldrich, St. Louis, MO, EUA);
- FM1-43 (Molecular Probes Inc., Eugene, OR, EUA);
- 4-aminopiridina (4AP) (Sigma-Aldrich St. Louis, MO, EUA);
- Veratridina (VER) (Sigma-Aldrich, St. Louis, MO, EUA)
- Tetrodotoxina (TTX) (Sigma-Aldrich, St. Louis, MO, EUA);
- ω -Conotoxina GIIIB (Sigma-Aldrich, St. Louis, MO, EUA);
- Sevoflurano 1 ml/1ml (Instituto BioChimico, RJ, Brasil)
- Isoflurano 1 ml/ml (Instituto BioChimico, RJ, Brasil)

3.4 Marcação dos aglomerados vesiculares e monitoramento do ciclo de vesículas sinápticas com o marcador fluorescente FM1-43

O ciclo das vesículas sinápticas pode ser monitorado utilizando sondas fluorescentes captadas durante a endocitose e liberadas durante a exocitose (LICHTMAN *et al*., 1985; BETZ, MAO, BEWICK, 1992; RIBCHESTER, MAO,

BETZ, 1994). Desta maneira podemos visualizar a reciclagem de vesículas em um terminal neuronal.

O desenvolvimento de tais ferramentas para estes estudos foi um passo fundamental para a melhor compreensão dos processos que envolvem a reciclagem das vesículas sinápticas e, com isso, a comunicação neuronal (COUSIN e ROBINSON, 1999).

Para a realização de nossos estudos de monitoramento do ciclo de vesículas sinápticas, músculos diafragma de camundongos foram dissecados, montados em câmara própria forrada com Sylgard®, fixados com alfinetes entomológicos e banhados por solução Ringer aerada por uma mistura de 5%CO^2/ 95%O^2.

Os aglomerados de vesículas sinápticas foram marcados utilizando a sonda fluorescente FM1-43 (4 μM) (BETZ & BEWICK, 1993). Esta molécula anfipática apresenta em uma extremidade duas caudas lipofílicas compostas por quatro grupos metilenos e um grupo metil terminal, o que facilita sua ligação reversível com membranas celulares (BETZ & BEWICK, 1993). Na outra extremidade, uma porção carregada positivamente previne a completa inserção do marcador nas membranas biológicas (BETZ e BEWICK, 1993; WU *et al.,* 2009). Entre estas duas porções da molécula encontra-se o fluoróforo, formado por dois anéis aromáticos conectados entre si por uma ligação dupla (FIGURA 5A). Tal fluoróforo é responsável pela emissão do espectro luminoso quando há excitação da sonda. Em nosso estudo, o marcador FM1-43 era adicionado a câmara contendo a preparação neuromuscular, permitindo a ligação deste na membrana da terminação nervosa. Seguido a isto, adicionávamos uma solução despolarizante de KCl 60 mM (solução Ringer Alto K^+), durante 10 minutos, com o objetivo de evocar a exocitose das vesículas sinápticas. Esta solução era acrescida da toxina d-tubocurarina (16 μM) - potente bloqueador de nAChR – para impedir as contrações do músculo durante a estimulação. Após corrido o tempo, a solução despolarizante era substituída por Ringer normal, contendo FM1-43 e d-tubocurarina e o músculo era incubado durante 15 minutos para garantir a captação da sonda durante o processo de endocitose compensatória. Este processo possibilita a internalização do marcador (BETZ *et.al*., 1992) fazendo com que as vesículas sinápticas endocitadas apresentem o marcador aprisionado em seu interior e aderido a sua membrana. (FIGURA 5B). Isto possibilitará a visualização de aglomerados vesiculares marcados com a sonda, em um microscópio de fluorescência, sob a forma de pontos fluorescente. Como o FM1-43 não é específico para membranas de terminais nervosos, mas sim para

todas e qualquer tipo de membrana lipídica, se fez necessário um período de lavagem da preparação por cerca de 20 minutos para que o excesso do marcador fosse removido e, consequentemente, uma diminuição do background fosse obtida para a captura de imagens de melhor qualidade. Tal lavagem era feita utilizando solução Ringer normal adicionada de d-tubocurarina (16 μM).

Para visualizar a exocitose de aglomerados de vesículas sinápticas, um novo estímulo, após o procedimento de marcação com o FM1-43, era aplicado. A sonda era então liberada no meio externo, levando a uma diminuição do sinal fluorescente, uma vez que o FM1-43 é 300 vezes menos fluorescente quando não está ligado às membranas celulares (BETZ *et.al*., 1992) (FIGURA 6).

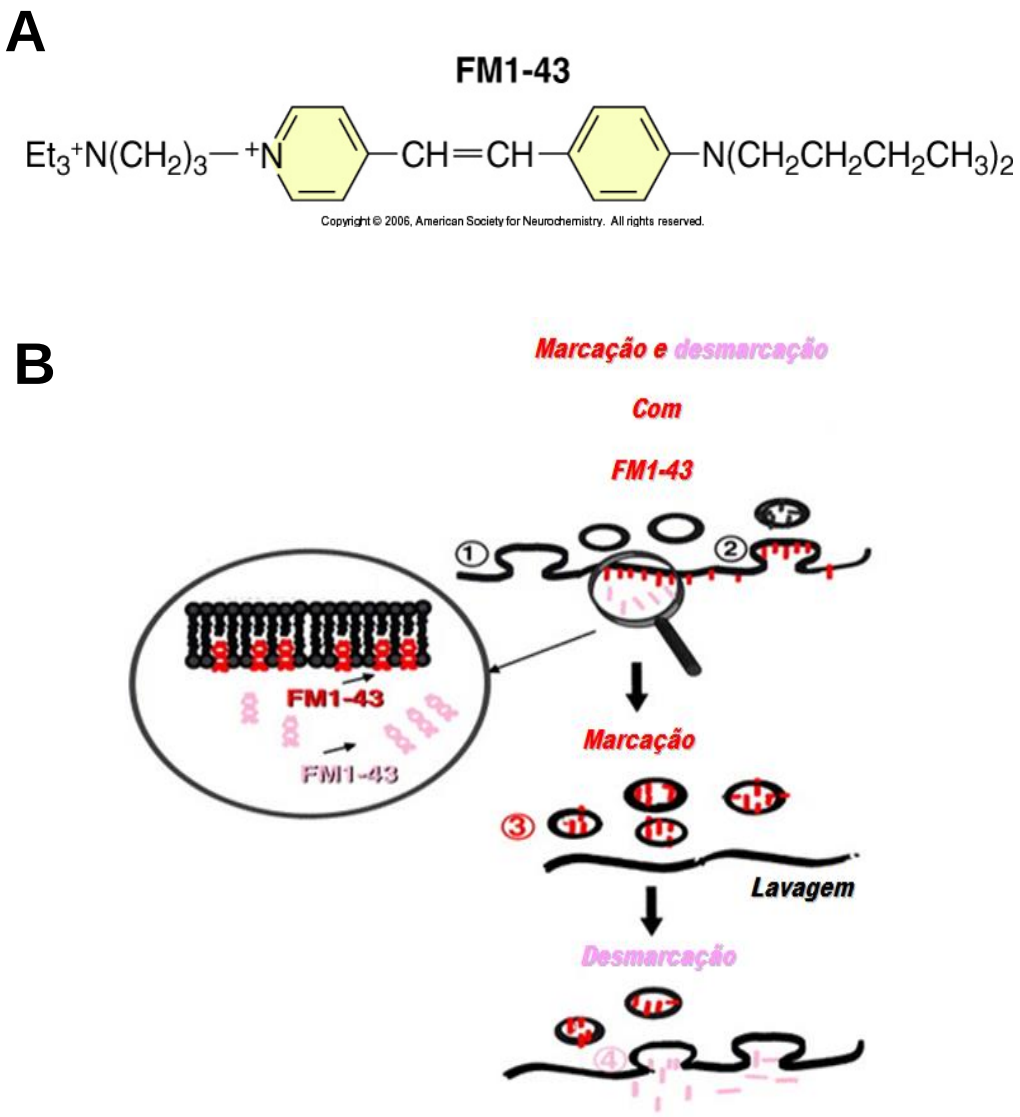

Figura 5. O marcador fluorescente FM1-43 é utilizado para monitoramento dos passos de endocitose e exocitose de vesículas sinápticas em neurônios. (A) Estrutura molecular do FM1-43, sonda fluorescente utilizada para o monitoramento do ciclo de vesículas sinápticas. *(Basic Neurochemistry, seventh edition. Edited by Siegel et. al., 2006)* **(B) Marcação de aglomerados vesiculares com a sonda fluorescente FM1-43.** (1,2) Marcação da membrana do terminal pré-sináptico com o FM1-43 adicionado à solução. O neurônio foi estimulado na presença de FM1-43. Observe no detalhe em aumento maior que a sonda não emite sinal fluorescente quando não ligada a membrana devido a seu baixo rendimento quântico. Notar que a membrana que originou uma nova vesícula sináptica está marcada com a sonda. (3) Uma breve lavagem remove as moléculas de FM que não foram internalizadas. (4) Um segundo ciclo de exocitose induzido por estimulação resulta na liberação da sonda que foi internalizada durante a endocitose. *(Modificado de GUATIMOSIM and VON GERSDORFF. Optical monitoring of synaptic vesicle trafficking in ribbon synapses. Neurochemistry International Volume 41, Issue 5, November 2002, Pages 307–312).*

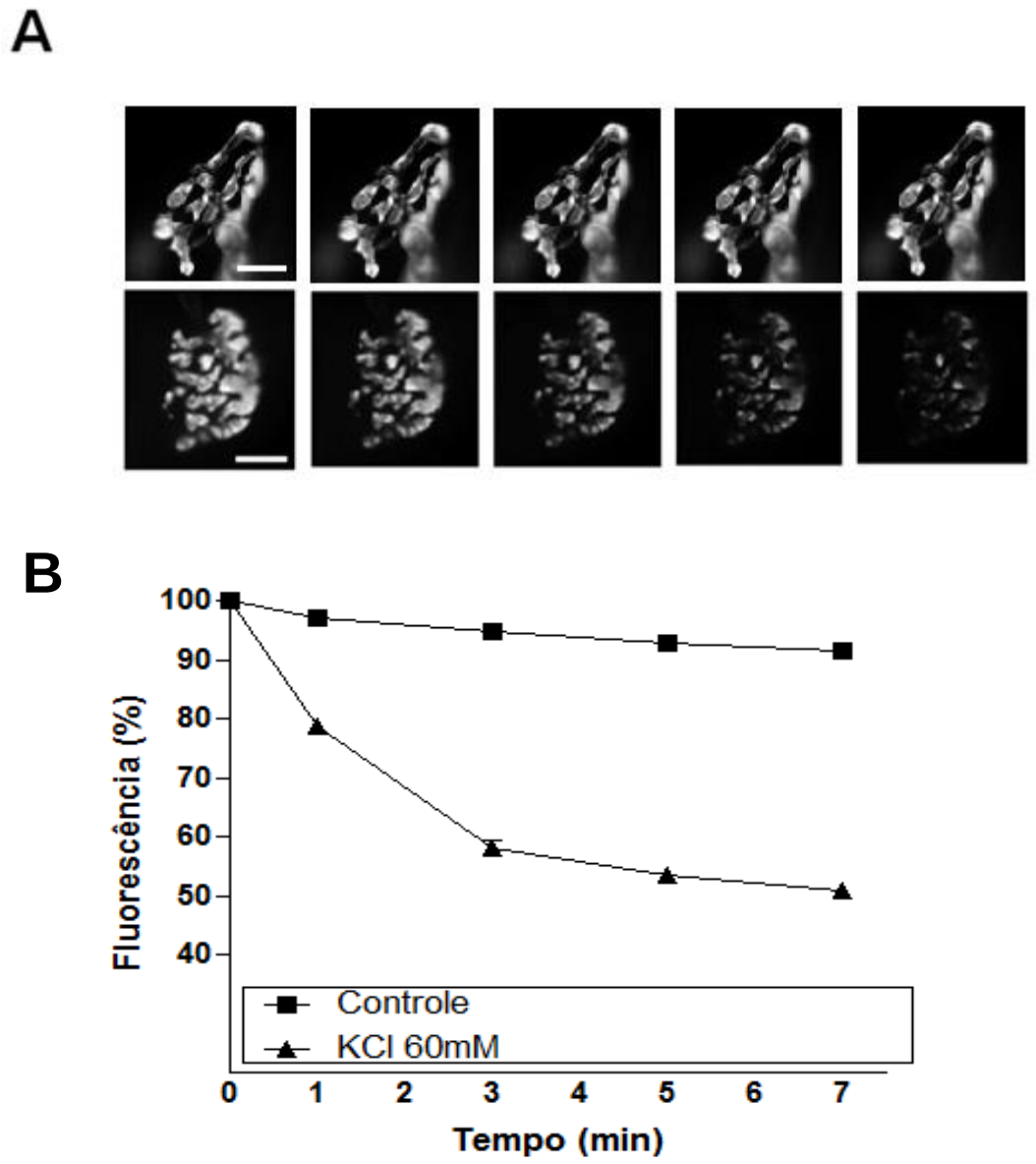

Figura 6. **Ciclo de vesículas sinápticas marcadas com o marcador FM1-43 visualizados por microscopia óptica de fluorescência. A)** Imagens representativas de duas terminações nervosas motoras de músculo diafragma com seus respectivos aglomerados de vesículas sinápticas marcados com FM1-43, submetidos à fotodesmarcação (painel superior) ou à estimulação com solução Ringer Alto Potássio (painel inferior) durante sete minutos. Observar perda do sinal fluorescente. **B)** Quantificação da perda de sinal fluorescente devido à fotodesmarcação (~10%) e ao estímulo com KCl 60mM (~50%). N= 3 animais para cada grupo experimental (fotodesmarcação e KCl 60mM); 30 pontos fluorescentes analisados para cada grupo experimental. Barra de escala: 10µm

3.5 Exposição da preparação ao anestésico e neurotoxinas

Depois de marcadas com FM1-43, as preparações neuromusculares foram submetidas a diferentes concentrações do anestésico sevoflurano ou isoflurano (0,45 mM, 0,6 mM e 0,9 mM). Devido à volatilidade destes agentes, a preparação neuromuscular foi perfundida continuamente com a solução anestésica preparada, através de uma bomba de perfusão Samtronic ST670, com o objetivo de se manter a concentração anestésica testada constante durante o procedimento. O efeito do anestésico na exocitose de vesículas sinápticas foi investigado na presença apenas do anestésico ou conjuntamente com neurotoxinas e agentes despolarizantes, com o objetivo de verificar se este fármaco bloqueia a exocitose evocada por esses estímulos.

3.6 Aquisição e análise das imagens

As imagens foram adquiridas utilizando um microscópio de fluorescência (Leica DM 2500) acoplado a uma câmera Leica DFC345FX nos seguintes valores de tempo: 0, 1, 3, 5 e 7 minutos após o início da perfusão. A aquisição foi feita pelo programa Leica Application Suite 4.0, em que foi possível selecionar o tempo de exposição da preparação e o ganho da imagem para evitar possíveis saturações que poderiam vir a distorcer a análise. Utilizamos uma lente objetiva de imersão com aumento de 63X e abertura numérica de 0,90. A luz utilizada na excitação do fluoróforo era proveniente de uma lâmpada HXP R120/45C – VIS e filtrada (505/530nm) para que o comprimento de onda excitação/ emissão desejado pudesse ser selecionado. Todos os experimentos foram realizados com no mínimo três réplicas.

3.7 Análise estatística

As análises cromatográficas foram avaliadas através do software Varian Star 5.5 em que as áreas das curvas obtidas em cada injeção eram obtidas e comparadas. As análises estatística foram feitas utilizando o programa GraphPad Prisma 5.0, através do test-t pareado de Student. $P<0,05$ foi considerado estatisticamente significante.

Já para os experimentos de microscopia de fluorescência, as análises das imagens foram realizadas utilizando os softwares Image J e Microsoft Office Excel. A média da intensidade da fluorescência foi determinada para cada grupo de aglomerado de vesículas e tabelada em gráficos criados utilizando o programa GraphPad Prisma 5.0. As análises estatísticas foram feitas utilizando o test-t pareado de Student. $P<0,05$ foi considerado estatisticamente significante.

4. RESULTADOS

4.1 Efeito do sevoflurano e isoflurano na exocitose espontânea de vesículas sinápticas de JNMs de diafragma de camundongo

No primeiro conjunto de experimentos investigamos o efeito do sevoflurano e isoflurano na exocitose espontânea de vesículas sinápticas na JNM de camundongos. Para isso, preparações de músculo diafragma contendo terminais nervosos motores marcados com FM1-43 foram continuamente perfundidas com concentrações clínicas (0,45 mM e 0,6 mM) ou supra-clínica (0,9 mM) de sevoflurano ou isoflurano durante 7 minutos (FIGURAS 7 e 8). Imagens representativas dos terminais nervosos antes (painéis superiores) e após (painéis inferiores) a fotodesmarcação são mostrados nas Figuras 7A e 8A. Como representado, após 7 minutos de exposição à luz, uma redução de ~10% na fluorescência é observada. As Figuras 7B-D mostram que as preparações perfundidas durante 7 minutos com sevoflurano em qualquer uma das concentrações testadas (0,45, 0,6 ou 0,9 mM) não apresentaram redução significativa do sinal fluorescente quando comparadas com o controle (fotodesmarcação). O mesmo resultado foi observado com isoflurano (FIGURAS 8B-D) nas mesmas concentrações acima. O gráfico da FIGURA 9 representa a quantificação da redução do sinal fluorescente devido à fotodesmarcação ($P > 0.05$; $N = 9$ animais, 63 pontos fluorescentes analisados), tratamento com sevoflurano/isoflurano 0,45 mM ($P > 0.05$; $N = 4$ animais, 28 pontos fluorescentes analisados), tratamento com sevoflurano/isoflurano 0,6 mM ($P > 0.05$; $N = 4$ animais, 28 pontos fluorescentes analisados) e tratamento com sevoflurano/isoflurano 0,9 mM ($P > 0.05$; $N = 4$ animais, 28 pontos fluorescentes analisados). Como observado, estes dados nos permite concluir que os anestésicos inalatórios sevoflurano e isoflurano não são capazes de evocar a exocitose de vesículas sinápticas na JNM de diafragma de camundongos.

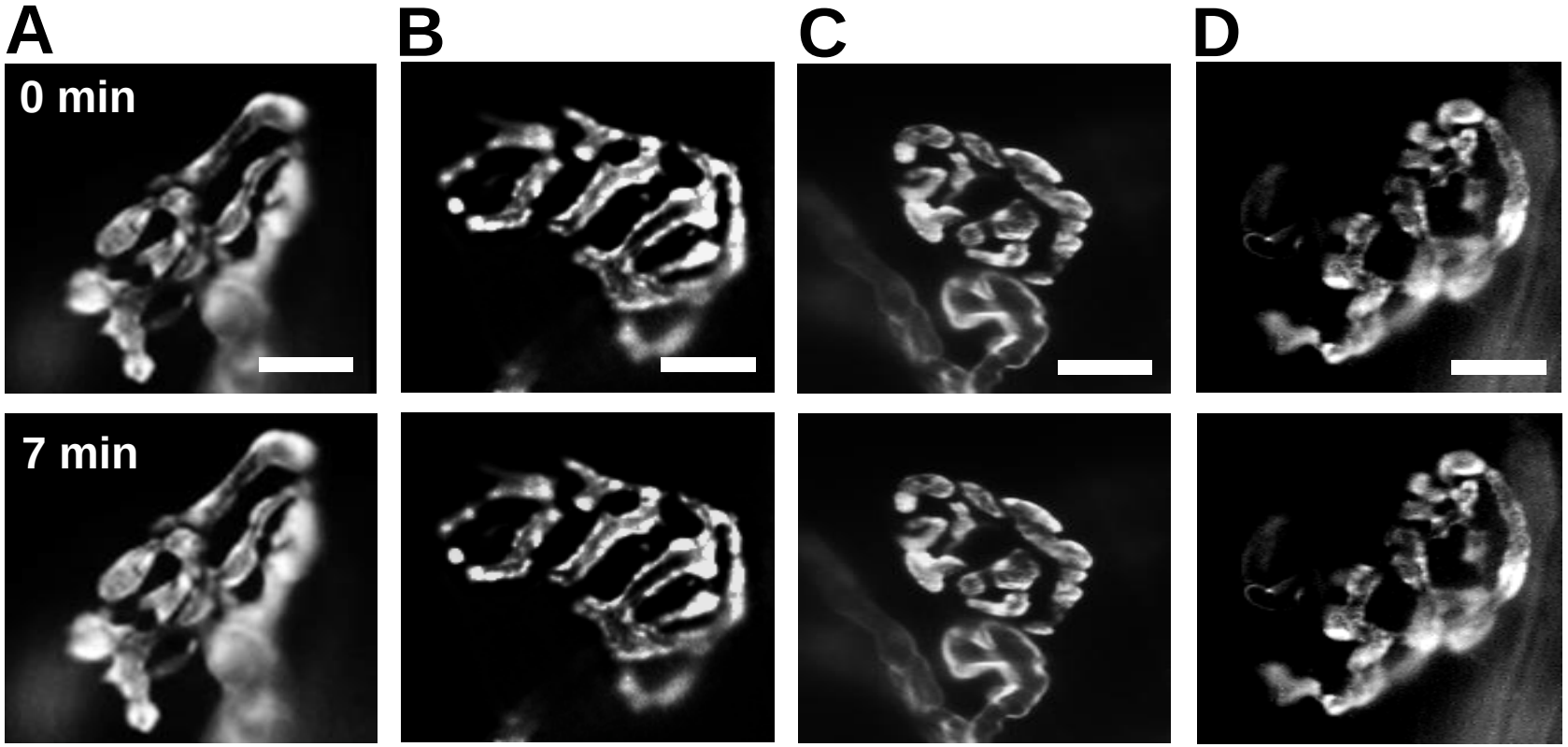

Figura 7: O anestésico inalatório sevoflurano não induz a exocitose de vesículas sinápticas na JNM de diafragma de camundongo. (A) Imagens representativas da redução da fluorescência devido à iluminação durante 7 minutos (fotodesmarcação). Painel superior: antes da iluminação. Painel inferior: após 7 minutos de iluminação. **(B)** Imagens representativas de terminações nervosas antes (painel superior) e após incubação com sevoflurano 0,45 mM por 7 minutos (painel inferior). **(C)** Imagens representativas de terminações nervosas antes (painel superior) e após incubação com sevoflurano 0,6 mM por 7 minutos (painel inferior). **(D)** Imagens representativas de terminações nervosas antes (painel superior) e após incubação com sevoflurano 0,9 mM por 7 minutos (painel inferior). Barra de escala = 10 μm

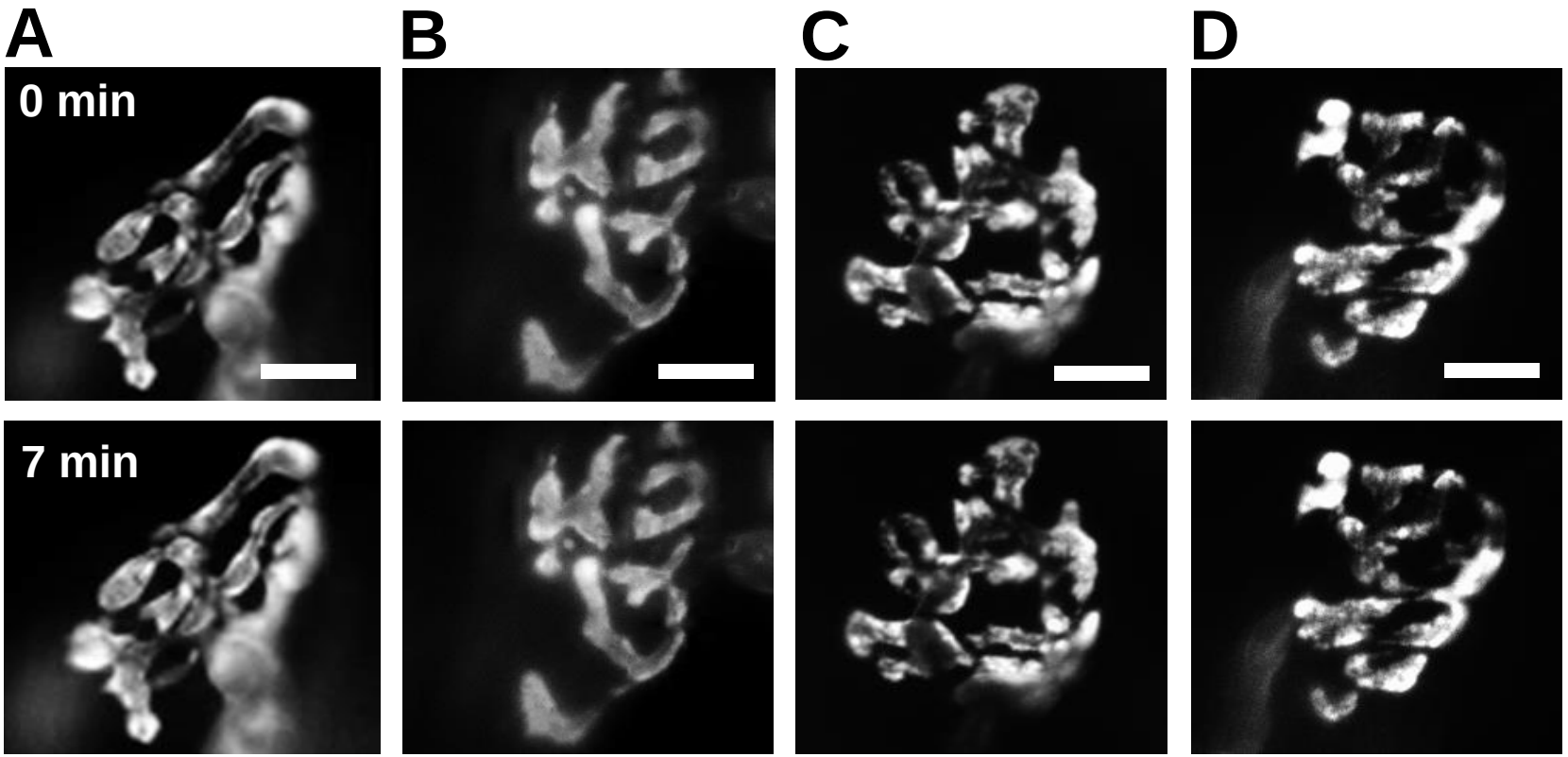

Figura 8: O anestésico inalatório isoflurano também não é capaz de evocar a exocitose de vesículas sinápticas na JNM de diafragma de camundongo. **(A)** Imagens representativas da redução da fluorescência devido à iluminação durante 7 minutos (fotodesmarcação). Painel superior: antes da iluminação. Painel inferior: após 7 minutos de iluminação. **(B)** Imagens representativas de terminações nervosas antes (painel superior) e após incubação com isoflurano 0,45 mM por 7 minutos (painel inferior). **(C)** Imagens representativas de terminações nervosas antes (painel superior) e após incubação com isoflurano 0,6 mM por 7 minutos (painel inferior). **(D)** Imagens representativas de terminações nervosas antes (painel superior) e após incubação com isoflurano 0,9 mM por 7 minutos (painel inferior). Barra de escala = 10 μm

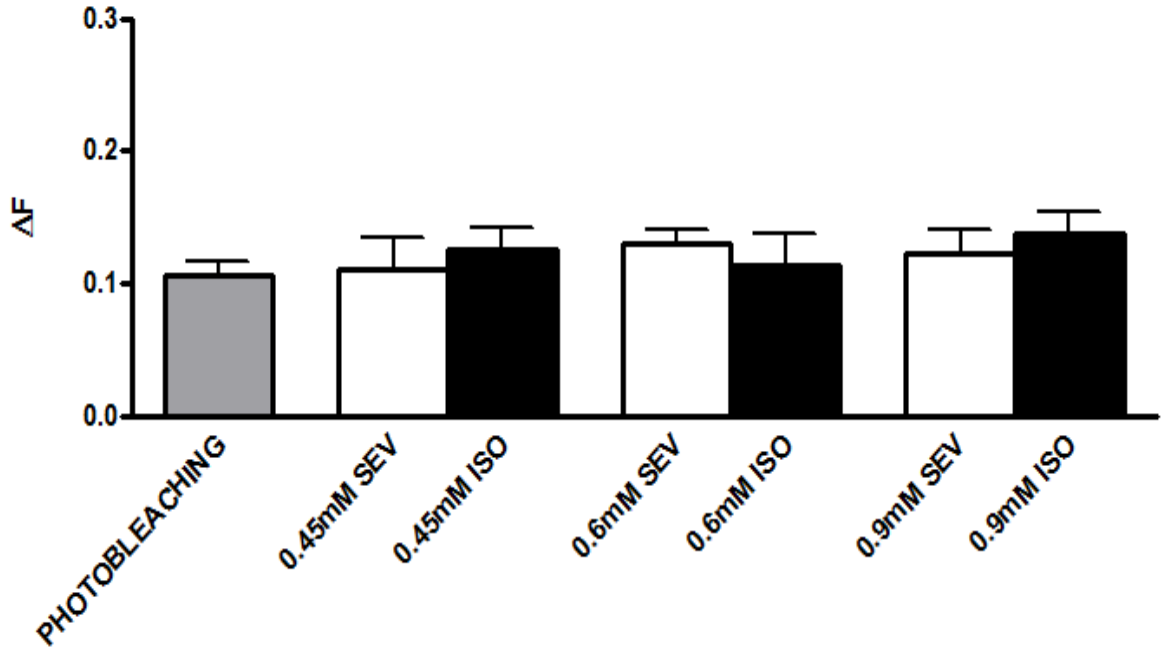

Figura 9: Sevoflurano e isoflurano não estimulam a exocitose de vesículas sinápticas na JNM. Quantificação do sinal fluorescente após fotodesmarcação ou incubação com diferentes concentrações de sevoflurano ou isoflurano. ΔF, fluorescência normalizada (F-F0/100). Os resultados expressos constituem a média ±EPM de 147 pontos fluorescentes de 15 terminações nervosos de 15 animais para fotodesmarcação e 28 pontos fluorescentes de 4 terminações nervosas de 4 animais para cada uma das outras condições experimentais (sevoflurano ou isoflurano 0,45 mM; sevoflurano ou isoflurano 0,6 mM e sevoflurano ou isoflurano 0,9 mM).

4.2 Sevoflurano e isoflurano não inibem a exocitose de vesículas sinápticas evocada por solução despolarizante de KCl.

Estudos apontam que os anestésicos gerais podem interagir com diferentes tipos de canais iônicos ativados por voltagem, dentre eles os canais para $Na^{+,}$ K^{+}, e Ca^{2+} (Hemmings et al., 2009). Além disso, alguns estudos tem demonstrado que os anestésicos gerais inalatórios causam relaxamento muscular e podem potencializar o efeito de drogas bloqueadoras neuromusculares como o vecurônio (SUZUKI *et al*., 1999; GHATGE *et.al.,* 2003). Sendo assim, para investigar um possível mecanismo pelo qual o sevoflurano e o isoflurano geram tal relaxamento muscular, o subsequente conjunto de experimentos investigou se estes anestésicos são capazes de bloquear diferentes estímulos despolarizantes que mimetizam um potencial de ação fisiológico, sejam dependentes ou independentes do influxo de íons Na^{+}.

Soluções altamente concentradas de KCl são rotineiramente utilizadas como um método farmacológico para evocar a exocitose de vesículas sinápticas em terminações nervosas de maneira independente de Na^{+} (NICHOLLS, 1993). Um nível aumentado na concentração extracelular de K^{+} despolariza a membrana celular por deslocar o equilíbrio de íons K^{+} que leva a ativação de canais para Ca^{2+} dependentes de voltagem. A ativação destes canais leva a um influxo de Ca^{2+} para o interior da terminação nervosa e, consequentemente, exocitose de vesículas sinápticas independente de Na^{+}. Para investigar se sevoflurano e isoflurano eram capazes de interferir com a exocitose induzida por KCl (60 mM), terminações nervosas marcadas com FM1-43 foram pré-incubadas com sevoflurano ou isoflurano nas concentrações de 0,45 ou 0,9 mM. Em seguida, as preparações foram continuamente perfundidas com solução de KCl 60mM acrescida do anestésico nas mesmas concentrações mencionadas. Preparações tratadas com KCl 60mM exibem uma perda de ~60% na intensidade de fluorescência após 7 minutos de tratamento. Terminações nervosas pré-incubadas e continuamente perfundidas com sevoflurano ou isoflurano 0,45 ou 0,9mM e estimulados com KCl 60mM, exibiram um padrão de desmarcação similar às preparações tratadas apenas com KCl 60mM. Imagens representativas de terminações nervosas antes e após a fotodesmarcação, estimulação com KCl 60mM na ausência ou presença dos anestésicos estudados são apresentadas nas FIGURAS 10 e 11. Resultados de diferentes experimentos estão quantificados na FIGURA 12. A desmarcação evocada por KCl 60 mM foi estatisticamente diferente da fotodesmarcação ($P < 0,001$; N=10 animais, 100

pontos fluorescentes analisados), mas similar à desmarcação de todos os outros grupos experimentais (KCl 60 mM + sevoflurano 0,45; KCl 60 mM + sevoflurano 0,9 mM; KCl 60 mM + isoflurano 0,45 e KCl 60 mM + sevoflurano 0,90 ($P > 0,05$; N= 3 animais, 21 pontos fluorescentes analisados para cada condição experimental). Este resultado sugere, portanto, que sevoflurano e isoflurano não inibem a exocitose de vesículas sinápticas evocada por KCl, um estímulo despolarizante independente do influxo de Na^+.

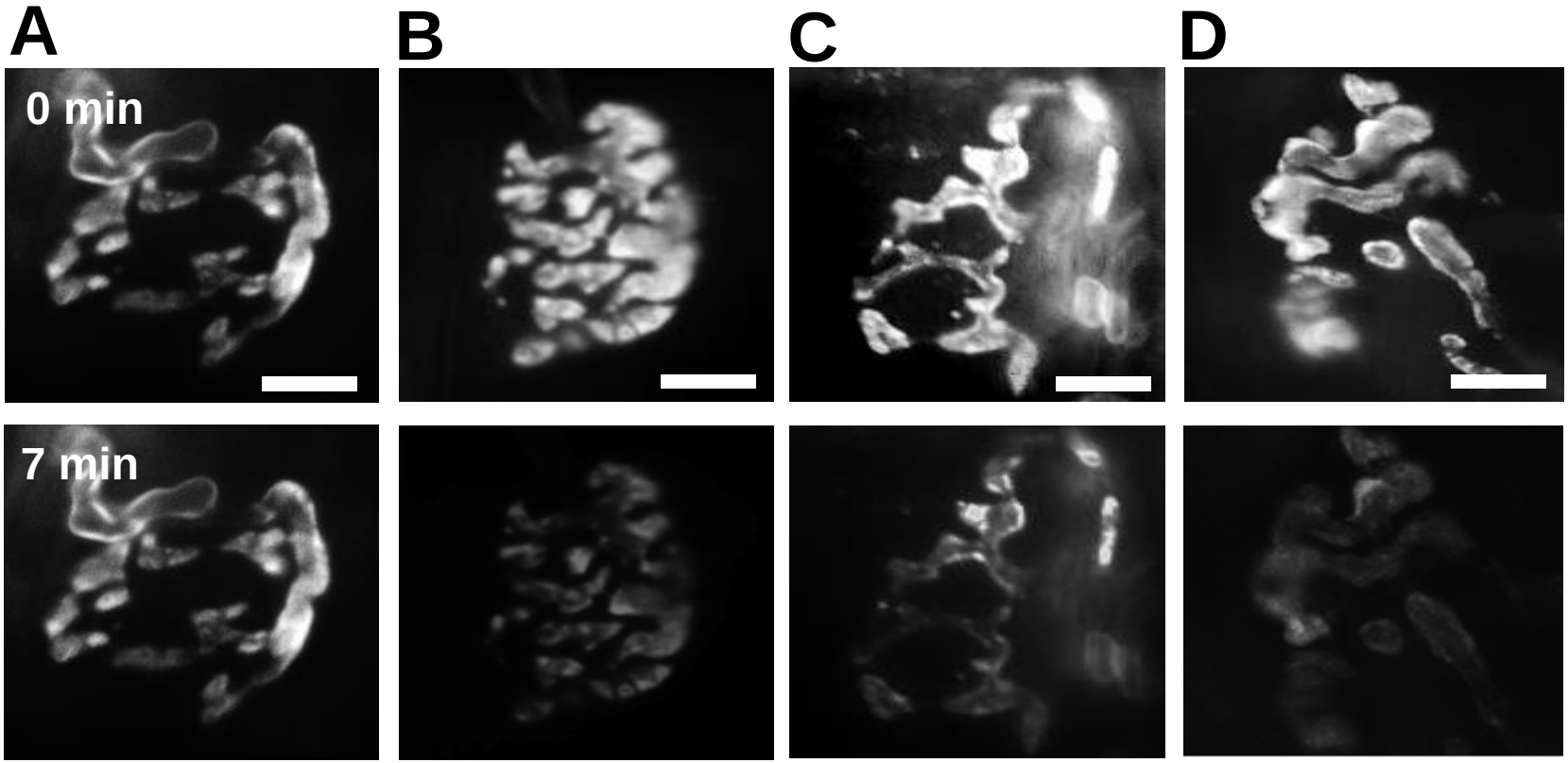

Figura 10: O anestésico inalatório sevoflurano não é capaz de bloquear a exocitose de vesículas sinápticas evocada por KCl 60 mM na JNM de diafragma de camundongo. (A) Imagens representativas da redução da fluorescência devido à iluminação durante 7 minutos (fotodesmarcação). Painel superior: antes da iluminação. Painel inferior: após 7 minutos de iluminação. **(B)** Imagens representativas de terminação nervosa antes (painel superior) e após 7 minutos de tratamento com KCl 60 mM (painel inferior). **(C)** Imagens representativas de terminação nervosa antes (painel superior) e após 7 minutos de tratamento com KCl 60 mM + sevoflurano 0,45 mM (painel inferior). **(D)** Imagens representativas de terminação nervosa antes (painel superior) e após 7 minutos de tratamento com KCl 60 mM + sevoflurano 0,9 mM. Barra de escala = 10 μm

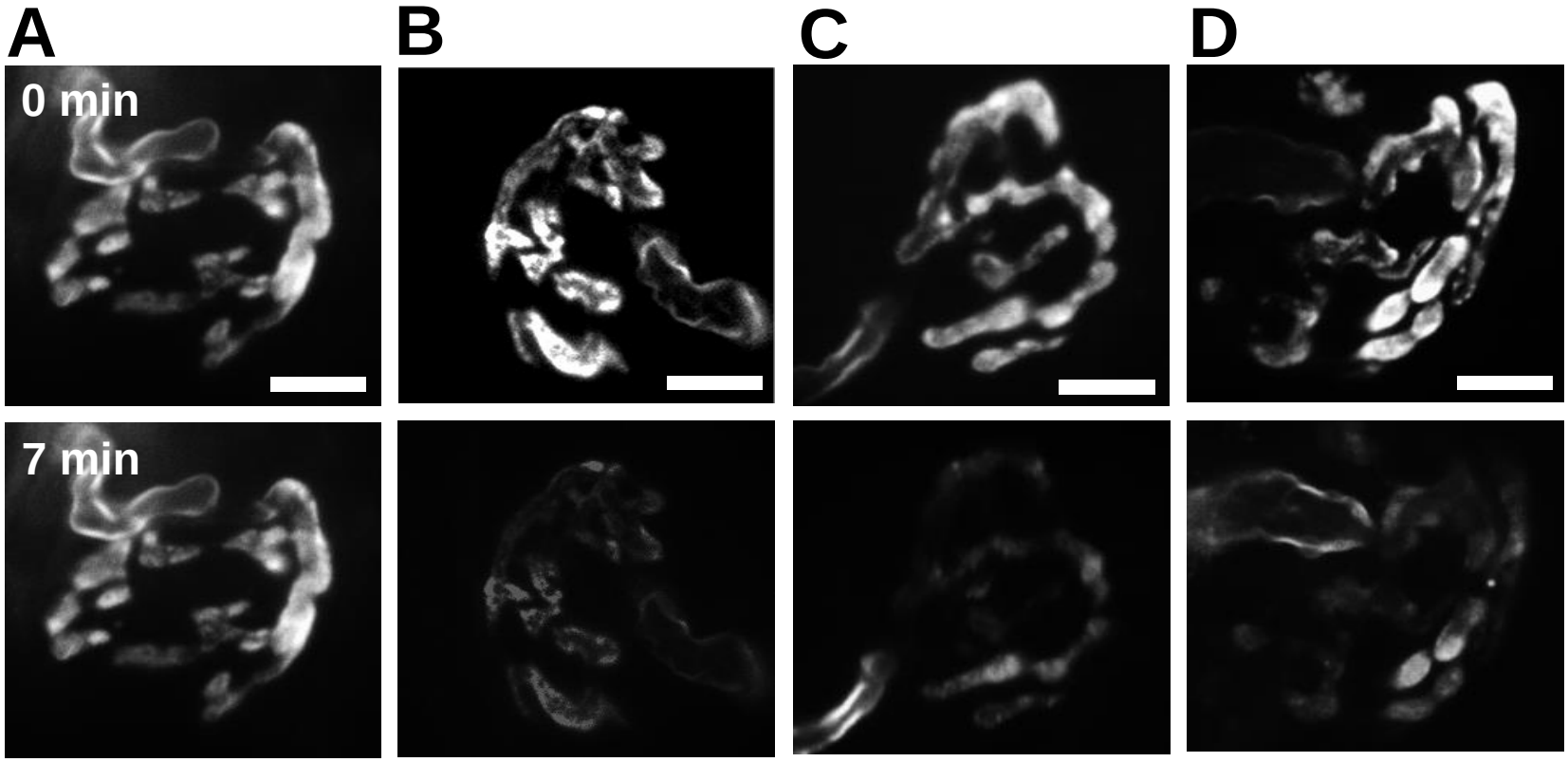

Figura 11: O anestésico inalatório isoflurano não é capaz de bloquear a exocitose de vesículas sinápticas evocada por KCl 60 mM na JNM de diafragma de camundongo. (A) Imagens representativas da redução da fluorescência devido à iluminação durante 7 minutos (fotodesmarcação). Painel superior: antes da iluminação. Painel inferior: após 7 minutos de iluminação. **(B)** Imagens representativas de terminação nervosa antes (painel superior) e após 7 minutos de tratamento com KCl 60 mM (painel inferior). **(C)** Imagens representativas de terminação nervosa antes (painel superior) e após 7 minutos de tratamento com KCl 60 mM + sevoflurano 0,45 mM (painel inferior). **(D)** Imagens representativas de terminação nervosa antes (painel superior) e após 7 minutos de tratamento com KCl 60 mM + sevoflurano 0,9 mM. Barra de escala = 10 μm

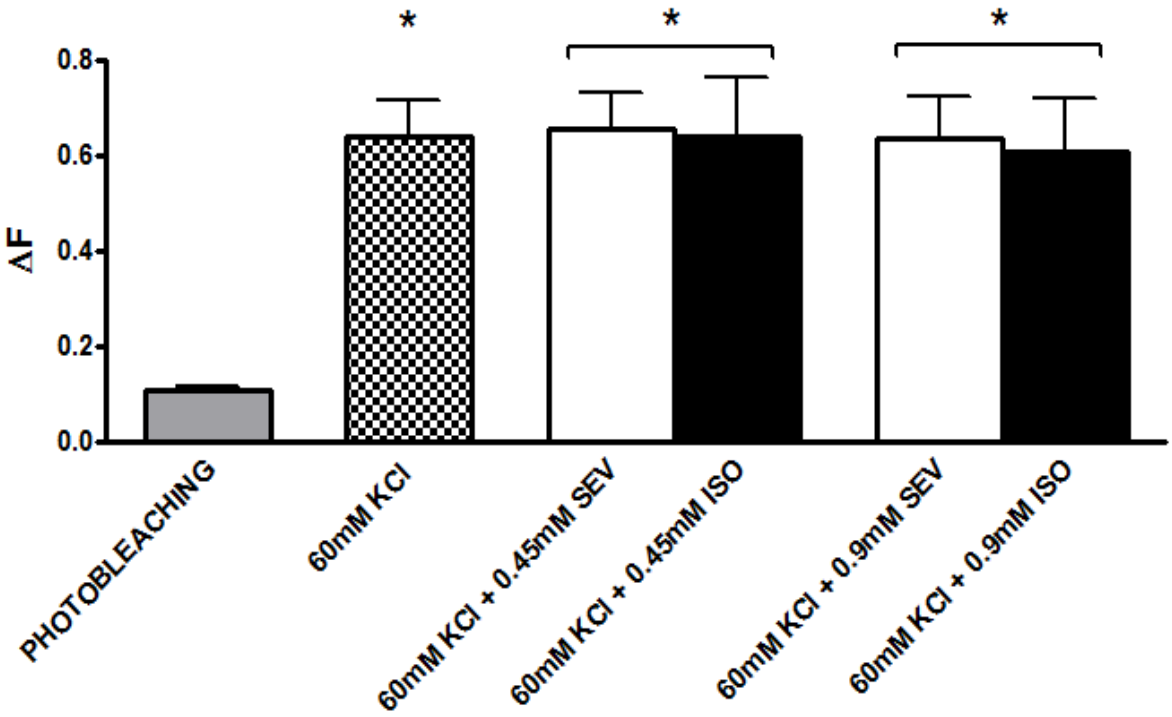

Figura 12. Sevoflurano, isoflurano e a exocitose evocada por KCl 60mM. Quantificação do sinal fluorescente após fotodesmarcação (primeira barra), evocada por KCl 60 mM (segunda barra), KCl 60 mM + sevoflurano ou isoflurano 0,45 mM (terceiras barras pareadas) e KCl 60 mM + sevoflurano ou isoflurano 0,9 mM (quartas barras pareadas) ou incubação com diferentes concentrações de sevoflurano ou isoflurano. ΔF, fluorescência normalizada (F-F0/100). Os resultados expressos são da média ±EPM de 150 pontos fluorescentes de 15 terminações nervosas de 15 animais para fotodesmarcação, 100 pontos fluorescentes de 10 terminações nervosas de 10 animais para KCl 60 mM e 21 pontos fluorescentes de 3 terminações nervosas de 3 animais para cada uma das outras condições experimentais (KCl 60 mM + sevoflurano ou isoflurano 0,45 ou 0,9 mM). *P<0.05 comparado à primeira barra (fotodesmarcação).

4.3 Sevoflurano e isoflurano inibem a exocitose de vesículas sinápticas evocada por 4-aminopiridina em JNMs de diafragma de camundongo.

Canais para Na^+ ativados por voltagem têm sido considerados como importantes alvos para os anestésicos gerais, especialmente para os anestésicos inalatórios. Já é bem elucidado que concentrações clínicas de anestésicos inalatórios inibem canais para Na^+ em terminações nervosas isoladas de neurônios de ratos, assim como possuem atividade inibitória de subunidades alfa de canais para Na^+ de mamíferos heterologamente expressos. (HEMMINGS, 2009). Baseado nessas observações, nosso próximo passo foi investigar em nosso modelo experimental se o sevoflurano poderia interferir com a exocitose de vesículas sinápticas evocada por 4AP (1 mM) ou por veratridina (100 µM). A despolarização de membrana evocada por 4AP é associada com a extensão temporal do potencial de ação causado pelo bloqueio da corrente de K^+, o que leva a abertura de canais para Na^+ e consequente abertura de canais para Ca^{2+}, ocasionando a liberação de neurotransmissores na fenda sináptica. (ENOMOTO & MAENO, 1981). A Figura 13B mostra que terminações nervosas incubadas com 4AP (1 mM) por 7 minutos exibem uma redução na intensidade do sinal fluorescente da sonda FM1-43 (Quantificação expressa na FIGURA 15; $P < 0,0001$ quando comparado a fotodesmarcação; N = 7 animais, 49 pontos fluorescentes analisados).

Preparações neuromusculares pré-incubadas e continuamente perfundidas com sevoflurano na concentração de 0,45 mM ($P = 0,0158$; N = 4 animais, 28 pontos fluorescentes analisados) e 0,6 mM ($P = 0,0024$; N = 4 animais, 28 pontos fluorescentes) apresentaram uma significativa redução da exocitose evocada por 4AP (decaimento de ~15% do sinal fluorescente) (FIGURAS 13C e 15). O sevoflurano na concentração de 0,9 mM inibiu de forma ainda mais significativa a desmarcação do FM1-43 induzida pelo 4AP (1 mM) ($P < 0,01$; N = 4 animais, 28 pontos) quando comparado com 4AP + sevoflurano 0,6 mM mM (FIGURA 13D e 15, decaimento de ~10% no sinal fluorescente). Podemos então inferir que na JNM de camundongos o sevoflurano inibe consideravelmente a exocitose de vesículas sinápticas evocada por 4AP, um mecanismo dependente de Na^+, na JNM de camundongos.

De maneira similar, observamos que o anestésico isoflurano foi capaz de inibir a exocitose evocada por 4AP, porém de maneira menos pronunciada que sevoflurano. (FIGURA 14). De fato, preparações neuromusculares pré-incubadas e continuamente perfundidas com isoflurano nas concentrações testadas (0,45, 0,6 ou 0,9 mM) exibiram

uma redução de ~20% do sinal fluorescente quando estimuladas com 4AP (1 mM) ($P < 0,05$ quando comparado com 4AP sozinho; N = 3 animais, 28 pontos fluorescentes analisados para cada grupo experimental) (FIGURAS 14 e 15). Com isso, mostramos que isoflurano inibe consideravelmente a exocitose de vesículas sinápticas evocada 4AP na JNM de camundongo, porém com uma eficiência estatisticamente menor do que sevoflurano.

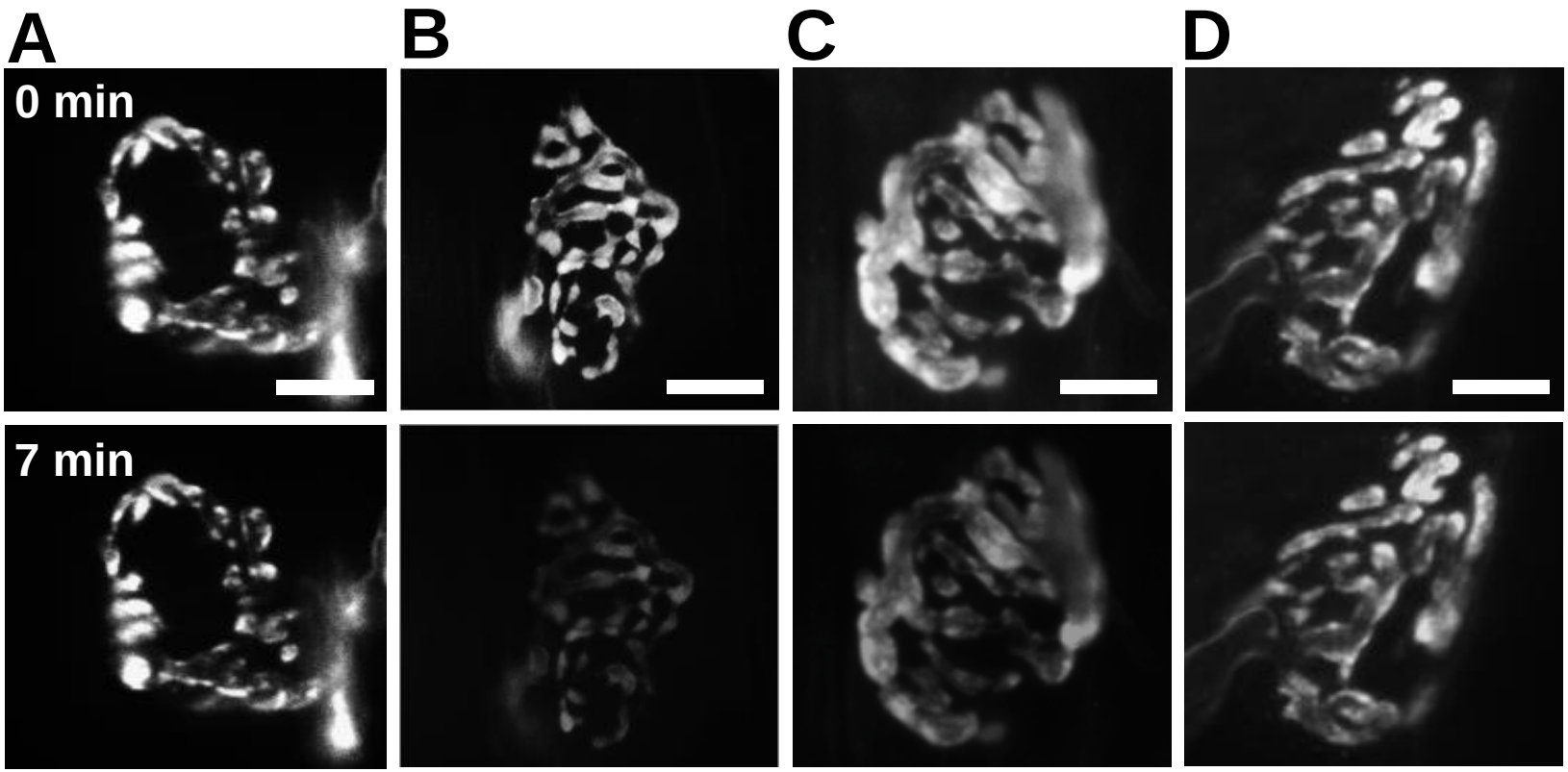

Figura 13: **O anestésico inalatório sevoflurano inibe a exocitose de vesículas sinápticas evocada por 4AP (1 mM) em JNM de diafragma camundongos** (A) Imagens representativas da redução da fluorescência devido à iluminação durante 7 minutos Painel superior: antes da iluminação. Painel inferior: após 7 minutos de iluminação. (B) Imagens representativas de terminação nervosa antes (painel superior) e após tratamento com 4AP 1 mM (painel inferior). (C) Imagem representativa de terminação nervosa antes (painel superior) e após tratamento com 4AP 1 mM + sevoflurano 0, 45 mM durante 7 minutos. (D) Imagem representativa de terminação nervosa antes (painel superior) e após 7 minutos de tratamento com 4AP 1 mM + sevoflurano 0, 9 mM (painel inferior). Barra de escala = 10 µm

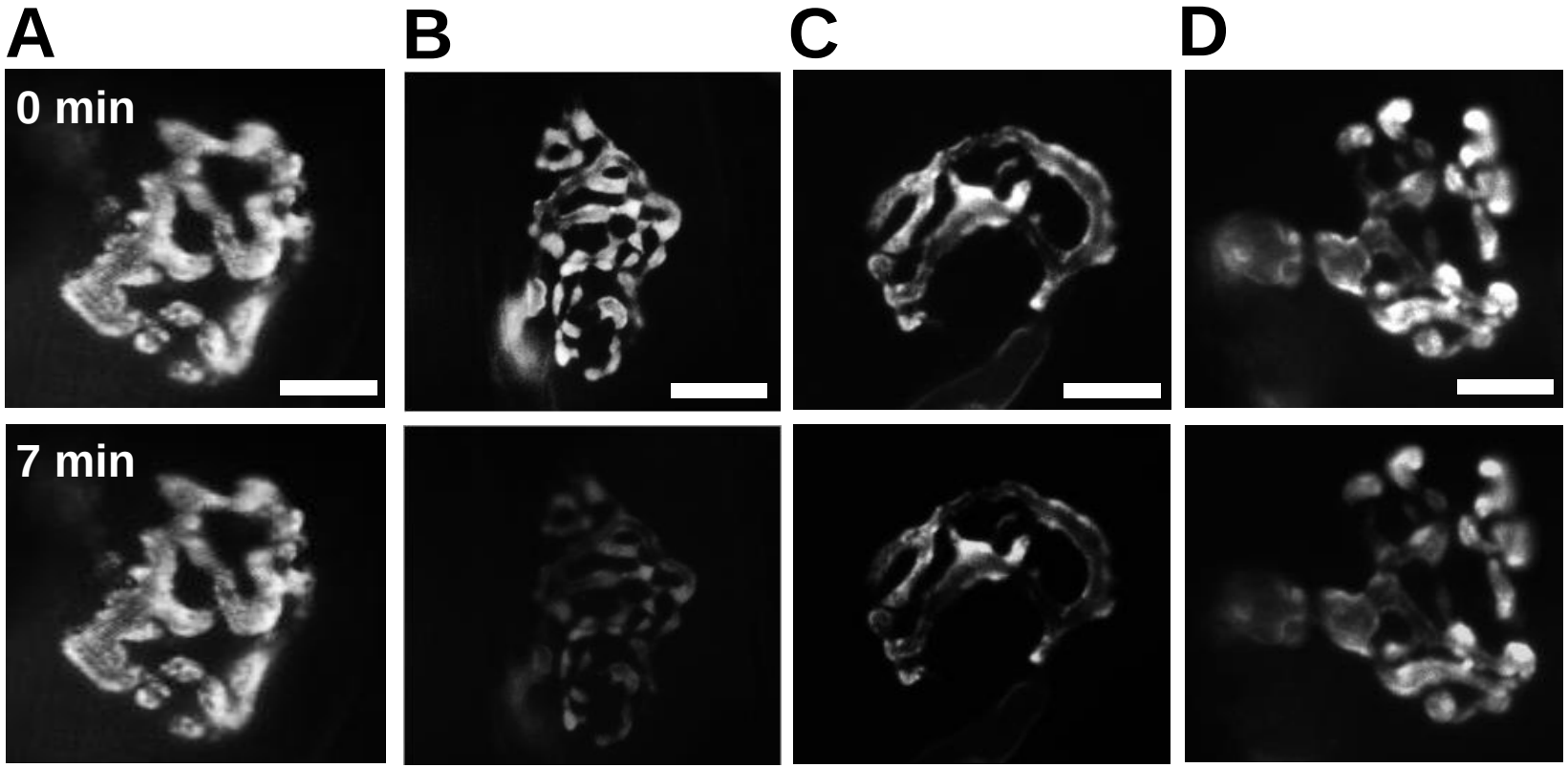

Figura 14: O anestésico inalatório isoflurano inibe a exocitose de vesículas sinápticas evocada por 4AP (1 mM) (A) Imagens representativas da redução da fluorescência devido à iluminação durante 7 minutos Painel superior: antes da iluminação. Painel inferior: após 7 minutos de iluminação. **(B)** Imagens representativas de terminação nervosa antes (painel superior) e após tratamento com 4AP 1 mM (painel inferior). **(C)** Imagem representativa de terminação nervosa antes (painel superior) e após tratamento com 4AP 1 mM + isoflurano 0, 45 mM durante 7 minutos. **(D)** Imagem representativa de terminação nervosa antes (painel superior) e após 7 minutos de tratamento com 4AP 1 mM + isoflurano 0, 9 mM (painel inferior). Barra de escala = 10 µm

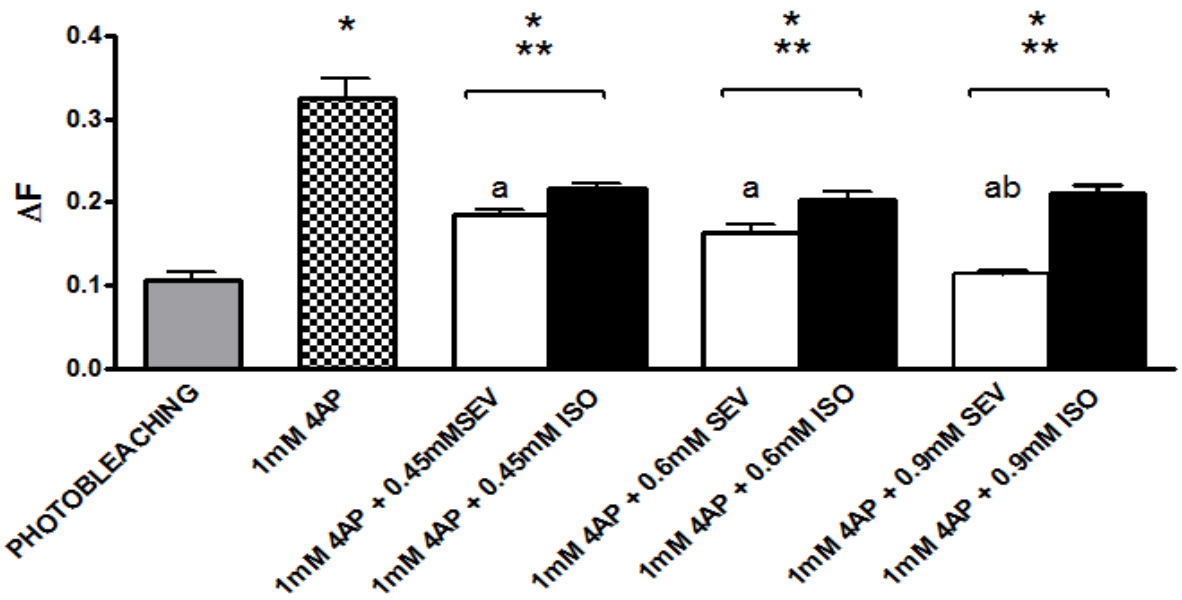

Figura 15: Os anestésicos inalatórios sevoflurano e isoflurano inibe a exocitose de vesículas sinápticas evocada por 4AP (1 mM) em JNM de diafragma camundongos (A) Quantificação da perda de fluorescência devido à fotodesmarcação (primeira barra), tratamento com 4AP (1 mM) (segunda barra), tratamento com 4AP (1 mM) + sevoflurano 0,45 mM (terceira barra), tratamento com 4AP (1 mM) + sevoflurano 0,6 mM (quarta barra) e tratamento com 4AP (1 mM) + sevoflurano 0,9 mM (quinta barra). ΔF, fluorescência normalizada (F-F0/100). Os resultados expressos representam a média ±EPM de 49 pontos fluorescentes de 7 animais de 7 terminações nervosas para 4AP 1mM e 28 pontos fluorescentes de 4 terminações nervosas de 4 animais para cada uma das outras condições experimentais. *P<0,05 quando comparado com a primeira barra (fotodesmarcação). **P<0,05 quando comparado com a segunda barra (4AP 1 mM). a P<0,05 quando comparado com isoflurano (cada concentração) . b P<0.05 quando comparado com sevofluran0 0, 45 ou 0,6mM.

4.4 Sevoflurano e isoflurano inibem a exocitose de vesículas sinápticas evocada por veratridina em JNM de diafragma de camundongo.

Em sequência, investigamos se sevoflurano e isoflurano inibem a exocitose de vesículas sinápticas evocada pela veratridina, outro estímulo despolarizante dependente de canais para Na^+. Este fármaco atua de maneira distinta de 4AP, por atuar de forma direta no canal para Na^+. A veratridina impede a inativação de canais para Na^+ previamente ativados e, desta maneira, causa uma despolarização de membrana (BARNES e HILLE, 1988).

Preparações tratadas com veratridina (100 µM) durante 7 minutos exibem uma significativa exocitose de vesículas sinápticas (~45% de redução do sinal fluorescente) ($P<0,0001$ quando comparado à fotodesmarcação; N=10 animais, 70 pontos fluorescentes analisados) (FIGURA 16). Preparações neuromusculares pré-incubadas e continuamente perfundidas com sevoflurano 0,45 mM exibiram uma redução no estímulo despolarizante evocado pela veratridina (~25% de redução do sinal fluorescente) ($P <0,05$; N=4 animais, 28 pontos fluorescentes analisados). Na presença do anestésico, a redução no sinal fluorescente foi menor do que na ausência do fármaco e não houve efeito inibitório mais proeminente quando concentrações mais altas foram utilizadas. (0,6 ou 0,9 mM, $P < 0,05$; N=4 animais, 28 pontos fluorescentes analisados para cada condição) (FIGURA 16). Desta maneira, conclui-se que o sevoflurano inibe a exocitose de vesículas sinápticas evocada pela veratridina.

Resultados similares foram observados quando isoflurano foi utilizado no lugar de sevoflurano. Preparações pré-incubadas e continuamente perfundidas com isoflurano 0,45, 0,6 ou 0,9 mM também inibiram significativamente a exocitose induzida pela veratridina (~25% de redução do sinal fluorescente) ($P<0,05$; N=4 animais e 28 pontos fluorescentes analisados para cada condição experimental) (FIGURA 17)

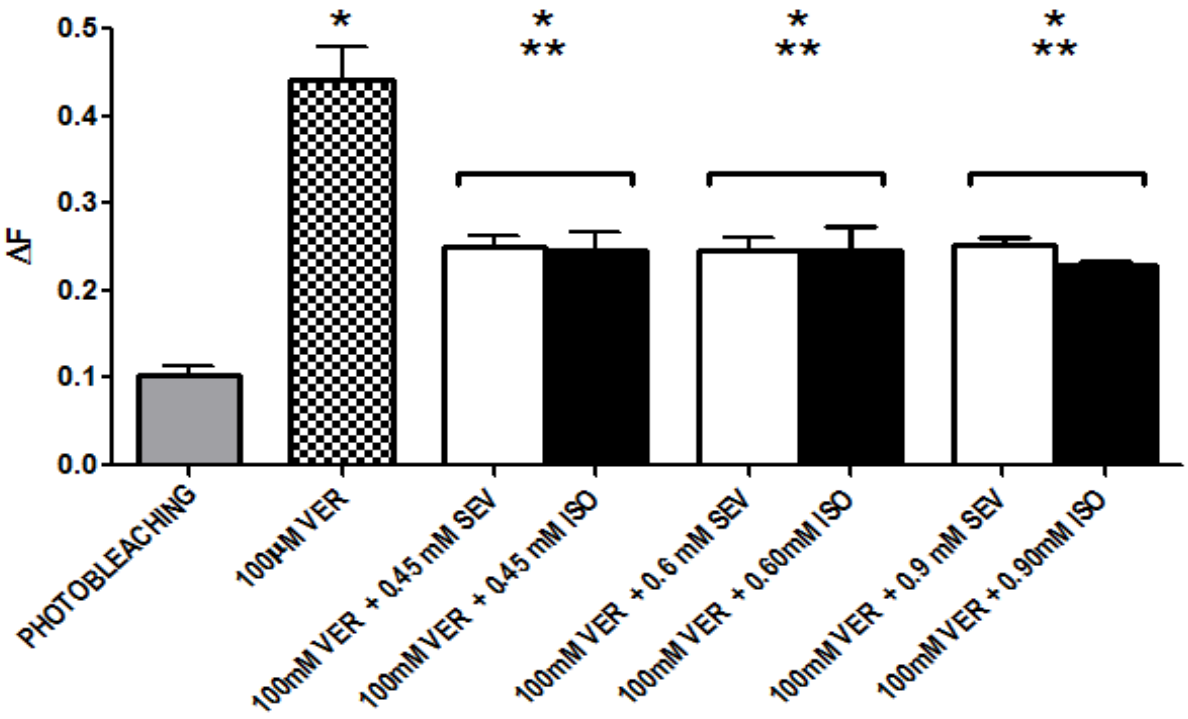

Figura 16: Sevoflurano e isoflurano inibem a exocitose de vesículas sinpaticas evocada por veratridina (100 µM) em JNMs de diafragma. Quantificação do sinal fluorescente após fotodesmarcação (primeira barra), evocada por veratridina 100µM (segunda barra), veratridina 100µM + sevoflurano ou isoflurano 0,45mM (terceiras barras pareadas), veratridina 100µM + sevoflurano ou isoflurano 0,6mM (quartas barras pareadas), veratridina 100µM + sevoflurano ou isoflurano 0,9mM (quintas barras pareadas). ΔF, fluorescência normalizada (F-F0/100). Os resultados expressos são da média ±EPM. Os resultados expressos representam a média ±EPM de 150 pontos fluorescentes de 15 terminações nervosas de 15animais para fotodesmarcação, 100 pontos fluorescentes de 10 terminações nervosas de 10 animais para veratridina 100µM e 28 pontos fluorescentes de 4 terminações nervosas de 4 animais para cada uma das outras condições experimentais (veratridina 100µM + sevoflurano ou isoflurano 0,45, 0,6 e 0,9mM). *P<0,05 quando comparado à primeira barra (fotodesmarcação). ** P< 0,05 quando comparado à segunda barra (veratridina 100µM).

A exocitose evocada pela veratridina é praticamente abolida (~80%) pela tetrodotoxina (TTX) na concentração de 1 µM (P = 0.0027 quando comparado com veratridina 100 µM; N=3 animais, 21 pontos fluorescentes analisados) e em aproximadamente 45% por TTX 0,5 µM (FIGURA 17) (P = 0,00236 quando comparado com a veratridina 100 µM; N=3 animais, 21 pontos fluorescentes analisados). Os resultados mostrados anteriormente nos levaram a perguntar se sevoflurano/isoflurano e TTX poderiam exercer um efeito aditivo em inibir a exocitose evocada pela veratridina. Como a TTX 1 µM quase aboliu completamente o estímulo da veratridina, para responder a esta pergunta nós utilizamos a concentração de 0,5 µM de TTX (FIGURA 18). Nossos resultados mostraram que incubação simultânea de terminações nervosas com TTX 0,5 µM e sevoflurano ou isoflurano 0,45 mM produziram um efeito sinérgico aditivo em inibir a exocitose de vesiculas induzida pela veratridina (~15% de redução do sinal fluorescente) quando comparado com sevoflurano ou isoflurano 0,45 mM sozinhos (~25% de redução do sinal fluorescente) (P = 0,022; N=4 animais, 28 pontos fluorescentes analisados, para cada condição experimental) ou com TTX 0,5 µM sozinha (~25% de redução do sinal fluorescente) (P = 0,0432; N=4 animais, 28 pontos fluorescentes analisados) (FIGURA 17).

Desta maneira, em conjunto, nossos dados mostram que sevoflurano e isoflurano reduzem a exocitose de vesículas sinápticas através de um bloqueio nos canais para Na^+ sensíveis a TTX na JNM de diafragma de camundongos e oferecem novas informações acerca dos mecanismos de ação do sevoflurano neste sistema.

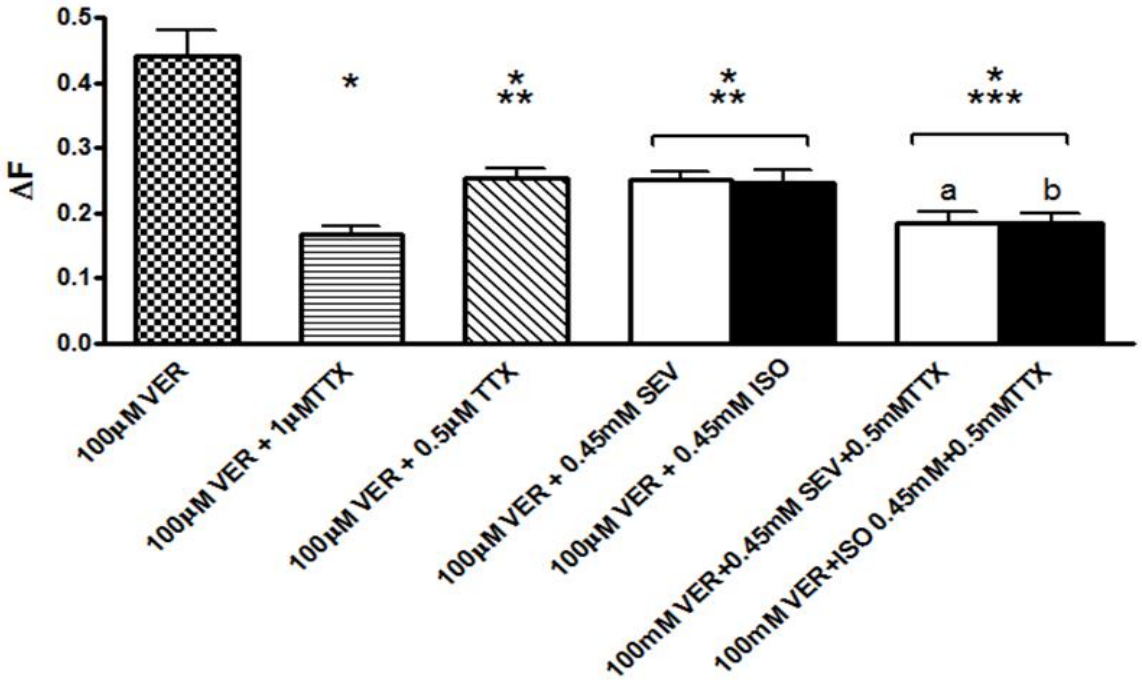

Figure 17. Os anestésicos isoflurano e sevoflurano inibem com a exocitose de vesículas sinápticas induzida por veratrina (100 µM) em JNMs de diafragma de camundongo. (A) Quantificação do sinal fluorescente após incubação com veratridina 100µM (primeira barra), veratridina 100µM + TTX (1 µM) (segunda barra), veratridina 100µM + TTX (0,5 µM) (terceira bar), veratridina 100µM + 0,45mM sevoflurano ou isoflurano (quartas barras pareadas) e veratridina 100µM + 0,45 mM isoflurano ou isoflurano + TTX 0,5 µM (quintas barras pareadas). ΔF, fluorescência normalizada (F-F0/100). Os resultados expressos são da média ±EPM de 100 pontos fluorescentes de 10 terminais nervosos de 10 animais (veratridina 100 µM) e 28 pontos fluorescentes de 4 terminais nervosos de 4 animais pra cada uma das outras condições experimentais (veratridina 100 µM + TTX 1 µM; veratridina 100 µM + 0,5 µM TTX; veratridina 100 µM + sevoflurano ou isoflurano 0,45mM e veratridina 100 µM +sevoflurano ou isoflurano 0,45mM + TTX 0,5 µM). *P<0,05 comparado a primeira barra (veratridina 100uM). ** P< 0,05 comparado à segunda barra (veratridina 100µM+ TTX 1 µM). *** P<0,05 comparado a terceira barra (TTX 0,5 µM) a,b P<0,05 quando comparado respectivamente a veratridina 100 µM + sevoflurano 0,45mM e veratridina 100 µM + isoflurano 0,45mM.

5. DISCUSSÃO

Os anestésicos gerais agem no sistema nervoso central e periférico, levando à ausência de consciência e da resposta à dor, além de promover a imobilização do paciente, necessário nos procedimentos cirúrgicos, através de um relaxamento muscular (JONES, 1999). Os anestésicos voláteis são administrados pela via inalatória e são eliminados principalmente pelos pulmões (TREVOR & WHITE, 2004). Além disso, alguns destes agentes, como o sevoflurano e isoflurano, são rapidamente eliminados do organismo permitindo uma rápida recuperação anestésica, o que reduz a ação de metabólitos tóxicos em outros órgãos, como fígado e rins (MUIR et al, 2007).

Diversos estudos têm sido publicados anualmente tentando esclarecer os mecanismos celulares e moleculares envolvidos na ação dos anestésicos inalatórios. Isso é de extrema importância, uma vez que cerca de 13,5% da população é submetido a algum tipo de anestesia a cada ano (CLERGUE *et al*., 1998). Sabe-se que esses agentes atuam primariamente em sinapses e parece não afetar a condução axonal (GRIFFTHS & NORMAN, 1993). Classicamente, a ação destas drogas envolve a potencialização da neurotransmissão inibitória, marcadamente as sinapses GABAérgicas no sistema nervoso central, e depressão da neurotransmissão excitatória seja ela central ou periférica (HEMMINGS, 2009).

Os anestésicos inalatórios sevoflurano e isoflurano apresentam diversas propriedades que os fazem como drogas de escolhas em procedimentos clínicos necessários. Atualmente, o sevoflurano é o anestésico inalatório mais utilizado em seres humanos enquanto que o isoflurano é o fármaco de escolha para procedimentos anestésicos envolvendo animais tanto em laboratórios de pesquisa quanto em clínicas veterinárias (CESAROVI *et al.* 2010)

Contudo, como qualquer anestésico moderno, estes agentes também produzem alguns efeitos colaterais considerados mínimos quando comparados com outros anestésicos. Adicionalmente, sevoflurano e isoflurano apresentam uma propriedade extremamente desejável para a anestesia: o relaxamento muscular (SUZUKI *et.al.*, 1996). Os anestésicos inalatórios sevoflurano, isoflurano, enflurano e desflurano produzem um relaxamento muscular esquelético considerado duas vezes maior do que o halotano. (WENKER, 1998). Muitos estudos mostram como estas drogas agem no sistema nervoso central, porém ainda não está bem estabelecido o efeito destes agentes anestésicos no sistema nervoso periférico, em especial, na JNM. Encontrar a resposta

para esta pergunta poderia nos oferecer mais informações sobre como estas drogas causam o relaxamento muscular observado durante a anestesia. Seria este apenas um efeito central ou poderia haver também alguma atuação marcadamente periférica?

Os efeitos inibitórios dos anestésicos voláteis na comunicação neuromuscular têm sido demonstrados em estudos *in vitro* (KENNEDY & GALINDO, 1975; BHATTACHARYYA *et.al.,* 1994) e *in vivo* (SUZUKI, 1996). SUZUKI e colaboradores (1999) mostraram que o sevoflurano deprime potencias de ação compostos em músculos e causa uma diminuição na amplitude dos mesmos sob estimulação repetitiva. Além disso, todos os anestésicos voláteis, incluindo sevoflurano e isoflurano, potencializam o efeito de agentes bloqueadores não despolarizantes que impedem a comunicação neuromuscular (SUZUKI *et al*., 1999; MOTAMED & DONATI, 2002). Além disso, VIOLET *et al* (1997) demonstraram que estes anestésicos por si só são também capazes de bloquear receptores nicotínicos musculares e neuronais.

Todos estes efeitos mencionados anteriormente vêm a sugerir que os anestésicos voláteis interferem de alguma maneira com a comunicação na JNM, podendo exercer tanto efeitos pré como pós-sinápticos. Alguns estudos têm tido foco nos efeitos dos anestésicos voláteis sob os componentes pós-sinápticos envolvidos com a comunicação neuromuscular (PAUL *et al*., 2002; SUZUKI *et al*., 2009). Contudo, os componentes pré-sinápticos que poderiam ser alvo dos anestésicos voláteis para causar o relaxamento muscular ainda são pouco investigados. Sendo assim, neste trabalho investigamos os efeitos dos anestésicos inalatórios sevoflurano e isoflurano sob a exocitose espontânea e evocada de vesículas sinápticas marcadas com a sonda fluorescente FM1-43 na JNM de diafragma de camundongos.

Estudos prévios já mostraram que os anestésicos isoflurano e halotano aumentam a liberação basal de dopamina em corpo estriado de ratos (KEITA *et al*., 1999). Além disso, apesar de SILVA e colaboradores (2007) terem demonstrado que o sevoflurano na concentração de 0,46mM aumenta significativamente a liberação de dopamina, esta ocorria por um mecanismo não-vesicular, sendo assim independente do ciclo de vesículas sinápticas. Estudos executados por SCHICHINO *et al* (1998) mostram que anestésicos voláteis como isoflurano e sevoflurano inibem a liberação de ACh de maneira dose-dependente em fatias corticais de rato não-estimuladas. NARUO e colaboradores (2005) sugerem que quando neurônios de gânglio de caramujos são isolados e incubados com concentrações clínicas de sevoflurano na presença de FM1-43

e na ausência de estimulação, nenhum efeito no ciclo de vesículas sinápticas é observado. Em nosso modelo, também um sistema colinérgico, nós investigamos se sevoflurano e isoflurano seriam capazes de evocar a exocitose de vesículas sinápticas em uma preparação não-estimulada.

Quando as preparações neuromusculares contendo as vesículas sinápticas marcadas com FM1-43 foram incubadas com diferentes concentrações de sevoflurano ou isoflurano (0,45, 0,6 e 0,9mM), nós não observamos decaimento significativo na fluorescência do FM1-43 quando comparado com preparações não tratadas com os anestésicos. Este resultado sugere, portanto, que sevoflurano e isoflurano não são capazes de estimular a exocitose de vesículas sinápticas na JNM de camundongos. (FIGURAS 7 e 8).

Já é documentado que anestésicos voláteis halogenados como sevoflurano e isoflurano causam relaxamento muscular esquelético durante cirurgias nas quais esses agentes são empregados (WAUD e WAUD, 1975 a e b; GHATGE *et al.*, 2003). Este efeito poderia ocorrer devido a um efeito inibitório sobre a exocitose evocada de vesículas sinápticas. Apesar de alguns trabalhos mostrarem que anestésicos voláteis podem inibir canais para Na^+ e canais para Ca^{2+} dos tipos P e Q, sejam eles somáticos ou heterologamente expressos (KAMATCHI, 1999), nesse trabalho nós observamos que sevoflurano e isoflurano não foram capazes de inibir a exocitose evocada por solução de KCl 60mM, um estímulo despolarizante independente de Na^+ que atua diretamente nos canais para Ca^{2+} dependentes de voltagem, levando a abertura dos mesmos (NICHOLLS, 1993).

Corroborando este achado, WESTPHALEN e colaboradores (2013) sugerem que o isoflurano inibe de uma maneira bem mais pronunciada a liberação de neurotransmissores evocada por 4AP do que a evocada por KCl. HEMMINGS *et al*. (2005) também demonstraram em modelo de neurônios hipocampais que, apesar de ter sido observada uma inibição da exocitose de vesículas sinápticas evocada por estímulo elétrico, este anestésico não inibe a exocitose de vesículas induzida por KCl. Esses dados, em conjunto com os que foram apresentados nesse trabalho sugerem que tanto no SNC quanto na periferia, o sítio pré-sináptico de ação dos anestésicos voláteis sevoflurano e isoflurano deve estar localizado numa etapa anterior ao influxo de Ca^{2+} para o terminal neuronal.

Diversas evidências sugerem um papel importante desempenhado pelos anestésicos inalatórios como bloqueadores de canais para Na^+ gerando, desta forma, um

bloqueio na comunicação celular (RATNAKUMARI & HEMMINGS, 1998; LINGAMANENI *et al*., 2001; OUYANG *et al*., 2003; WESTPHALEN *et al*., 2003; WU *et al*., 2004, HEROLD & HEMMINGS, 2012). Com o objetivo de investigar e adquirir novas informações acerca das ações pré-sinápticas de sevoflurano e isoflurano na JNM, nós testamos se estes agentes anestésicos seriam capazes de abolir ou inibir a exocitose de vesículas sinápticas evocada por estímulos despolarizantes dependentes de Na^+, como 4AP e veratridina.

Preparações nervo-músculo estimuladas por 4AP, um estímulo despolarizante que mimetiza um potencial de ação capaz de induzir a liberação de neurotransmissores através da ativação de canais para Na^+ e Ca^+ respectivamente, exibiram um decaimento considerável na fluorescência do marcador FM1-43. Este efeito observado foi significativamente inibido quando as preparações foram pré-incubadas e continuamente perfundidas com sevoflurano ou isoflurano (FIGURAS 11 e 12). WESTPHALEN e equipe (2013) também demonstraram que o volátil isoflurano inibe a liberação de vários neurotransmissores no sistema nervoso central, como dopamina, GABA, glutamato, norepinefrina e ACh, quando evocada por 4AP. Além disso, LEITE *et al* (2010) mostrou que altas concentrações de propofol, um agente anestésico intravenoso, inibem a exocitose de vesículas sinápticas evocada por 4AP na JNM de rãs. Evidências eletrofisiológicas também oferecem evidências de que isoflurano e outros anestésicos inalatórios inibem as correntes de Na^+ e a amplitude dos potencias de ação em terminais nervosos isolados da neurohipófise, via bloqueio dos canais pra Na+ desta preparação (OUYANG *et al*., 2003; OUYANG & HEMMINGS, 2005).

É importante destacar que OUYANG e colaboradores (2009) mostraram que tanto isoflurano quanto sevoflurano inibem de forma similar os canais para Na^+ dependentes de voltagem por diferentes mecanismos. Contudo, em nosso modelo nós demonstramos que isoflurano inibe a exocitose evocada por 4AP de forma significativamente menos eficiente quando comparado com sevoflurano, como mostrado nas FIGURAS 11 e 12. Diferenças em potência de efeito entre os diferentes anestésicos inalatórios já é observada e, ao mesmo tempo, controversa. PARK e colaboradores (1997), por exemplo, mostraram que tanto isoflurano quanto halotano são equipotentes em causar relaxamento muscular em um modelo de brônquio de rato contraído. Por outro lado, quando preparações de nervo ciático e músculo gastrocnêmico de gatos foram incubados com isoflurano, halotano ou sevoflurano, só foi observado efeito neuromuscular inibitório na presença de sevoflurano (SUZUKI,

1996). Além disso, WULF (1998) demonstrou que a potenciação dos efeitos neuromusculares inibitórios do bloqueador neuromuscular cisatracúrio é mais eficiente em procedimentos anestésicos com sevoflurano do que com isoflurano. Estas diferenças podem ocorrer devido a diferenças físico-químicas entre os diferentes anestésicos voláteis (STRUM *et al.*, 1987; YASUDA *et al*., 1989). Também não podemos excluir diferentes interações destes anestésicos com outros componentes celulares como PKC, cAMP etc. o que poderia gerar diferentes potências inibitórias. Contudo, o mecanismo preciso que poderia explicar estas diferenças continua obscuro e necessita de mais investigação.

O papel dos canais para Na^+ como possível alvo para os efeitos inibitórios dos anestésicos inalatório sevoflurano e isoflurano na JNM foi mais profundamente analisado por nosso grupo. Para isso, testamos qual seria o efeito destes anestésicos sobre a exocitose de vesículas sinápticas evocada pela veratridina. Esta toxina ativa diretamente os canais para Na^+ e impedem a inativação dos mesmos (NICHOLLS, 1993). Sevoflurano e isoflurano inibiram de maneira similar a exocitose de vesículas sinapticas evocada pela veratridina. (FIGURAS 13A e 14A). Este resultado vai ao encontro com muitos outros achados da literatura em que o efeito de diversos anestésicos sob os canais para Na^+ foram investigados. RATNAKUMARI & HEMMINGS (1997) observaram que o anestésico intravenoso propofol inibe de maneira dose-dependente a liberação de glutamato a partir de sinaptosomas de ratos. RATNAKUMARI & HEMMINGS (1998) e LINGAMANENI *et al*. (2001) também demonstraram que os anestésicos inalatório halotano e isoflurano também causam uma redução de aproximadamente 50% da liberação de glutamato evocada pela veratridina. Em adição, HARRIS & BRUNO (1985) sugeriram que o éter, halotano, enflurano e até mesmo o álcool apresentam efeito inibitório sobre os canais para Na^+.

Muitos estudos prévios já foram realizados investigando o efeito intrínseco da veratridina sobre os canais para Na^+ e os resultados encontrados sugerem fortemente que esta toxina prolonga a atividade destes canais e seu efeito é inibido pela toxina TTX (revisado por CATTERAL *et.al*., 2005). Todas as isoformas conhecidas de canais para Na^+ voltagem-dependentes (Na_v) podem ser bloqueadas com alta especificidade e potência pela TTX, porém algumas isoformas, conhecidas como tetrodotoxina-resistentes, são menos responsivas aos efeitos dessa toxina quando comparadas com as outras isoformas (GOLDIN, 2001).

Em nosso modelo, a concentração de 0,5 µM de TTX inibiu significativamente a exocitose evocada pela veratridina a 100 µM. Sevoflurano e isoflurano acentuaram de forma significativa o efeito da TTX, fazendo com que a exocitose fosse menor quando as preparações eram expostas a veratridina 100 µM. Isto sugere a possibilidade de um sinergismo farmacológico entre dois antagonistas moduladores dos canais para Na^+ (sevoflurano/isoflurano e TTX) diminuindo, assim, o efeito despolarizante da veratridina e, com isso, a exocitose de vesículas sinápticas (FIGURAS 17 e 18). Corroborando nossos achados, ZHANG *et.al*., (2010) mostraram que, ao realizar infusão intratecal de TTX em camundongos, a potência do anestésico isoflurano era aumentada consideravelmente. Esta interação entre drogas é consistente com a especificidade farmacológica da TTX para os canais para Na^+ e reforça a hipótese de que estes canais como tendo um papel importante produzido pelos anestésicos inalatórios (HEMMINGS, 2009)

Em um estudo utilizando registros eletromiográficos com estimulação trem-de quatro (do inglês, *train-of-four*, TOF) realizado por NITAHARA e colaboradores (2007), foi mostrado que pacientes miastênicos e normais apresentavam uma grande depressão das funções neuromusculares quando eram submetidos à anestesia com sevoflurano. Porém, este efeito inibitório do sevoflurano era mais proeminente em pacientes miastênicos. Logo após o término da administração da droga, os registros voltavam aos seus valores normais, indicando, portanto, um restabelecimento das atividades neuromusculares para os níveis considerados normais. Baseado neste resultado e em nossos outros achados, nós sugerimos que o efeito pré-sináptico destes anestésicos inalatórios contribui de forma importante para o relaxamento muscular observado em procedimentos clínicos em que a utilização destas drogas é necessária. Sendo assim, este estudo sugere que um bloqueio dos canais para Na^+ efetuado pela anestesia com sevoflurano e isoflurano, pode contribuir para o relaxamento muscular

Em conjunto, o corpo de nossos dados sugere que sevoflurano e isoflurano inibem a exocitose de vesículas sinápticas por atuarem de forma direta em canais para Na^+, efetuando o bloqueio dos mesmos, sem qualquer efeito direto nos canais para Ca^{2+}. Este trabalho oferece novas informações na compreensão de como estes anestésicos causam o relaxamento observado durante sua administração em procedimentos cirúrgicos.

6. CONCLUSÃO

Em resumo, através da utilização de técnicas de microscopia óptica de fluorescência, este trabalho demonstrou que os anestésicos halogenados, sevoflurano e isoflurano não se apresentam com potencial de evocar a exocitose de vesículas sinápticas. Em adição, estes agentes não afetaram a exocitose evocada por KCl 60mM, estímulo independente de íons Na^+. Contudo, concentrações clínicas destes anestésicos inibem consideravelmente a exocitose evocada por estímulos dependentes de íons Na^+, como veratridina e 4AP, sendo este efeito mais pronunciado quando as preparações foram pré-incubadas e continuamente perfundidas com sevoflurano. Estes dados indicam que tanto sevoflurano quanto isoflurano interferem com a liberação de neurotransmissores por atuar em passos anteriores ao influxo de Ca^{2+} para o terminal neuronal, provavelmente por atuar nos canais para Na^+ dependentes de voltagem. Desta maneira, este trabalho oferece novos dados acerca dos mecanismos pelos quais estes anestésicos causam os efeitos neuromusculares observados durante a anestesia geral.

7. REFERÊNCIAS

ALABI, A.A., TSIEN, R.W. Synaptic vesicle and dynamics. **Cold Spring Harb Perspect Biol**. 4(8), 1-18. 2012.

BARNES, S., HILLE, B.. Veratridine modifies open sodium channels. **J Gen Physiol**. 91, 421-443, 1988

BETZ, W. J., MAO, F., BEWICK, G. S. Activity dependent fluorescent staining and destaining of living vertebrate motor nerve terminals. **J Neurosci**. 12, 363-375, 1992

BETZ, W.J, BEWICK, G.S. Optical monitoring of transmitter release and synaptic vesicle recycling at the frog neuromuscular junction. **J Physiol**. 460, 287-309, 1993.

BHATTACHARYYA, B.J, TSEN, K., SOKOLL, M.D. Age-induced alteration of neuromuscular transmission: effect of halothane. **Eur J Pharmacol**. 254 (1-2), 97-104, 1994

CATTERALL, W.A., GOLDIN, A.L., WAXMAN, S.G. **International Union of Pharmacology**. XLVII. Nomenclature and structure-function relationships of voltage-gated sodium channels. 57, 397-409, 2005.

CECCARELLI, B.; HULBURT, W. P.; MAURO, A. Turnover of transmitter and **Cell Biology,** 133,1237-1250, 1996.

CESAROVIC, N., NICHOLLS, F., RETTICH, A., KRONEN, P., HÄSSIG, M., JIRKOF, P., ARRAS, M. Isoflurane and sevoflurane provide equally effective anaesthesia in laboratory mice**. Lab Anim.** 44, 329-336, 2010.

CHAPMAN, E. R. How does synaptotagmin trigger neurotransmitter release? Annual CHT1**. Journal of Neurochemistry**. 97,1-12, 2006

CLERGUE, F.; AUROY, Y.; PEQUIGNOT, F.; JOUGLA, E.; LIENHART, A.;LAXENAIRE, M. C. French survey of anesthesia in 1996. **Anesthesiology** 91, 1509–1520, 1999.

COUSIN, M. A.; ROBINSON, P. J. Mechanisms of Synaptic Vesicle Recycling Illuminated by Fluorescent Dyes. **Journal of Neurochemistry**, v.73, n.6, p.2227-39, 1999

DINIZ, P. H. ; SILVA, J.H.; GOMEZ, R.S, GUATIMOSIM, C ; GOMEZ, M.V. . Halothane Increases Non-vesicular [(3)H]dopamine Release from Brain Cortical Slices. **Cellular and Molecular Neurobiology**, 27, 757-770, 2007.

DINIZ, P.H ; GUATIMOSIM, C. ; BINDA, N. S. ; COSTA, F. ; GOMEZ, M. V. ; GOMEZ, M. V. ; GOMEZ RS . The Effects of Volatile Anesthetics on the Extracellular Accumulation of [3H]GABA in Rat Brain Cortical Slices.. **Cellular and Molecular Neurobiology** 44,188-195, 2013.

ENOMOTO, K., MAENO, T. Presynaptic effects of 4-aminopyridine and streptomycin on the neuromuscular junction. **Eur J Pharmacol**. 19; 76, 1-8, 1981.

GAFFIELD M.A., BETZ W.J. Imaging synaptic vesicle exocytosis and endocytosis with FM dyes. **Nat Protoc**; 1, 2916−21, 2006.

FRANKS, N.P. Molecular targets underlying general anaesthesia. **Br J Pharmacol**. 147, 1, 72-81, 2006.

GARNER, C. C.; KINDLER, S.; GUNDELFINGER, E. D. Molecular determinants of presynaptic active zones. **Current Opinion in Neurobiology**, v. 10, p. 321-327, 2000.

GHATGE, S., LEE, J., SMITH, I. Sevoflurane: an ideal agent for adult day-case anesthesia? **Acta Anaesthesiol Scand**. 47, 917-931, 2003.

GOLDIN, A.L. Resurgence of sodium channel research. **Annu Rev Physiol**. 63, 871-894, 2001

GRIFFITHS R., NORMAN R.I. Effects of anaesthetics on uptake, synthesis and release of transmitters. **Br. J. Anaesth**. 71:96–107, 1993.

HALL, Z. W. An Introduction to Molecular Neurobiology. **Sunderland, MA: Sinauer**, 1992.

HALL, Z. W.; SANES, J. R. Synaptic structure and development: the neuromuscular junction. **Cell.** 72, 99-121,1993.

HAITAO, WU., XIONG, W.C., MEI, L. To build a synapse: signaling pathways in neuromuscular junction assembly. **Development**. 137(7), 1017-1033, 2010.

HARRIS, R.A., BRUNO, P. Effects of ethanol and other intoxicant-anesthetics on voltage-dependent sodium channels of brain synaptosomes. **J Pharmacol Exp Ther**. 232, 401-406, 1985.

HEDENSTIERNA, G., EDMARK, L. The effects of anesthesia and muscle paralysis on the respiratory system. **Intensive Care Med**. 31, 1327-1335, 2005.

HEMMINGS, H.C. JR., AKABAS, M.H., GOLDSTEIN, P.A., TRUDELL, J.R., ORSER, B.A., HARRISON, N.L. Emerging molecular mechanisms of general anesthetic action. **Trends Pharmacol Sci**. 26, 503-510, 2005.

HEMMINGS, H.C.JR., YAN, W., WESTPHALEN, R.I., RYAN, T.A. The general anesthetic isoflurane depresses synaptic vesicle exocytosis. **Mol Pharmacol**. 67, 1591-1599, 2005.

HEMMINGS, H. C. JR. Sodium channels and the synaptic mechanisms of inhaled anaesthetics. **Br J Anaesth**. 103, 61-69, 2009.

HEROLD, K.H., HEMMINGS, H.C.JR. Sodium channels as targets for volatile anesthetics. **Front Pharmacol**. 30, 3:50, 2012.

HEUSER, J.E., REESE, T.S., Evidence for recycling of synaptic vesicle membrane during transmitter release at the frog neuromuscular junction. J Cell Biol. 57(2), 315-344. 1973.

HOFMEISTER E.H, BRAINARD B.M, SAMS L.M, ALLMAN D.A, CRUSE A.M. Evaluation of induction characteristics and hypnotic potency of isoflurane and sevoflurane in healthy dogs. **Am J Vet Res**. 69:451-456, 2008.

HORMUZDI, S.G., FILIPOVV, M.A., MITROPOULOU, G., MONYER, H., BRUZZONE, R. Electrical synapses: a dynamic signaling system that shapes the activity of neuronal networks. **Biochim Biophys Acta.** 1662(1-2): 113-137.

JACOB, A.K.; KOPP, S.L.; BACON, D.R.; SMITH, H.M. The History of Anesthesia. In: BARASH, P.G.; CULLEN, B.F.; STOELTING, R.K.; CAHALAN, M.K.; STOCK, M.C. **Clinical Anesthesia**. 6.ed. Phliadelphia: Lippincott Williams & Wilkins, 2009. 1640p. cap.1, p.3-26.

JONES, R.M. Desflurane and sevoflurane: Inhalation anesthetics for this decade? **Br J Anaesth.** 65:527–536, 1990

JONES, R.S. The practice of veterinary anaesthesia and analgesia. In C. Seymour and R. Gleed (Eds). *Manual of small animal anaesthesia and analgesia*. United Kingdom: BSAVA. 1999

KAMATCHI, G.L., CHAN, C.K., SNUTCH, T., DURIEUX, M.E., LYNCH, C. Volatile anesthetic inhibition of neuronal Ca channel currents expressed in Xenopus oocytes. **Brain Res.** 831, 85-96, 1999.

KATZ, B.; , MILEDI, R. The effect of calcium on acetylcholine release from motor nerve terminals. **Proc R Soc Lond B Biol Sci.** 161, 496-503, 1965.

KEITA, H., HENZEL-ROUELLÉ, D., DUPONT, H., DESMONTS, J.M., MANTZ, J. Halothane and isoflurane increase spontaneous but reduce the N-methyl-D-aspartate-evoked dopamine release in rat striatal slices: evidence for direct presynaptic effects. **Anesthesiology.** 91, 1788-1797, 1999.

KENNEDY, R., GALINDO, A. Neuromuscular transmission in a mammalian preparation during exposure to enflurane**. Anesthesiology**. 42, 432-442, 1975.

KUMMER, T. T.; MISGELD, T.; SANES, J. R. Assembly of the Postsynaptic Membrane at the Neuromuscular Junction: Paradigm Lost. ***Current Opinion in Neurobiology***. v.16, n.1, p.74-82, 2006.

LEITE, L.F., GOMEZ, R.S., FONSECA, M.C., GOMEZ, M.V., GUATIMOSIM, C. Effect of intravenous anesthetic propofol on synaptic vesicle exocytosis at the frog neuromusuclar junction. **Acta Pharmacol Sin**. 32, 31-37, 2010.

LI, C., YAO, S., NIE, H., LÜ, B. Effects of isoflurane on the action of neuromuscular blockers on the muscle acetylcholine receptors. **J Huazhong Univ Sci Technolog Med Sci**. 24, 605-614, 2004.

LI,C., CHIN, L.S. The molecular machinery of synaptic vesicles exocytosis. **Cell Mol Life Sci.** 60(5), 942-950, 2003.

LICHTMAN, J. W.; WILKINSON, R. S.; RICH, M. M. Multiple innervation of tonic endplates revelead by activity-dependent uptake of fluorescent probes. **Nature** 314, 357-9, 1985.

LINGAMANENI, R., BIRCH, M.L., HEMMINGS, H.C.JR. Widespread inhibition of sodium channel-dependent glutamate release from isolated nerve terminals by isoflurane and propofol. **Anesthesiology.** 95, 1460-1466, 2001.

MATTHEWS N.S, HARTSFIELD S.M, MERCER D, BELEAU M.H AND MACKENTHUN A. Recovery from sevoflurane anesthesia in horses: comparison to isoflurane and effect of post medication with xylazine. **Veterinary Surgery** 27:480-485. 1998.

MERRETT K.L, JONES R.M. Inhalational anaesthetic agents. **Br J Hosp Med**. 52:260–263, 1994.

MILLER, M.S., GANDOLFI, A.J. A rapid, sensitive method for quantifying enflurane in whole blood. **Anesthesiology** 51, 542-544,1979.

MOTAMED, C., DONATI, F. Sevoflurane and isoflurane, but not propofol, decrease mivacurium requirements over time. **Can J Anaesth**. 49, 907-912, 2002.

MUIR, W. W., HUBBELL, J. A. E., SKARDA, R. T., Bednarski, R. M. *Handbook of veterinary anesthesia* (4th ed.). 2000

MURTHY, V. N.; DE CAMILLI, P. Cell Biology of the Presynaptic Terminal, **Annual Review of Neuroscience**. 26, 701–28, 2003.

NARUO, H., ONIZUKA, S., PRINCE, D., TAKASAKI, M., SYED, N.I. Sevoflurane blocks cholinergic synaptic transmission postsynaptically but does not affect short-term potentiation. **Anesthesiology.** 102, 920-928, 2005.

NICHOLLS, D.G. The glutamatergic nerve terminal. **Eur J Biochem**. 212, 613-631, 1993.

NITAHARA, K., SUGI, Y., HIGA, K., SHONO, S., HAMADA, T. Neuromuscular effects of sevoflurane in myasthenia gravis patients. **Br J Anaesth**. 98, 337-341, 2007.

NITAHARA, K., SUGI, Y., KUSUMOTO, G., SHONO, S., IWASHITA, K., HIGA, K. Neuromuscular blockade by vencuronium during induction with 5% sevoflurane or propofol. **J Int Med Res**. 38, 1997-2003, 2010.

OUYANG, W., WANG, G., HEMMINGS, H.C.JR. Isoflurane and propofol inhibit presynaptic Na^+ channels in isolated rat neurohypophysial nerve terminals. **Mol Pharmacol**. 64, 373-381, 2003.

OUYANG, W., HEMMINGS, H.C.JR. Depression by isoflurane of the actionpotential and underlying voltage-gated ion currents in isolated rat neurohypophysial nerve terminals. **J Pharmacol Exp Ther**. 312, 801-808, 2005.

OUYANG, W., HEROLD, K.F., HEMMINGS, H.C.JR. Comparative effects of halogenated inhaled anesthetics on voltage-gated Na^+ channel function. **Anesthesiology.** 110, 582-590, 2009.

PARK, K.W., DAI, H.B., LOWESTEIN, E., KOCHER, O.N., SELKE, F.W. Isoflurane-and-halothane mediated dilation of distal bronchi in the rat depends on the epithelium. **Anesthesiology.** 86: 1078-1087, 1997.

PEROUANSKY, M. General anesthetics and long-term neurotoxicity. **Handb Exp Pharmacol**. 182, 209-223, 2008.

PASHKOV, V.N., HEMMINGS, H.C. JR. The effects of general anesthetics on norepinephrine release from isolated rat cortical nerve terminals. **Anesth Analg.** 95, 1274-1281, 2002.

PAUL, M., FOKT, R.M., KINDLER, C.H., DIPP, N.C., YOST, C.S. Characterization of the interactions between volatile anesthetics and neuromuscular blockers at the muscle nicotinic acetylcholine receptor. **Anesth Analg**. 95, 362-367, 2002.

RATNAKUMARI, L., HEMMINGS, H.C.JR. Effects of propofol on sodium channel-dependent sodium influx and glutamate release in rat cerebrocortical synaptosomes. **Anesthesiology.** 86, 428-439, 1997.

RATNAKUMARI, L., HEMMINGS, H.C. JR. Inhibition of presynaptic sodium channels by halothane. **Anesthesiology** 88,1043–1054, 1998.

RIBCHESTER, R.R.; MAO F.; BETZ, W. J. Optical measurements of activitydependent membrane recycling in motor nerve terminals of mammalian skeletal muscle. **Proceedings of the Royal Society B: Biological Sciences,** 255, (1342), 61-66,1994

RICHARDS, D. A.; GUATIMOSIM, C.; BETZ, W. J. Two Endocytic Recycling Routes Selectively Fill Two Vesicle Pools in Frog Motor Nerve Terminals. **Neuron.** 27,551-559, 2000.

RICHARDS, C.D. Anaesthetic modulation of synaptic transmission in the mammalian CNS. **Br. J. Anaesth**. 89, 79-90, 2002.

RIZZOLI, S.O., RICHARDS, D.A., BETZ, W.J. Monitoring synaptic vesicle recycling in frog motor nerve terminals with FM dyes. **J Neurocytol**. 32, 539-549, 2003.

RIZZOLI, S. O.; BETZ, W. J. Synaptic Vesicle Pools. ***Nature Reviews/Neuroscience*** 6, 57-69, 2005.

ROOS, J. & KELLY, R. B. The endocytic machinery in nerve terminals surrounds sites of exocytosis. **Curr. Biol**., 9,1411-1414, 1999.

ROYLE, S. G.; LAGNADO L. Endocytosis at the synaptic terminal. **The Journal of Physiology,** 553, (2), 345-355, 2003.

SCHERRINGTON, C.S. The integrative action of the nervous system. **Charles Scribner's sons.** Nova York, 1906.

SCHWEIZER, F. E.; RYAN, T. A. The Synaptic Vesicle: Cycle of Exocytosis and Endocytosis. **Current Opinion in Neurobiology.** 16, 298-304, 2006.

SHICHINO, T., MURAKAWA, M., ADACHI, T., ARAI, T., MIYAZAKI, Y., MORI, K. Effects of inhalation anaesthetics on the release of acetylcholine in the rat cerebral cortex in vivo. **Br J Anaesth**. 80, 365-370, 1998.

SILVA, J.H., GOMEZ, R.S., DINIZ, P.H., Gomez, M.V., Guatimosim, C. The effect of sevoflurane on the release of [3H] dopamine from rat brain cortical slices. **Brain Res Bull.** 30; 72, 309-314, 2008.

SOLT, K., FORMAN, S.A. Correlating the clinical actions and molecular mechanism of general anesthetics. **Curr Opin Anaesthesiol**. 20(4), 300-306, 2007.

SÖLLNER, T.; BENNETT, M. K.; WHITEHEART, S. W.; SCHELLER, R. H.; ROTHMAN, J. E. A protein assembly-disassembly pathway in vitro that may correspond to sequential steps of synaptic vesicle docking, activation, and fusion. ***Cell,*** 75,(3) 409-18, 1993.

STRUM, D.O., EGER, E.I. Partition coeficientes for sevoflurane in human blood, saline and olive oil. **Anesth Analg.** 66:654-656, 1987.

SÜDHOF, T. C. The Synaptic Vesicle Cycle. **Annual Review of Neuroscience**. 27, 509-547, 2004.

SÜDHOF, T.C. Neurotransmitter release: the last millisecond in the life of a synaptic vesicle. **Neuron**. 80(3):675-690, 2013.

SUZUKI, T., NAGAI, H., OGAWA, S., SUZUKI, H. Comparative neuromuscular inhibitory effects of volatile anesthetics. **Masui.** 45, 599-607, 1996.

SUZUKI, T., MUNAKATA, K., WATANABE, N., KATSUMATA, N., SAEKI, S., OGAWA, S. Augmentation of vencuronium-induced neuromuscular block during sevoflurane anaesthesia: comparison with balanced anaesthesia using propofol or midazolam. **Br J Anaesth.** 83, 485-487, 1999.

TAKEI, K.; MUNDIGL, O.; DANIELL, L.; DE CAMILLI, P. The synaptic vesicle cycle: a single vesicle budding step involving clathrin and dynamin. **The Journal of Cell Biology**.133,1237-1250, 1996.

TASSONYI, E., CHARPANTIER, E., MULLER, D., DUMONT, L., BERTRAND, D. The role of nicotinic acetylcholine receptors in the mechanisms of anesthesia. **Brain Res Bull**. 15; 57, 133-150, 2002.

TOPF, N., JENKINS, A., BARON, N., HARRISON, N.L. Effects of isoflurane on gamma-aminobutyric acid type A receptors activated by full and partials agonists. **Anesthesiology**. 98, 306-311, 2003

TORREJAIS, M.M.;, SOARES, J.C.; MATHEUS, S.M.; CASSEL, F.D.; MELLO, J.M.; BASSO, N.A . Histochemical and SEM evaluation of the neuromuscular junctions from alcoholic rats. **Tissue Cell.** 34(2) 117-123, 2002.

TORRI, G. Inhalation anesthetics: a review. **Minerva Anesthesiol**. 76(3), 215-228, 2010.

TREVOR, A.J., WHITE, P.F. General Anesthetics. In B.G. Katzung (Ed), **Basic & clinical pharmacology** (9th). (pp.401-417). 2004

VALADÃO, P.A., NAVES, L.A., GOMEZ, R.S., GUATIMOSIM, C. Etomidate evokes synaptic vesicle exocyosis without increasing miniature endplate potentials frequency at the mice neuromuscular junction. **Neurochemistry International**. 63(5), 576-582, 2013.

VANDAM, L.D. Concerning neurologic sequelae of spinal anesthesia. **Anesthesiology**. 100(1), 176-177, 2004.

VIOLET, J.M., DOWNIE, D.L., NAKISA, R.C., LIEB, W.R., FRANKS, N.P. Differential sensitivities of mammalian neuronal and muscle nicotinic acetylcholine receptors to general anesthetics. **Anesthesiology**. 86, 866-874, 1997.

WALLIN, R.F., REGAN, B.M., NAPOLI, M.D., Stern, I.J. Sevoflurane: a new inhalational anesthetic agent. **Anesth Analg**. 54(6), 758-766, 1975.

WAUD, B.E., WAUD, D.R. Comparison of the effects of general anesthetics on the end-plate of skeletal muscle. **Anesthesiology.** 43, 540-547, 1975a.

WAUD, B.E., WAUD, D.R. The effects of diethyl ether, enflurane and isoflurane at the neuromuscular junction. **Anestehsiology.** 42, 275-280, 1975b.

WENKER, O. Review of currently used inhalation anesthetics: part II. The internet **Journal of Anesthesiology**. Volume 3, Number 3, 1998.

WESTPHALEN, R.I., HEMMINGS, H.C.JR. Selective depression by general anesthetics of gluatamate vs. GABA release from isolated nerve terminals. **J Pharmacol Exp Therm.** 304, 1188-1196, 2003.

WESTPHALEN, R.I., DESAI, K.M., HEMMINGS, H.C. JR. Presynaptic inhibition of the release of multiple major central nervous system neurotransmitter types by the inhaled anaesthetic isoflurane. **Br J Anaesth**. 110, 592-599, 2013.

WU, X.S., SUN, J.Y., EVERS, A.S., CROWDER, M., WU, L.G. Isoflurane inhibits transmitter release and the presynaptic action potential. **Anesthesiology**. 100, 663-670, 2004.

WU Y., YEH F. L., MAO F., CHAPMAN E. R. Biophysical characterization of styryl dye-membrane interactions. **Biophysical Journal**, v. 97, n. 1, p. 101-109, 2009

WULF, H., KAHL, M., LEDOWSKI, T. Augmentation of the neuromuscular blocking effects of cisatracurium during desflurane, sevoflurane, isoflurane or i.v anaesthesia. **Br J of Anaesth.** 80(3): 308-312, 1998.

YASUDA, N., TARG, A.G., EGER, E.L. Solubility of I-653, sevoflurane, isoflurane and halothane in human tissues. **Anesth Analg**. 69:370-373, 1989.

ZHAI, R.G., BELLEN, H.J. The architecture of the active zone in the presynaptic nerve terminal. **Physiology (Bethesda)**. 19: 262-270,2004.

ZHANG, Y., GUZINSKI, M., EGER E.L.2ND., LASTER, M.J., SHARMA, M., HARRIS, R.A., HEMMINGS H.C.JR. Bidirectional modulation of isoflurane potency by intrathecal tetrodotoxin and veratridine in rats. **Br J Pharmacol**. 159, 872-878, 2010.

8. ANEXO 1: Artigo aceito para publicação, após revisão, referente à essa dissertação de mestrado

---

Comparison of the presynaptic effects of the volatile anesthetics sevoflurane and isoflurane at the mouse neuromuscular junction

Matheus de Castro Fonseca [a], Janice Henriques da Silva [a], Vany Perpetua Ferraz [b], Renato Santiago Gomez [c], Cristina Guatimosim [a *]

[a] Departamento de Morfologia, Instituto de Ciências Biológicas, Universidade Federal de Minas Gerais, MG, Brasil.

[b] Departamento de Química, Instituto de Ciências Exatas, Universidade Federal de Minas Gerais, MG, Brasil.

[c] Departamento de Cirurgia, Faculdade de Medicina, Universidade Federal de Minas Gerais, Belo Horizonte, MG, Brasil.

* **Corresponding author**:

Cristina Guatimosim

Associate Professor

Departamento de Morfologia, ICB

Universidade Federal de Minas Gerais

Av. Antônio Carlos, 6627

Belo Horizonte, MG

31270-901

Brazil

Email: cguati@icb.ufmg.br

Running title: Presynaptic effects of sevoflurane and isoflurane

Abbreviations

ACh, acetylcholine;

GABA, γ-amino butyric acid;

nAChR, nicotinic acetylcholine receptor;

NMJ, neuromuscular junction;

TTX, tetrodotoxin;

4AP, 4-aminopyridine

Comparative presynaptic effects of the volatile anesthetics sevoflurane and isoflurane at the mouse neuromuscular junction

Abstract

Introduction: Sevoflurane and isoflurane are anesthetics that cause muscle relaxation and potentiate the effect of neuromuscular blocking agents. Their presynaptic mechanisms of action are not clearly understood, especially at the motor nerve terminal level. **Methods:** We compared the presynaptic effects of these anesthetics on the exocytosis of synaptic vesicles labeled with the dye FM1-43 at the mouse neuromuscular junction. **Results:** Both anesthetics did not evoke spontaneous exocytosis of synaptic vesicles, but significantly inhibited the depolarization evoked by 4AP and veratridine, suggesting a putative action on sodium channels. Exocytosis evoked by veratridine was inhibited by tetrodotoxin alone or in conjunction with sevoflurane or isoflurane indicating that both agents may target in voltage-gated sodium channels. **Conclusion:** We suggest that sevoflurane and isoflurane inhibit exocytosis evoked by sodium-dependent depolarization and it might act on tetrodotoxin-sensitive sodium channels. These findings contribute to a better understanding of some clinical muscular effects induced by these anesthetics.

Keywords: Sevoflurane, Isoflurane, neuromuscular junction, FM1-43, synaptic vesicle, exocytosis.

1. Introduction

A great effort has been made during the last decades to understand the cellular and molecular mechanism underlying general anesthesia and how those anesthetics produce their related effects such as amnesia, hypnosis, unconsciousness and muscle relaxation [1-2]. Different molecular targets in several regions of the nervous system are involved in the multiple components of general anesthesia, and these targets can vary among the distinct anesthetics. In addition, the anesthetics affect both excitatory and inhibitory synaptic transmission in the nervous system[3]. Several experimental approaches support the action of general anesthetics at the synaptic level involving presynaptic and/or postsynaptic targets[2]. Nevertheless, the contributions of each of these targets have not been clearly defined yet. Since the 1980s, presynaptic ion channels have been considered as the most promising molecular target for general anesthetics[4], but further investigation is still remaining.

Sevoflurane and isoflurane are volatile anesthetics that present many properties that make them useful for induction and/or maintenance of general anesthesia with the ability to cause unconsciousness, analgesia and also muscle relaxation[1]. Although both drugs interact directly with nicotinic acetylcholine receptor (nAChR) and also potentiate the effect of nondepolarizing neuromuscular-blockade drugs, sevoflurane leads to more intense outcomes than other volatile anesthetics, such as halothane and isoflurane[5-6]

Because of the desirable muscle relaxation effect evoked by several anesthetics, one opened question is: how do volatile anesthetics interfere with neuromuscular transmission? For instance, Kennedy and Galindo (1975)[7] showed that enflurane is able to cause muscle relaxation, acting directly on the motor neuron endplate. Hedenstierna and Edmark (2005)[8] also showed the effects of general anesthesia and muscle paralysis

on the respiratory system. In addition, some works have already investigated the postsynaptic effects of inhalatory anesthetics. Violet et al. (1997)[9], for example, showed that muscle or neuronal nAChRs subtype are sensitive to general anesthetics, including sevoflurane, with different degrees of sensibility. Tassonyi et al. (2002)[10] showed that volatile anesthetics and ketamine are the most potent inhibitors of neuronal nAChRs subtype and also produce great inhibitory effect on the muscle subtype. However, the presynaptic mechanisms, more specifically, the basic steps for neurotransmission release involved in the effects caused by sevoflurane and isoflurane at neuromuscular junctions (NMJs) remain unclear.

In this work, we aimed to investigate the presynaptic effect of the volatile anesthetics sevoflurane and isoflurane at the NMJ level. By visualizing synaptic vesicles recycling with FM1-43, a powerful tool to study the synaptic vesicles cycle[11,12,13]. We provided direct evidences that sevoflurane and isoflurane have a presynaptic action at the mouse NMJ, by inhibiting voltage-gated sodium channels. Our study provides for the first time data that might help to explain some of the neuromuscular effects observed during the administration of volatile anesthetics.

2. Materials and Methods

2.1 Reagents

The fluorescent dye FM1-43 was purchased from Molecular Probes (Eugene, OR, USA); *d*-tubocurarine, 4-aminopyridine (4AP), veratridine, tetrodotoxin (TTX) and μ-conotoxin were purchased from Sigma-Aldrich (St.Louis, MO, USA). The inhalatory anesthetics were obtained from Instituto Biochimico Ind. Farm. Limitada (Itatiaia RJ,

Brazil). All other chemicals and reagents were of analytical grade. Experiments were performed in accordance with the local animal care committee (CETEA-UFMG). Efforts were made in order to minimize the suffering and number of animals used in this study.

2.2 Preparation of Anesthetic Solutions

For each experiment, the perfusion solution (134 mM NaCl, 5 mM KCl, 2 mM $CaCl_2$, 1 mM $MgCl_2$, 12 mM $NaHCO_3$, 1 mM NaH_2PO_4, 11 mM d-glucose) was saturated with sevoflurane or isoflurane and rotated for at least 6 hours at room temperature (23-25°C) in an airtight glass tube[14]. The saturated solution (13 – 16 mM for sevoflurane and 11 – 13 mM for isoflurane) was diluted with normal mouse Ringer in order to obtain the desired concentration of each anesthetic (0.45, 0.60 or 0.90 mM). The diluted anesthetic solution was introduced to the perfusion chamber through polyethylene tubing from a closed syringe. The perfusion of the preparation was performed by an infusion system (model ST670) from Samtronic (São Paulo, SP, Brazil) during 7 min. Because of the volatility of sevoflurane and isoflurane and attendant losses (~33%), the final anesthetic concentrations exiting the perfusion chamber were determined by gas-cromatography following n-heptane extraction as previously described[15]. Analysis by gas–liquid chromatography was performed on a Hewlett Packard Series II-5890gas chromatograph equipped with a DB-WAX capillary column 30m x 0.25mm with a film thickness of 0.33 μm (80ºC) and a flame ionization detector (100ºC). The volume of injection was 2μL.

2.3 Staining and Destaining with FM1-43

The experiments described below were performed according to Valadão et. al., (2013)[16]. Diaphragm nerve-muscle preparations were dissected from Swiss female adult

mice (30-40g), divided into two hemidiaphragms, and pinned flat in a sylgard-line perfusion chamber containing mouse Ringer solution (134 mM NaCl, 5 mM KCl, 2 mM $CaCl_2$, 1 mM $MgCl_2$, 12 mM $NaHCO_3$, 1 mM NaH_2PO_4, 11 mM *d*-glucose) gassed with 95% O_2 – 5% CO_2. FM1-43 (4 μM) was then used to stain the recycling pool of synaptic vesicles[12]. The structure of this dye presents a hydrophobic tail, which allows it to reversibly bind to biological membranes, and a polar head that impairs it to fully permeate the plasma membrane[11-17]. Therefore, FM1-43 binds to synaptic membrane and after stimulating the nerve terminal to cause synaptic vesicles exocytosis and consequently compensatory endocytosis, the fluorescent dye is incorporated resulting in a typical pattern of staining of the synaptic vesicles[12]. If the nerve terminals are resubmitted to a new round of stimulation, in the absence of FM1-43 in the external medium, the dye is released to the hydrophilic medium, resulting in a decrease of fluorescence intensity, which reflects the exocytosis of synaptic vesicles[11-17]. In our experiments, the muscles were incubated with *d*-tubocurarine (16 μM) to avoid contractions during stimulation. The muscles were stimulated for 10 min with modified Ringer solution containing a high concentration of KCl (80 mM NaCl, 60 mM KCl, 2 mM $CaCl_2$, 1 mM $MgCl_2$, 12 mM $NaHCO_3$, 1 mM NaH_2PO_4, 11mM *d*-glucose) in the presence of FM1-43 (4 μM). Thereafter, the preparation was kept resting in mouse Ringer solution for 10 min to guarantee FM1-43 uptake. The excess of FM1-43 adhered to the muscle membranes were removed during a 20 min washing period in gassed mouse Ringer solution. Images were acquired during 7 min with intervals of 2 min. The destaining at the absence of stimulus due to photobleaching of FM1-43 when it is exposed to illumination (around 10% of decrease in fluorescence) was used as a control for destaining.

2.4 Exposure to the anesthetic and other drugs

After labeling the recycling pool of synaptic vesicles, neuromuscular preparations were continuously exposed to different sevoflurane or isoflurane concentrations during 7 min to evaluate its effect on spontaneous exocytosis. We also performed experiments to investigate the anesthetics' effect on evoked synaptic vesicles exocytosis by Na^+-dependent (1 mM 4AP and 100 μM veratridine) or Na^+-independent (60 mM KCl) stimuli. In this case, preparations were pre-exposed to the anesthetic tested and then perfused with the depolarizing solution also containing the anesthetic, throughout the whole image acquisition period (7 min). All procedures were performed in room temperature (25 - 30ºC).

2.5 Fluorescence microscopy

All images were acquired using a fluorescence microscope (Leica DM2500) coupled to a CCD camera (12 bits, Leica DFC345FX) using a water immersion objective (63×, 0.95 NA) and visualized in a computer screen using Leica Application Suite 4.0 software. Excitation light came from a 100 W Hg lamp and passed through filters (505/530 nm) to select the desired fluorescence spectrum. The experimental parameters for collection of images were kept the same in control and test contra lateral hemidiaphragms in a given trial.

2.6 Image and statistical analysis

Images were analyzed using the softwares Image J and Microsoft Excel. The mean fluorescence intensity was determined for each cluster of fluorescent spots. Data were normalized and then converted to a percentage graphic representation using GraphPad Prisma 4.0. Statistical analysis was performed using unpaired Student's t-Test. $P < 0.05$ values were considered statistically significant.

3 Results

3.1 Effect of isoflurane and sevoflurane on spontaneous synaptic vesicles exocytosis

Figure 1A shows representative image of a control experiment showing nerve terminal fluorescence loss due to FM1-43 photobleaching during illumination time (7 min). As expected, the fluorescence loss due photobleaching was negligible (Figure 1G). Figures 1B and C show representative images of nerve terminals from neuromuscular preparations that were continuously perfused with 0.45 mM sevoflurane and 0.45 mM isoflurane, respectively, for 7 min and we observed no change in fluorescence intensity. No further fluorescence decay was detected when the preparations were exposed to any of clinical (0.45 mM or 0.6 mM) or supra-clinical sevoflurane concentrations tested (0.9 mM) (not shown). Likewise, the preparations perfused with isoflurane at the same concentrations did not show further fluorescence decay when compared to photobleaching. Quantification of normalized fluorescence loss due to photobleaching and treatment with 0.45 mM sevoflurane or isofluanre is represented on Figure 1G. Therefore, these data show that neither sevoflurane nor isoflurane evoke synaptic vesicles exocytosis at the mouse NMJ

Effect of sevoflurane and isoflurane on evoked synaptic vesicles exocytosis

It is already known that general anesthetics affect voltage-gated $Na^{+,}$ K^{+}, and Ca^{2+} channels[18]. In addition, some studies have shown that inhaled anesthetics cause a great muscle relaxation and potentiate the effect of neuromuscular blocking agents[1]. Thereby, in order to access how sevoflurane and isoflurane are able to generate such muscle relaxation, the next set of experiments aimed to investigate whether these volatile

anesthetics may block different depolarizing stimuli, mainly Na^+-dependent or Na^+-independent.

Elevated extracellular KCl concentration has been used extensively as a pharmacological tool for evoking synaptic vesicles exocytosis in isolated nerve terminals on a Na^+-independent manner[19]. Increased extracellular K^+ levels depolarize the membrane by shifting the K^+ equilibrium potential above the threshold for activation of voltage-gated Ca^{2+} channels, leading to Ca^{2+} influx and then a Na^+ channel-independent neurotransmitter release. We therefore tested whether sevoflurane and isoflurane could interfere with exocytosis evoked by KCl (60 mM). Preparations treated with 60mM KCl exhibit a ~ 60% fluorescence decay, as shown on Figure 1D. Nerve terminals pre-incubated and continuously perfused with 0.45 mM sevoflurane or isoflurane also showed a loss in fluorescence intensity due to stimulation with 60 mM KCl as similar as preparations untreated with the anesthetic. Same result was observed with 0.9 mM sevoflurane or isoflurane (data not shown). Figure 1E shows representative images of a nerve terminal treated with 60 mM KCl + 0.45 mM sevoflurane. Figure 1F shows representative images of a nerve terminal treated with 60mM KCl + 0.45 mM isoflurane. Results from independent experiments are summarized in Figure 1G. FM1-43 destaining evoked by 60 mM was statically different from photobleaching but similar to all the other experimental groups (60 mM KCl + 0.45 mM sevoflurane, 60 mM KCl + 0.90 mM sevoflurane, 60 mM KCl + 0.45 mM isoflurane and 60 mM KCl + 0.90 mM isoflurane. Thereby, this result suggests that sevoflurane and isoflurane are not able to block synaptic vesicles exocytosis evoked by high KCl concentrations, a stimulus that is independent on extracellular Na^+ influx.

Voltage-gated sodium channels have been emerging as important targets for some inhaled anesthetics. It is now evident that volatile anesthetics at clinical concentrations

inhibit sodium channels in isolated rat nerve terminals and neurons, as well as in heterologously expressed mammalian Na^+-channel α subunits[2]. We therefore tested in our system whether sevoflurane and isoflurane might interfere with exocytosis evoked by Na^+-dependent stimuli such as 4-aminopyridine (4AP) (1 mM) and veratridine (100 μM). 4AP depolarization is associated with prolongation of the presynaptic action potential evoked by blocking the K^+ current, thus leading to Na^+ channels activation and neurotransmitter release[20]. Incubation of nerve terminals with 4AP (1 mM) during 7 min induced a ~35% decay in FM1-43 fluorescence intensity (Figure 2B). Preparations pre-incubated and continuously perfused with 0.45 mM sevoflurane (Figure 2C) or 0.6 mM presented a reduced 4AP-evoked exocytosis (~15% decay in fluorescence intensity). Moreover, preparations pre-incubated and continuously perfused with 0.90 mM sevoflurane showed a complete inhibition of 4AP-evoked exocytosis (~10% decay in fluorescence intensity, similar to photobleaching) (Figure 2E). Although crescent concentrations of isoflurane such as 0.45mM, 0.60 mM or 0.90 mM also induced an inhibition of 4AP-evoked exocytosis, it is noteworthy that this was less pronounced than that caused by the same concentrations of sevoflurane. All preparations treated with any of the isoflurane concentrations showed an approximately 20% decay in FM1-43 fluorescence intensity evoked by 4AP. Figure 2D shows representative images of a nerve terminal treated with 0.45 mM isoflurane. These data indicate that although both anesthetics inhibit synaptic vesicles exocytosis evoked by a 4AP, the inhibition caused by sevoflurane is greater than the one induced by isoflurane

To further test this hypothesis, we next investigated the effect of sevoflurane and isoflurane on veratridine-evoked exocytosis. This pharmacological agent acts in a different manner than 4AP by interacting directly with the sodium channel, and therefore leading to its activation (by slowing inactivation), and consequently

depolarizing the plasma membrane[21]. Incubation of neuromuscular preparations with veratridine (100 µM) during 7 min induced a significant FM1-43 destaining (~45%) (Figure 3). The destaining evoked by veratridine was approximately 70% abolished by 1 µM TTX and significantly reduced (~ 45%) by 0.5 µM TTX (Figure 3). Preparations pre-incubated and continuously perfused with 0.45 mM sevoflurane showed a great inhibition on veratridine-evoked exocytosis (~ 25% decay in fluorescence intensity) (Figure 3). Increased concentrations of sevoflurane (0.6 mM and 0.9 mM) did not provide any further inhibition (data not shown). The same result was observed when was used (Figure 3). Preparations pre-incubated and continuously perfused with 0.45 mM isoflurane significantly inhibited veratridine-evoked synaptic vesicles exocytosis (~ 25% decay in fluorescence intensity). Increased concentrations (0.6 mM and 0.9 mM) did not show further inhibition either (data not shown).

Our previous results prompt us to ask if sevoflurane/isoflurane and TTX have an additive effect on inhibiting veratridine-evoked FM1-43 destaining. Since 1 µM TTX almost completely abolish veratridine-evoked stimulus, we performed experiments using a lower TTX concentration (0.5 µM). Our results showed that simultaneous pre-incubation of nerve terminals with 0.45 mM sevoflurane and 0.5 µM TTX produced a significant inhibition of veratridine-induced vesicle exocytosis (~ 15% decay in fluorescence intensity) with an additive effect when compared to 0.5 µM TTX alone. The same result was observed when 0.45 mM isoflurane and 0.5 µM TTX were used combined (Figure 3). Taken together, these results suggest that sevoflurane and isoflurane reduce sodium-dependent synaptic vesicles exocytosis by blocking Na^+ sodium channels sensitive to TTX at the mouse NMJ.

4 Discussion

The inhaled anesthetics sevoflurane and isoflurane have many properties that make them very useful for surgical procedures. Nowadays, sevoflurane is the most common anesthetic used for inhalation anesthesia in humans while isoflurane is the most used in animals[22]. However, as any modern anesthetic, both agents produce side effects. Previous studies showed that isoflurane and sevoflurane might cause hypercapnia, acidosis and a marked decrease in respiration rate[22]. In addition, volatile anesthetics do not only potentiate the action of neuromuscular blocking agents but also have muscle relaxants properties of their own. Enflurane, isoflurane, desflurane, and sevoflurane produce skeletal muscle relaxation that is about twice as high as that associated with halothane[23]. This relaxation might occur due to a blockage on neuromuscular transmission at the pre and/or postsynaptic level[5,6,9].

Inhibitory effects of volatile anesthetics on neuromuscular transmission have been shown in *in vitro*[7,24] and *in vivo* studies[25]. For example, Suzuki et al. (1999)[26] showed that sevoflurane depressed compound muscle action potentials and caused fading amplitudes under a train of repetitive stimulation. Volatile anesthetics were already reported to reinforce the effects of non-depolarizing blocking agents [26,27,28]. In addition, Violet et al. (1997) showed that these drugs are also able to inhibit the muscular and neuronal nAChR all by itself. All these effects mentioned above show that volatile anesthetics interfere somehow with the neuromuscular transmission, either at the pre-synaptic or post-synaptic levels or both. Some studies have focused on the postsynaptic effects of sevoflurane and isoflurane [6,9,26]. Nevertheless, the presynaptic mechanisms behind this volatile anesthetics capacity to produce muscle relaxation are not clear. Therefore, in this work, we investigated the effects of sevoflurane and isoflurane on spontaneous and evoked synaptic vesicles exocytosis labeled with the vital fluorescence

dye FM1-43 at the mouse NMJ, an experimental model that provides a direct way to investigate neurotransmitter release in an isolated synapse.

Regarding the presynaptic effects of these anesthetics, it is already known that isoflurane and halothane increases basal dopamine release in the rat striatum[29]. In addition, although Silva and colleagues (2007)[30] have shown that sevoflurane (0.46 mM) increases significantly the release of dopamine, it was by a non-vesicular process, independent of synaptic vesicles exocytosis. Moreover, Schichino et al. (1998)[31] showed that volatile anesthetics such as sevoflurane and isoflurane suppressed acetylcholine (ACh) release in a dose-dependent manner in non-stimulated rat cerebral cortex. Interestingly, Naruo et al. (2005)[32] showed that when non-stimulated neurons isolated from ganglia of snails were incubated with clinical sevoflurane concentrations in the presence of FM1-43, there was no alteration on synaptic vesicles recycling. In our model, also a cholinergic system, we investigate if sevoflurane and isoflurane would be able to evoke synaptic vesicles exocytosis, leading to ACh release. When preparations were treated with sevoflurane or isoflurane (0.45, 0.60 and 0.90 mM) we observed no decay in fluorescence intensity of FM1-43-labeled nerve terminals. This result indicates that these anesthetics do not stimulate synaptic vesicles exocytosis at the mouse NMJ (Figure 1).

It has been reported that ether derivative fluorinated volatile anesthetics such as sevoflurane and isoflurane causes skeletal muscle relaxation during surgical procedures[1,33,34]. This effect could be due to an inhibitory effect on evoked synaptic vesicles exocytosis. Although there are some findings showing that somatic and heterologously expressed Na^+ and also P/Q-type voltage-gated Ca^{2+} channels can be inhibited by volatile anesthetics[35], here we showed that, for the NMJ, neither sevoflurane nor isoflurane were able to inhibit FM1-43 destaining evoked by 60 mM

KCl, a Na+ independent stimulus that acts directly by opening Ca^{2+} channels (Figure 1). Westphalen and colleagues (2013)[36] suggested that the volatile anesthetic isoflurane significantly inhibits the 4AP-evoked release of neurotransmitter (Na^{+}-dependent stimulus) with greater sensitivity compared with KCl-evoked exocytosis. Hemmings et al. (2005)[4] also showed that in hippocampal neurons, despite isoflurane inhibition of synaptic vesicles exocytosis evoked by electrical pulses of stimulation, this drug does not abolish this process when high K^{+} solution is used as stimulus. Since KCl-evoked exocytosis was not inhibited, the major presynaptic target for inhibition of exocytosis by these volatiles must lie upstream of Ca^{2+} entry through nerve terminal voltage-gated Ca^{2+} channels coupled to synaptic vesicle exocytosis.

It is already known that accumulation of Na^{+} at both vertebrate and invertebrate nerve terminals augments transmitter release by triggering the increase of intracellular Ca^{2+} concentrations and, in addition, Na^{+} *per se* can activate the asynchronous neurotransmitter release [56]. Therefore, the Na^{+} influx to the terminal is a key point for the release of neurotransmitters. Considerable evidences support a role for Na^{+} channel blockade in the inhibition of synaptic vesicle exocytosis by volatile anesthetics[37,38,39,40,41,42]. In order to gain further insight about the presynaptic actions of sevoflurane and isoflurane at the NMJ, we tested if sevoflurane and isoflurane would be able to inhibit synaptic vesicles exocytosis evoked by 4AP or veratridine.

Preparations stimulated by 4AP, a stimulus that mimics synaptic action-potential-evoked neurotransmitter release in requiring activation of Na^{+} and Ca^{2+} channels exhibited a significant decrease in fluorescence intensity (Figure 2). This effect was significantly inhibited by clinical sevoflurane or isoflurane concentrations (Figure 2). Accordingly, Westphalen and colleagues (2013)[36] showed that the volatile anesthetic isoflurane inhibits the 4AP-evoked release of many neurotransmitters, such as

dopamine, (γ-amino butyric acid) GABA, glutamate, norepinephrine and ACh, at central nervous system. In addition, Leite et al. (2011)[43] also showed that high concentrations of an intravenous anesthetic (propofol) inhibited synaptic vesicles exocytosis evoked by 4AP. Indeed, electrophysiological data evidence offers some evidence that isoflurane inhibits nerve terminal Na^+ currents and action potential amplitude through Na^+ channels blockage in isolated neurohypophysial nerve terminals[39,44]. Although Ouyang and colleagues (2009)[45] showed that isoflurane and sevoflurane inhibits equally voltage-gated Na+ channels by voltage- and use-dependent mechanisms, we observed in our experimental model that inhibition of 4AP-evoked exocytosis by sevoflurane was greater than the inhibition caused by isoflurane as shown on Figure 3. These differences in potency among many different volatile anesthetics are already observed and controversial. Park and colleagues[46], for instance, studying the 5-HT-precontracted rat bronchi found that isoflurane and halothane are equipotent in relaxing it. On the other hand, previous work showed a neuromuscular inhibitory effect of sevoflurane (not isoflurane or halothane) on the cat sciatic nerve and gastrocnemius muscle[25] complex. In addition, the augmentation of the neuromuscular blocking effects of cisatracurium during sevoflurane anesthesia is also more efficient than isoflurane anesthesia[47]. These variations might be due the different physicochemical properties of these halogenated anesthetics[48,49]. However, the precise mechanism why these differences observed for the volatile anesthetics, explaining the seemingly more potent effect of sevoflurane compared with isoflurane and other halogenated drugs, remain unclear and need further investigation.

The role of Na^+ channels as a putative target for volatile anesthetics at the mouse NMJ was further analyzed by testing the effects of sevoflurane and isoflurane on veratridine-evoked synaptic vesicles exocytosis, since it directly acts on Na^+ channels

[19]. Sevoflurane and isoflurane significantly inhibited veratridine-evoked FM1-43 destaining (Figure 3), similar to previous studies showing that intravenous anesthetic propofol inhibits the veratridine-evoked glutamate release in synaptosomes in a dose-dependent manner[50]. Halothane and isoflurane also causes a 50% inhibition of veratridine-evoked glutamate release from synaptosomes [37,38]. Moreover, Harris and Bruno, (1985)[51] suggested that ethanol and other anesthetic drugs such as diethyl ether, halothane and enflurane are able to inhibit sodium channel.

It is well known that veratridine enhances the activity of most Na^+ channels (reviewed[52]) and its effect is blocked by TTX. All isoforms of voltage-gated Na^+ channels (Na_v) can be blocked with high potency and specificity by the TTX, however some isoforms, known as TTX-resistant, are less sensitive compared with other isoforms[53]. In our model, TTX (0.5 μM) significantly inhibited FM1-43 destaining and both anesthetics sevoflurane and isoflurane caused further inhibition of veratridine-evoked destaining by TTX. In accordance to our data, Zhang et al. (2010)[54] have shown that intrathecal infusion of TTX increases the potency of the volatile anesthetic isoflurane. These drug interactions are consistent with the known pharmacological specifity of this Na^+ channel modulator, and further support a role for this channel action in the immobilization produced by inhaled anesthetics[2].

In common anesthetic practice, nondepolarizing muscle relaxant agents are currently used to facilitate intubation of the trachea, mechanical ventilation, and surgical access and there are evidences that volatile anesthetics might enhance the effect these agents (reviewed by Tassonyi et al 2002[10]). In addition, several clinical studies have reported that volatile anesthetics such as iso and sevoflurane potentiate the inhibitory effect of non-depolarizing muscle relaxants [57, 58, 59]. In general, nondepolarizing muscle relaxants are competitive antagonists of nicotinic receptors and at the NMJ level, these receptors

are expressed both pre and post-synapticaly [60, 61]. Considering that at the NMJ, nicotinic pre-synaptic receptors are stimulatory autoreceptors that increases ACh release upon demand [61], we cannot rule out the possibility that the inhibitory effect of iso and sevoflurane on exocytosis might be due to an inhibition of those channels. However, because all the experiments here, to avoid muscle contraction during imaging, had to be performed in the presence of d-tubocurarine (that inhibits both neuronal and muscle nicotinic receptor), we cannot address the sole contribution of pre-synaptic nicotinic autoreceptors in the anesthetics effect on synaptic vesicles exocytosis.

Finally, in a study using electromyography with train-of-four (TOF) stimulation, Nitahara and colleagues (2007)[55] showed that in control and myastenic patients, sevoflurane has an inhibitory effect on neuromuscular transmission. Interestingly, this inhibitory effect of sevoflurane was more prominent in myasthenic patients. Based on this observation and in our data showing that sevoflurane and isoflurane block presynaptic Na^+ channels (Figure 2 and 3), we therefore suggest that this presynaptic effect of volatile anesthetics contribute to the muscular relaxation observed during surgical procedures under these volatile anesthetics.

Taken together, our data show that sevoflurane and isoflurane inhibit synaptic vesicles exocytosis by directly acting on Na^+ channels with no action on voltage-gated Ca^{2+} channels. This mechanism of action give further information of how these anesthetics might cause neuromuscular depression observed in clinical procedures.

5 Acknowledgements

This work was supported by grants from CNPq, FAPEMIG and CAPES. Cristina Guatimosim and Renato S. Gomez are Bolsistas de Produtividade em Pesquisa (CNPq).

6 References

1. Ghatge, S., Lee, J., Smith, I. Sevoflurane: an ideal agent for adult day-case anesthesia? Acta Anaesthesiol Scand 2003; 47(8):917-931.
2. Hemmings, H. C. Jr. Sodium channels and the synaptic mechanisms of inhaled anaesthetics. Br J Anaesth 2009; 103(1):61-69.
3. Richards, C.D. Anaesthetic modulation of synaptic transmission in the mammalian CNS. Br. J. Anaesth 2002; 89(1):79-90.
4. Hemmings, H.C. Jr., Akabas, M.H., Goldstein, P.A., Trudell, J.R., Orser, B.A., Harrison, N.L. Emerging molecular mechanisms of general anesthetic action. Trends Pharmacol Sci 2005; 26(10):503-510.
5. Nitahara, K., Sugi, Y., Kusumoto, G., Shono, S., Iwashita, K., Higa, K. Neuromuscular blockade by vencuronium during induction with 5% sevoflurane or propofol. J Int Med Res 2010; 38(6):1997-2003.
6. Paul, M., Fokt, R.M., Kindler, C.H., Dipp, N.C., Yost, C.S. Characterization of the interactions between volatile anesthetics and neuromuscular blockers at the muscle nicotinic acetylcholine receptor. Anesth Analg 2002; 95(2):362-367.
7. Kennedy, R., Galindo, A. Neuromuscular transmission in a mammalian preparation during exposure to enflurane. Anesthesiology 1975; 42(4):432-442.
8. Hedenstierna, G., Edmark, L. The effects of anesthesia and muscle paralysis on the respiratory system. Intensive Care Med 2005; 31(10):1327-1335.
9. Violet, J.M., Downie, D.L., Nakisa, R.C., Lieb, W.R., Franks, N.P. Differential sensitivities of mammalian neuronal and muscle nicotinic acetylcholine receptors to general anesthetics. Anesthesiology 1997; 86(4):866-874.

10. Tassonyi, E., Charpantier, E., Muller, D., Dumont, L., Bertrand, D. The role of nicotinic acetylcholine receptors in the mechanisms of anesthesia. Brain Res Bull 2002; 15:57(2): 133-150.
11. Betz, W.J, Bewick, G.S. 1993. Optical monitoring of transmitter release and synaptic vesicle recycling at the frog neuromuscular junction. J Physiol. 460, 287-309.
12. Betz, W. J., Mao, F., Bewick, G. S. Activity dependent fluorescent staining and destaining of living vertebrate motor nerve terminals. J Neurosci 1992; 12(2):363-375.
13. Gaffield M.A., Betz W.J. Imaging synaptic vesicle exocytosis and endocytosis with FM dyes. Nat Protoc 2006; 1(6):2916−21
14. Hemmings, H.C.Jr., Yan, W., Westphalen, R.I., Ryan, T.A. The general anesthetic isoflurane depresses synaptic vesicle exocytosis. Mol Pharmacol 2005; 67(5):1591-1599.
15. Miller, M.S., Gandolfi, A.J., A rapid, sensitive method for quantifying enflurane in whole blood. Anesthesiology 1979; 51(6):542-544.
16. Valadão, P.A., Naves, L.A., Gomez, R.S., Guatimosim, C. Etomidate evokes synaptic vesicle exocyosis without increasing miniature endplate potentials frequency at the mice neuromuscular junction. Neurochemistry International 2013; 63(5):576-582.
17. Rizzoli, S.O., Richards, D.A., Betz, W.J. Monitoring synaptic vesicle recycling in frog motor nerve terminals with FM dyes. J Neurocytol 2003; 32(5-8):539-549.
18. Topf, N., Jenkins, A., Baron, N., Harrison, N.L. Effects of isoflurane on gamma-aminobutyric acid type A receptors activated by full and partials agonists. Anesthesiology 2003.; 98(2):306-311.

19. Nicholls, D.G. The glutamatergic nerve terminal. Eur J Biochem 1993; 212(3):613-631.
20. Enomoto, K., Maeno, T. Presynaptic effects of 4-aminopyridine and streptomycin on the neuromuscular junction. Eur J Pharmacol 1981; 76(1):1-8.
21. Barnes, S., Hille, B. Veratridine modifies open sodium channels. J Gen Physiol 1988; 91(3):421-443
22. Cesarovic, N., Nicholls, F., Rettich, A., Kronen, P., Hässig, M., Jirkof, P., Arras, M. Isoflurane and sevoflurane provide equally effective anaesthesia in laboratory mice. Lab Anim 2010; 44(4):329-336.
23. Wenker, O. Review of currently used inhalation anesthetics: part II. The internet Journal of Anesthesiology 1998; vol. 3, nº 3.
24. Bhattacharyya, B.J, Tsen, K., Sokoll, M.D. Age-induced alteration of neuromuscular transmission: effect of halothane. Eur J Pharmacol 1994; 254(1-2):97-104
25. Suzuki, T., Nagai, H., Ogawa, S., Suzuki, H. Comparative neuromuscular inhibitory effects of volatile anesthetics. Masui 1996; 45(5):599-607.
26. Suzuki, T., Munakata, K., Watanabe, N., Katsumata, N., Saeki, S., Ogawa, S. Augmentation of vencuronium-induced neuromuscular block during sevoflurane anaesthesia: comparison with balanced anaesthesia using propofol or midazolam. Br J Anaesth 1999; 83(3):485-487.
27. Li, C., Yao, S., Nie, H., Lü, B. Effects of isoflurane on the action of neuromuscular blockers on the muscle acetylcholine receptors. J Huazhong Univ Sci Technolog Med Sci 2004; 24:605-614.
28. Motamed, C., Donati, F. Sevoflurane and isoflurane, but not propofol, decrease mivacurium requirements over time. Can J Anaesth 2002; 49(9):907-912.

29. Keita, H., Henzel-Rouellé, D., Dupont, H., Desmonts, J.M., Mantz, J. Halothane and isoflurane increase spontaneous but reduce the N-methyl-D-aspartate-evoked dopamine release in rat striatal slices: evidence for direct presynaptic effects. Anesthesiology 1999; 91(6):1788-1797.
30. Silva, J.H., Gomez, R.S., Diniz, P.H., Gomez, M.V., Guatimosim, C. The effect of sevoflurane on the release of [3H] dopamine from rat brain cortical slices. Brain Res Bull 2007; 72(4-6):309-314.
31. Shichino, T., Murakawa, M., Adachi, T., Arai, T., Miyazaki, Y., Mori, K. Effects of inhalation anaesthetics on the release of acetylcholine in the rat cerebral cortex in vivo. Br J Anaesth 1998; 80(3):365-370.
32. Naruo, H., Onizuka, S., Prince, D., Takasaki, M., Syed, N.I. Sevoflurane blocks cholinergic synaptic transmission postsynaptically but does not affect short-term potentiation. Anesthesiology 2005; 102(5):920-928.
33. Waud, B.E., Waud, D.R. Comparison of the effects of general anesthetics on the end-plate of skeletal muscle. Anesthesiology 1975; 43(5):540-547.
34. Waud, B.E., Waud, D.R. The effects of diethyl ether, enflurane and isoflurane at the neuromuscular junction. Anestehsiology 1975; 42(3):275-280.
35. Kamatchi, G.L., Chan, C.K., Snutch, T., Durieux, M.E., Lynch, C. Volatile anesthetic inhibition of neuronal Ca channel currents expressed in Xenopus oocytes. Brain Res 1999; 831(1-2):85-96.
36. Westphalen, R.I., Desai, K.M., Hemmings, H.C. Jr. Presynaptic inhibition of the release of multiple major central nervous system neurotransmitter types by the inhaled anaesthetic isoflurane. Br J Anaesth 2013; 110(4):592-599.
37. Ratnakumari, L., Hemmings, H.C. Jr. Inhibition of presynaptic sodium channels by halothane. Anesthesiology 1998; 88(4):1043–1054.

38. Lingamaneni, R., Birch, M.L., Hemmings, H.C.Jr. Widespread inhibition of sodium channel-dependent glutamate release from isolated nerve terminals by isoflurane and propofol. Anesthesiology 2001; 95(6):1460-1466.
39. Ouyang, W., Wang, G., Hemmings, H.C.Jr. Isoflurane and propofol inhibit presynaptic Na^+ channels in isolated rat neurohypophysial nerve terminals. Mol Pharmacol 2003; 64(2):373-381.
40. Westphalen, R.I., Hemmings, H.C. Selective depression by general anesthetics of gluatamate vs. GABA release from isolated nerve terminals. J Pharmacol Exp Ther 2003; 304(3):1188-1196.
41. Wu, X.S., Sun, J.Y., Evers, A.S., Crowder, M., Wu, L.G. Isoflurane inhibits transmitter release and the presynaptic action potential. Anesthesiology 2004; 100(3):663-670.
42. Herold, K.H., Hemmings, H.C.Jr. Sodium channels as targets for volatile anesthetics. Front Pharmacol 2012; 3(50):1-7.
43. Leite, L.F., Gomez, R.S., Fonseca, M.C., Gomez, M.V., Guatimosim, C. Effect of intravenous anesthetic propofol on synaptic vesicle exocytosis at the frog neuromusuclar junction. Acta Pharmacol Sin 2011; 32(1):31-37.
44. Ouyang, W., Hemmings, H.C.Jr. Depression by isoflurane of the actionpotential and underlying voltage-gated ion currents in isolated rat neurohypophysial nerve terminals. J Pharmacol Exp Ther 2005; 312(2):801-808.
45. Ouyang, W., Herold, K.F., Hemmings, H.C.Jr. Comparative effects of halogenated inhaled anesthetics on voltage-gated Na^+ channel function. Anesthesiology 2009; 110(3):582-590.
46. Park, K.W., Dai, H.B., lowestein, E., Kocher, O.N., Selke, F.W. Isoflurane-and-halothane mediated dilation of distal bronchi in the rat depends on the epithelium. Anesthesiology 1997; 86(5):1078-1087.

47. Wulf, H., Kahl, M., Ledowski, T. Augmentation of the neuromuscular blocking effects of cisatracurium during desflurane, sevoflurane, isoflurane or i.v anaesthesia. Br J of Anaesth 1998; 80(3):308-312.

48. Strum, D.O., Eger, E.I. Partition coeficientes for sevoflurane in human blood, saline and olive oil. Anesth Analg 1987; 66(7):654-656.

49. Yasuda, N., Targ, A.G., Eger, E.L. Solubility of I-653, sevoflurane, isoflurane and halothane in human tissues. Anesth Analg 1989; 69(3):370-373

50. Ratnakumari, L., Hemmings, H.C.Jr. Effects of propofol on sodium channel-dependent sodium influx and glutamate release in rat cerebrocortical synaptosomes. Anesthesiology 1997; 86(2):428-439.

51. Harris, R.A., Bruno, P. Effects of ethanol and other intoxicant-anesthetics on voltage-dependent sodium channels of brain synaptosomes. J Pharmacol Exp Ther 1985; 232(2):401-406.

52. Catterall, W.A., Goldin, A.L., Waxman, S.G. International Union of Pharmacology. XLVII. Nomenclature and structure-function relationships of voltage-gated sodium channels. Pharmacol Rev 2005; 57(4):397-409.

53. Goldin, A.L. Resurgence of sodium channel research. Annu Rev Physiol 2001; 63:871-894.

54. Zhang, Y., Guzinski, M., Eger E.L.2nd., Laster, M.J., Sharma, M., Harris, R.A., Hemmings H.C.Jr. Bidirectional modulation of isoflurane potency by intrathecal tetrodotoxin and veratridine in rats. Br J Pharmacol 2010; 159(4):872-878.

55. Nitahara, K., Sugi, Y., Higa, K., Shono, S., Hamada, T. Neuromuscular effects of sevoflurane in myasthenia gravis patients. Br J Anaesth 2007; 98(3):337-341.

56. Meunier, F.A., Colasante, C., Molgo, J. Sodium-dependent increase in quantal secretion induced by brevetoxin-3 in Ca^{2+}-free medium is associated with

depletion of synaptic vesicles and swelling of motor nerve terminals in situ. Neuroscience 1997; 78(3): 883-893.

57. Takagi, S., Adachi, Y.U., Saubermann, A.J., Vizi, E.S. Presynaptic inhibitory effects of rocuronium and SZ1677 on [3H] acetylcholine release from the mouse hemidiaphragm preparation. Neurochem Int. 2002; 40(7): 655-659
58. Morita, T., Tsukagoshi, H., Sugaya, T., Yoshikawa, D., Fujita, T. The effects of sevoflurane are similar to those of isoflurane on the neuromuscular block produced by vecuronium. Br J Anaesth. 1994; 72(4): 465-467
59. Valinthout, L.E., Booij, L.H., van Egmond, J., Robertson, E.N. Effect of isoflurane and sevoflurane on the magnitude and time course of neuromuscular block produced by vecuronium, pancuronium and atracuium. Br J Anaesth 1996; 76(3): 389-395.
60. Flecther, P., Forrester, T. The effect of curare on the release of acetylcholine from mammalian motor nerve terminals and an estimate of quantum content. J Physiol 1975; 251(1):131-144.
61. Vizi, E.S., Lendvai, B. Side effects of nondepolarizing muscle relaxants: relationship to their antinicotinic and antimuscarinic actions. Pharmacol Ther 1997; 73(2): 75-89.

7 Figures

Figure 1

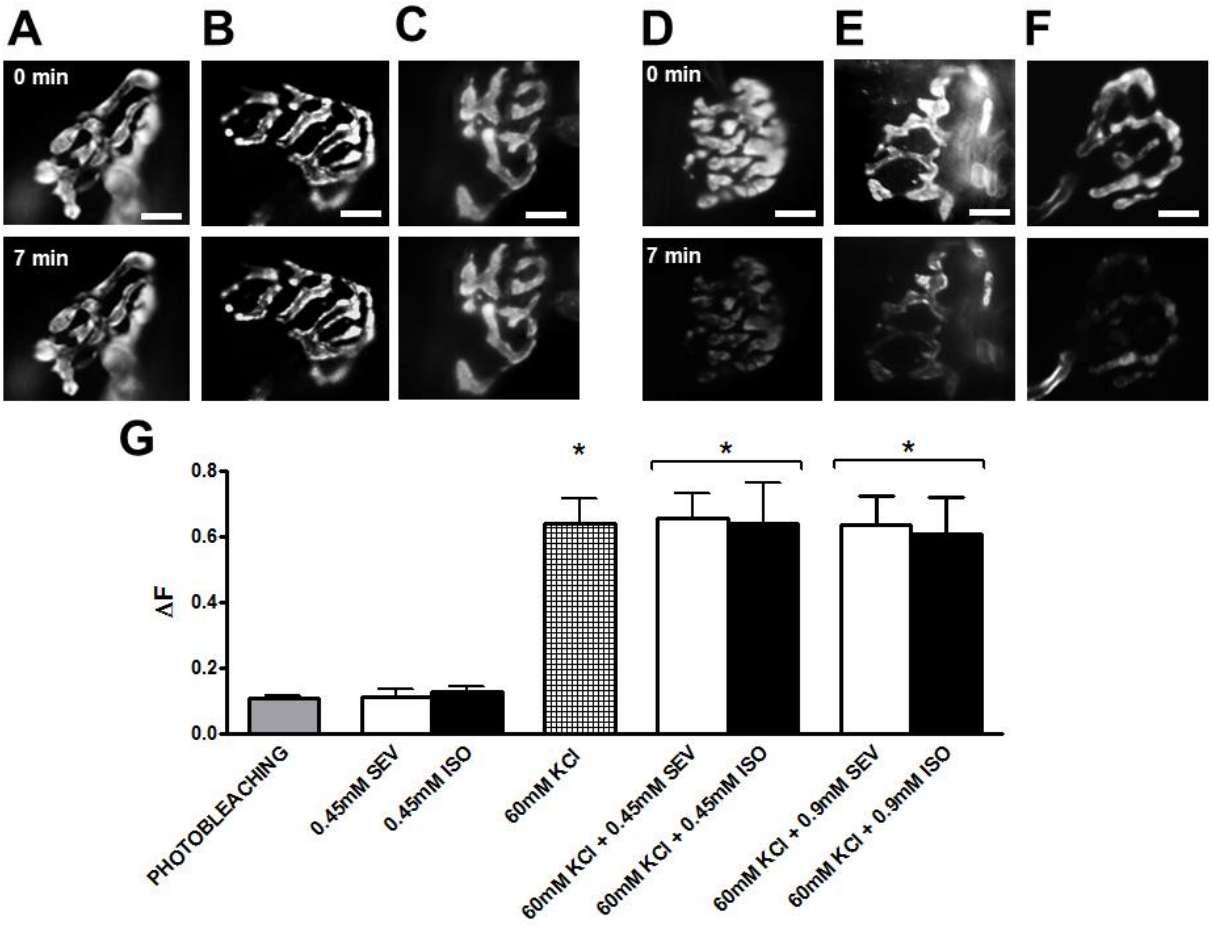

Figure 2

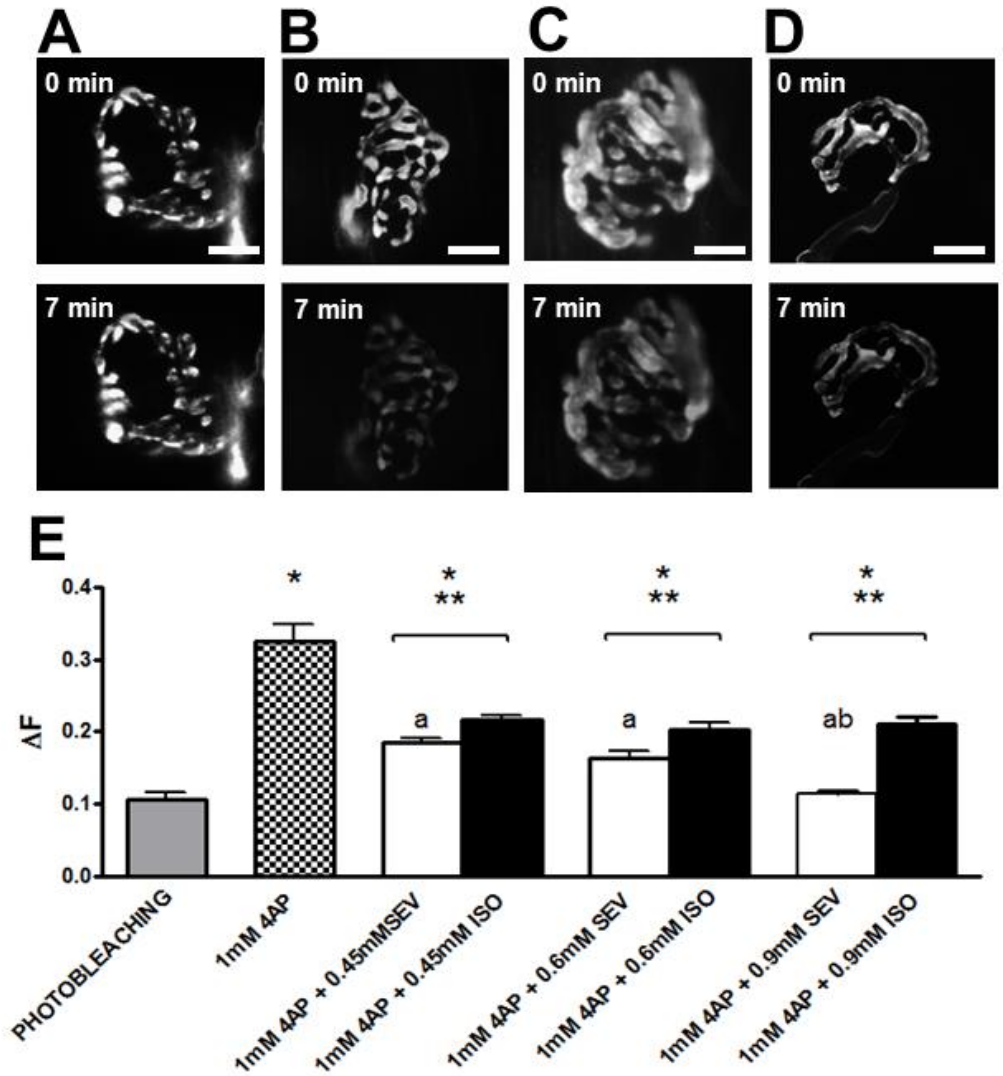
A
B
C
D
0 min
0 min
0 min
0 min
7 min
7 min
7 min
7 min
E
ΔF
0.4
0.3
0.2
0.1
0.0
*
*
**
*
**
*
**
a
a
ab
PHOTOBLEACHING
1mM 4AP
1mM 4AP + 0.45mMSEV
1mM 4AP + 0.45mM ISO
1mM 4AP + 0.6mM SEV
1mM 4AP + 0.6mM ISO
1mM 4AP + 0.9mM SEV
1mM 4AP + 0.9mM ISO

Figure 3

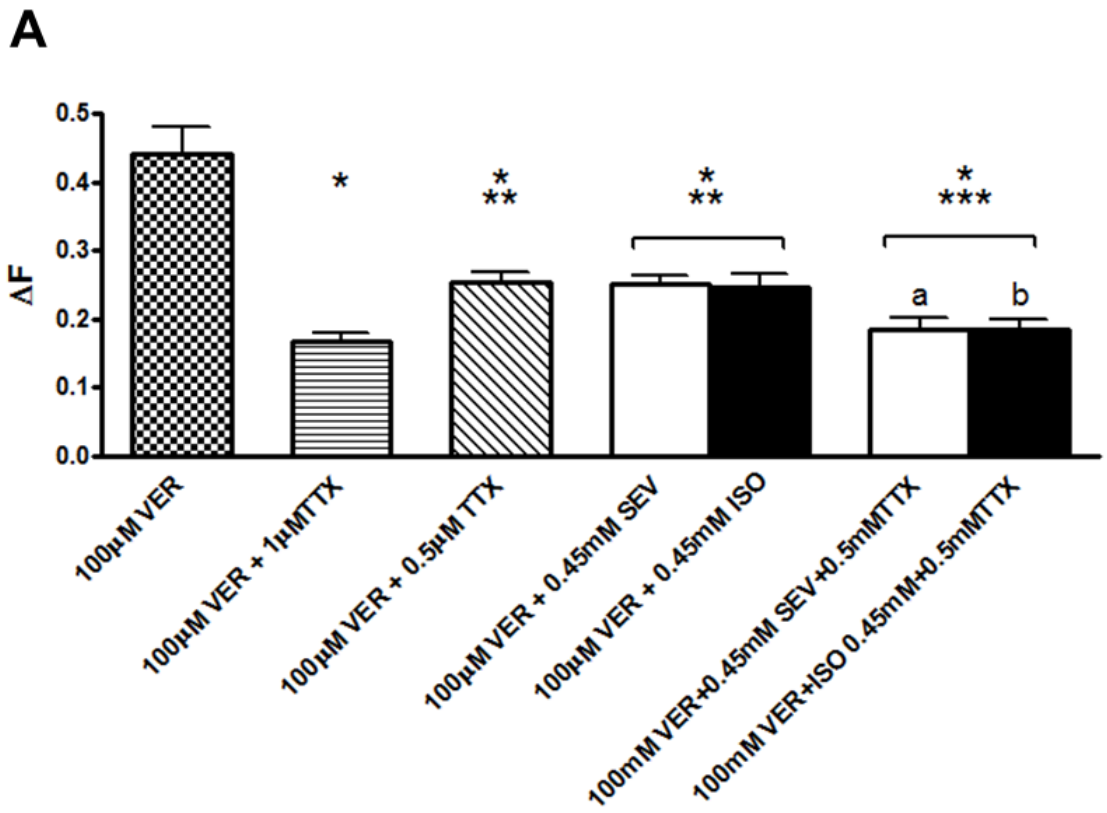

8 Figure legends

Figure 1. Sevoflurane and isoflurane neither evoke the exocytosis of synaptic vesicle nor interfere with the exocytosis evoked by 60 mM KCl at the mouse NMJ. (A) Representative image of fluorescence loss due to photobleaching during illumination for 7 min. Upper panel: before illumination. Lower panel: after 7 min of illumination. (B) Representative image of nerve terminal before (upper panel) and after incubation with 0.45 mM sevoflurane (lower panel). (C) Representative image of nerve terminal before (upper panel) and after incubation with 0.45 mM isoflurane (lower panel). (D) Representative image of nerve terminal before (upper panel) and after treatment with 60 mM KCl for 7 min (lower panel). (E) Representative image of nerve terminal before (upper panel) and after treatment with 60 mM KCl + 0.45 mM

sevoflurane for 7 min. (F) Representative image of nerve terminal before (upper panel) and after treatment with 60 mM KCl + 0.45 mM isoflurane for 7 min. (G) Quantification of fluorescence signal after photobleaching, incubation with 0.45 mM sevoflurane or isoflurane, 60 mM KCl and 60 mM KCl + 0.45 mM sevoflurane or isoflurane. ΔF =(F0-F/100), normalized fluorescence. The results are mean ± SEM of 150 fluorescent spots from 15 nerve terminals of 15 animals (photobleaching), 28 fluorescent spots from 4 nerve terminals of 4 animals for 0.45 mM sevoflurane or isoflurane, 100 fluorescent spots from 10 nerve terminals of 10 animals (60 mM KCl) and 21 fluorescent spots from 3 nerve terminals of 3 animals for each of the other experimental conditions (60 mM KCl + 0.45 mM sevoflurane or isoflurane). *P<0.05 when compared to the second bar (photobleaching). Scale Bar =10 μm

Figure 2. The anesthetic sevoflurane inhibits exocytosis of synaptic vesicles evoked by 4AP (1 mM) greater than isoflurane at the mouse NMJ (A) Representative image of fluorescence loss due to photobleaching during illumination for 7 min. Upper panel: before illumination. Lower panel: after 7 min of illumination. (B) Representative image of nerve terminal before (upper panel) and after treatment with 1mM 4AP for 7 min (lower panel). (C) Representative image of nerve terminal before (upper panel) and after treatment with 1 mM 4AP + 0.45 mM sevoflurane for 7 min (lower panel). (C) Representative image of nerve terminal before (upper panel) and after treatment with 1 mM 4AP + 0.45 mM isoflurane for 7 min (lower panel). (D) Quantification of destaining by photobleaching (first bar) and evoked by 1 mM 4AP (second bar), 1 mM 4AP + 0.45 mM sevoflurane or isoflurane (third paired bars), 1 mM 4AP + 0.6 mM sevoflurane or isoflurane (fourth paired bars) and 1 mM 4AP + 0.9 mM sevoflurane or isoflurane (fifth paired bars). ΔF=(F0-F/100), normalized fluorescence. The results are

mean ± SEM of 150 fluorescent spots from 15 nerve terminals of 15 animals (photobleaching), 100 fluorescent spots from 10 nerve terminals of 10 animals (1 mM 4AP) and 28 fluorescent spots from 4 nerve terminals from 4 animals per each experimental condition. *P<0.05 when compared to the first bar (photobleaching). **P<0.05 when compared to the second bar (1 mM 4AP). [a] P<0.05 when comparing 4AP + sevoflurane (each concentration) to 4AP + isoflurane each concentration. [b] P<0.05 comparing 1 mM 4AP + 0.45mM sevoflurane with 1 mM 4AP + 0.9 mM sevoflurane. Scale Bar =10 μm.

Figure 3. The anesthetics sevoflurane and isoflurane interfere with exocytosis of synaptic vesicles induced by veratridine (100 μM) probably targeting in voltage-gated sodium channels. Quantification of destaining by 100 μM veratridine (first bar), veratridine + TTX (1 μM) (second bar), 100 μM veratridine + TTX (0.5 μM) (third bar), 100 μM veratridine + 0.45mM sevoflurane or isoflurane (fourth paired bars) and 100 μM veratridine + 0.45 mM isoflurane or isoflurane + 0.5 μM TTX (fifth paired bars). ΔF=(F0-F/100), normalized fluorescence. The results are mean ± SEM of 150 fluorescent spots from 15 nerve terminals of 15 animals (photobleaching), 100 fluorescent spots from 10 nerve terminals of 10 animals (100 μM veratridine) *P < 0.05 when compared to the first bar (100 μM veratridine), 28 fluorescent spots from 4 nerve terminals of 4 animals per each experimental condition. **P<0.05 when compared to the second bar (100 μM veratridine + 1 μM TTX). *** P<0.05 when compared to the third bar 100 μM veratridine + 0.5 μM TTX. [a,b] P<0.05 when compared respectively to 100 μM veratridine + 0.45 mM sevoflurane and 100 μM veratridine + 0.45 mM isoflurane.

9. ANEXO 2: Artigo publicado durante a iniciação científica no LabNeuro

Acta Pharmacologica Sinica (2011) 32: 31–37
 1671-4083/11 $32.00
www.nature.com/aps

Original Article

Effect of intravenous anesthetic propofol on synaptic vesicle exocytosis at the frog neuromuscular junction

Luciana Ferreira LEITE[1], Renato Santiago GOMEZ[2, *], Matheus de Castro FONSECA[1], Marcus Vinicius GOMEZ[3], Cristina GUATIMOSIM[1, §]

[1]Department of Morphology, Federal University of Minas Gerais, Belo Horizonte, Minas Gerais, Brazil; [2]Department of Surgery, School of Medicine, Federal University of Minas Gerais, Belo Horizonte, Minas Gerais, Brazil; [3]Graduate Program of Santa Casa, Belo Horizonte, Minas Gerais, Brazil

Aim: To investigate the presynaptic effects of propofol, a short-acting intravenous anesthetic, in the frog neuromuscular junction.
Methods: Frog cutaneous pectoris nerve muscle preparations were prepared. A fluorescent tool (FM1-43) was used to visualize the effect of propofol on synaptic vesicle exocytosos in the frog neuromuscular junction.
Results: Low concentrations of propofol, ranging from 10 to 25 μmol/L, enhanced spontaneous vesicle exocytosis monitored by FM1-43 in a Ca^{2+}-dependent and Na^{+}-independent fashion. Higher concentrations of propofol (50, 100, and 200 μmol/L) had no effect on spontaneous exocytosis. By contrast, higher concentrations of propofol inhibited the Na^{+}-dependent exocytosis evoked by 4-aminopyridine but did not affect the Na^{+}-independent exocytosis evoked by KCl. This action was similar and non-additive with that observed by tetrodotoxin, a Na^{+} channel blocker.
Conclusion: Our data suggest that propofol has a dose-dependent presynaptic effect at the neuromuscular transmission which may help to understand some of the clinical effects of this agent on neuromuscular function.

Keywords: propofol; neuromuscular junction; frog; FM1-43; synaptic vesicle; general anesthetic

Acta Pharmacologica Sinica (2011) 32: 31–37; doi: 10.1038/aps.2010.175; published online 29 Nov 2010

Introduction

During the last decade, there was a significant progress related to the knowledge of the mechanism of action of general anesthetic. Cellular and molecular mechanisms underlying general anesthesia are not yet fully elucidated but general anesthetics seems to act in both presynaptic and postsynaptic molecular targets[1–4]. There is now a great body of evidences that clinical concentrations of most general anesthetics act on specific ligand-gated ion channels like GABA and glutamate receptors and/or other important ion channels, such as voltage gated sodium channels, potassium channels and HCN-pacemaker channels[3]. Nevertheless, characterizing the molecular targets of general anesthetics has challenged many research groups over the years.

Propofol is one of the most widely used general anesthetic agent for induction and maintenance of anesthesia. Previous works performed in central nervous system (CNS) synapses have shown an inhibition of calcium channels by propofol[5–7]. Other works showed that propofol inhibited calcium-dependent glutamate release evoked by veratridine and 4-AP with greater potency than Na^{+} channel-independent release evoked by KCl[8, 9]. In addition, there were evidences in the literature suggesting that high doses of propofol might have a direct effect on Na^{+} channels[9–13].

It is well described the sedative and hypnotic effects of propofol on CNS. Nevertheless, there are few studies investigating its effect on neuromuscular transmission. Indeed, it has been proposed that propofol has a dual effect on the neuromuscular junction. Low concentrations of propofol stimulate skeletal muscle contractions elicited direct and indirectly[14] but high concentrations of this agent inhibit skeletal muscle contractions evoked direct and indirectly[15, 16]. The mechanisms underlying the neuromuscular effects of propofol include reduction of muscular blood flow, a direct effect on the post-junctional membrane receptors, and reduction on acetylcholine (ACh) release on the neuromuscular junction[17–23].

§ Now in Center for Brain Sciences and Department of Molecular and Cellular Biology, Harvard University, 52 Oxford Street, Cambridge, MA 02138, USA.
* To whom correspondence should be addressed.
E-mail renatogomez2000@yahoo.com.br
Received 2010-07-13 Accepted 2010-09-14

FM1-43 is a fluorescent tool that has been used to study synaptic vesicle recycling at the neuromuscular junction[24–26]. The molecular characteristics of this fluorescent marker allow its internalization during synaptic vesicle endocytosis as well as its release during exocytosis[25]. In the present work, we investigated the effect of propofol on synaptic vesicle exocytosis, a crucial step for neurotransmitter release. We used FM1-43 to visualize the effect of several concentrations of propofol on spontaneous and evoked exocytosis at frog neuromuscular junction.

Materials and methods

Reagents

FM1-43 was purchased from Molecular Probes (Eugene, OR, USA), *d*-tubocurarine, 4-aminopyridine (4AP), tetrodotoxin (TTX), 2APB, dantrolene and omega-conotoxin GVIA were purchased from Sigma-Aldrich (St Louis, MO, USA). Propofol was obtained from Fresenius (Uppsala, Sweden) and azumolene was obtained from Proctor & Gamble (Norwich, NY, USA). All other chemicals and reagents were of analytical grade. All procedures were approved by the local animal care committee (CETEA-UFMG).

Staining and destaining with FM1-43

The frog neuromuscular junction has been an invaluable experimental model for elucidating many aspects of neurotransmission which is the basis of neuronal communication. Two decades ago, Betz and colleagues have introduced the use of the fluorescent dye FM1-43 to visualize synaptic vesicles recycling in motor nerve terminals of the frog neuromuscular junction[24, 25, 27]. Using this powerful tool, it was possible to elucidate the mechanisms that governed synaptic vesicle recycling and consequently neurotransmitter release in several neuronal cell types[28].

In the present work, frog cutaneous pectoris nerve muscle preparations were dissected from Rana catesbeiana (about 60 g) and mounted in a sylgard-lined chamber containing frog Ringer solution (115 mmol/L NaCl, 2.5 mmol/L KCl, 1.8 mmol/L $CaCl_2$, 5 mmol/L HEPES, pH 7.2). FM1-43 (4 μmol/L) was used to stain the recycling pool of synaptic vesicles[25]. This dye presents a hydrophobic tail that reversibly binds to membranes and a polar head that impairs it to fully permeate the plasma membrane[24–28]. Therefore, FM1-43 binds to synaptic membrane and when the nerve terminal is submitted to a stimulus that causes exocytosis of synaptic vesicles and, consequently, a compensatory endocytosis, the fluorescent dye is incorporated, resulting in a typical pattern of staining[25]. After a new round of stimulation, in the absence of FM1-43 in the external medium, the dye is released to the hydrophilic medium, resulting in a decrease of fluorescence intensity, reflecting the exocytosis of synaptic vesicle[24–26]. In our experiments, the muscles were incubated with *d*-tubocurarine (16 μmol/L) to prevent contractions during stimulation. The muscles were stimulated for 10 min with modified Ringer solution (57.5 mmol/L NaCl, 60 mmol/L KCl, 1.8 mmol/L $CaCl_2$, 5 mmol/L HEPES, pH 7.2) in the presence of FM1-43 (4 μmol/L). Thereafter, the preparation was kept resting for 15 min to guarantee FM1-43 uptake. The excess of FM1-43 adhered to the muscle membranes was removed during an one hour washing period in frog Ringer solution. Images were acquired in intervals of 5 min until the end of the experiments. The destaining at the absence of stimulus (photobleaching) was used as a control.

After labeling with FM1-43, neuromuscular preparations were exposed to different concentrations of propofol during 30 min to evaluate its effect on spontaneous exocytosis. Experiments were also performed to investigate the effect of propofol on Na^+-dependent exocytosis evoked by 4AP. After labeling neuromuscular preparations with FM1-43, muscles were exposed to 4AP (1 mmol/L) during 30 min. To test the role of extracellular Na^+ on 4AP-evoked exocytosis, the neuromuscular preparation was initially incubated for 30 min in frog Ringer containing 1.0 μmol/L TTX and, thereafter, it was exposed to 4AP for 30 min. The propofol effect on 4AP-induced exocytosis was investigated by pre-incubation in propofol (100 μmol/L) solution during 10 min before 4AP exposure. Similar protocols were applied to investigate the effects of propofol and TTX on Na^+-independent exocytosis evoked by 60 mmol/L KCl.

Experiments that investigated the role of extracellular Ca^{2+} on the vesicular release induced by propofol were performed in modified Ringer solution without Ca^{2+} but containing EGTA (2.0 mmol/L), an extracellular Ca^{2+} chelator. The preparations were incubated in modified Ringer during 30 min before application of propofol. In experiments performed with the calcium channel blocker omega-conotoxin GVIA, the preparations were pre-incubated in Ringer containing toxin for 30 min before propofol. The participation of intracellular Ca^{2+} stores on the exocytosis evoked by propofol was also investigated. For this purpose, preparations were incubated for 30 min in Ringer containing 2APB (100 μmol/L), an IP_3 receptor blocker, or azumolene (100 μmol/L), a ryanodine receptors blocker before the addition of propofol.

Fluorescence microscopy and imaging analyses

Images were acquired using a fluorescence microscope (Zeiss Axioskop) coupled to a CCD camera (Micromax) and visualized in a computer. The microscope was equipped with water immersion objectives (63×, 0.95 NA and 40×, 0.75 NA). Excitation light came from a 100 W Hg lamp and passed through filters (505/530 nm) to select the fluorescence spectrum. The experimental parameters for collection of images were always identical in control and test contralateral muscles in a given trial.

Statistical analysis

Image analysis was performed using the softwares Image J and Microsoft Excel. The mean fluorescence intensity was determined for each group of spots and plotted against the time as percentage of its mean initial fluorescence using the software Sigma Plot 9.0. Statistical analysis was performed using paired Student's *t*-Test or ANOVA. $P<0.05$ values were

considered statistically significant.

Results

FM1-43 staining and destaining of nerve terminals

Frog cutaneous-pectoris neuromuscular junctions were stained with FM1-43 as previously described[25]. The nerve terminal that was stained with FM1-43 shows fluorescent spots corresponding to clusters of synaptic vesicles that were able to pick up the dye (Figure 1A, upper panel). When this previously labeled terminal was submitted to a new depolarizing stimulus by modified Ringer containing 60 mmol/L KCl, in the absence of FM1-43 in external medium, we observed a significant reduction in fluorescence (Figure 1A, lower panel). The loss of fluorescence was due to dye release to external medium, that correspond to synaptic vesicle exocytosis[25]. Exposure of nerve terminals to illumination without any depolarizing stimulus resulted in a small decrease on fluorescence (maximum 10%) attributable to dye photobleaching[28]. A representative image of the terminal before (upper panel) and after illumination (lower panel), in the absence of stimulus, is shown in Figure 1B. To quantify the decrease in fluorescence that occurs after stimulation with 60 mmol/L KCl and photobleaching, the mean fluorescence intensity for each synaptic vesicle cluster was measured and plotted as gray levels against time (Figure 1C). The small reduction in fluorescence observed corresponds to photobleaching whereas the larger destaining curve obtained during depolarization stimulus corresponds to synaptic vesicle exocytosis.

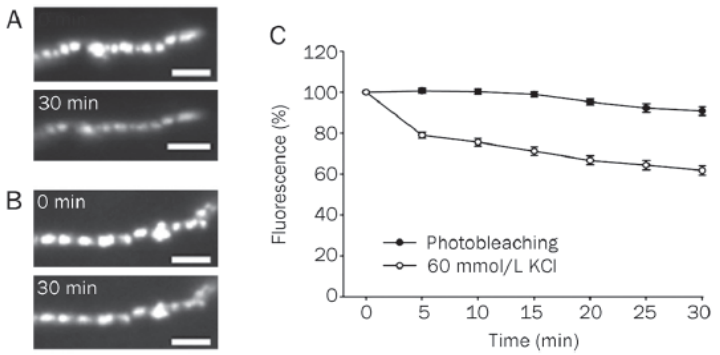

Figure 1. Synaptic vesicles recycling visualized by the fluorescent dye FM1-43. (A) Upper panel: Representative nerve terminal that was incubated in modified Ringer containing 60 mmol/L KCl for 10 min in the presence of FM1-43. Note the formation of fluorescent spots, corresponding to clusters of synaptic vesicles that were able to pick up dye. Lower panel: The same terminal after a second round of depolarization with modified Ringer containing 60 mmol/L KCl, now in the absence of extracellular dye. Note a pronounced destaining of fluorescent spots, corresponding to exocytosis of synaptic vesicles and dye release to the external medium. (B) Representative image of fluorescence loss due to photobleaching during illumination for 30 min. Upper panel: before illumination. Lower panel: after 30 min of illumination. (C) Quantification of FM1-43 fluorescence loss due to photobleaching and KCl fluorescence loss due to exocytosis of synaptic vesicles. The results are mean±SEM of 65 spots from 8 nerve terminals of 4 animals. Scale Bar=10 μm.

Effect of low concentrations of propofol on spontaneous synaptic vesicle exocytosis

Nerve terminals labeled with FM1-43 were bathed in different concentrations of propofol (10 to 200 μmol/L) for 30 min (Figure 2). Fluorescence of representative terminals before and after photobleaching (Figure 2A); propofol 10 μmol/L (Figure 2B), and propofol 200 μmol/L (Figure 2C) were obtained. Low concentrations of propofol ranging from 10 to 25 μmol/L significantly reduced FM1-43 fluorescence, corresponding to exocytosis of previously labeled vesicular clusters (*P<0.01 compared to photobleaching) (Figure 2D). On the other hand, high doses of propofol (50–200 μmol/L) had no effect on FM1-43 destaining from motor nerve terminals (Figure 2D), suggesting a dose-dependent effect of the anesthetic agent.

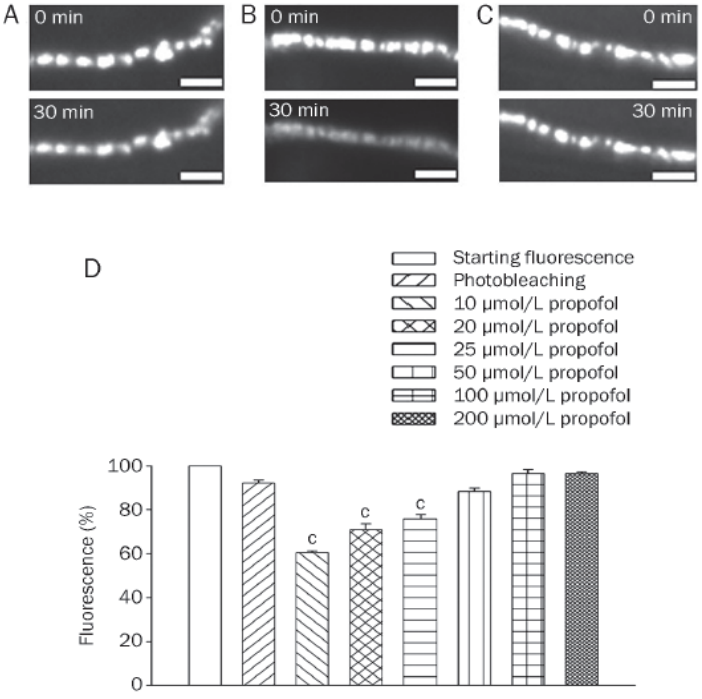

Figure 2. Dose-response curve of exocytosis induced by propofol. (A) Representative image of fluorescence loss due to photobleaching during illumination for 30 min. Upper panel: before illumination. Lower panel: after 30 min of illumination. (B) Representative image of fluorescence loss before (upper panel) and after (lower panel) 30 min in the presence of propofol 10 μmol/L. (C) Representative image of fluorescence loss before (upper panel) and after (lower panel) 30 min in the presence of propofol 200 μmol/L. (D) Quantification of exocytosis evoked by different concentrations of propofol. The results are mean±SEM of 131 fluorescent spots from 15 nerve terminals of 8 animals. °P<0.01 compared to the second bar (photobleaching). Scale Bar=10 μm.

The next set of experiments was performed to identify the mechanism(s) by which low doses of propofol induced exocytosis of synaptic vesicles. Pre-incubation of nerve terminals with TTX (1.0 μmol/L), a voltage-gated Na^+-channel blocker, did not affect the vesicle exocytosis evoked by propofol (data not shown). By contrast, the effect of low doses of propofol

on spontaneous exocytosis monitored by FM1-43 destaining was Ca^{2+}-dependent (Figure 3A). Indeed, we observed a statistically significant inhibition of exocytosis evoked by low doses of propofol in the presence of the external Ca^{2+} chelator EGTA (2.0 mmol/L) or in the presence of omega-toxin GVIA (5 μmol/L), that blocks N-type calcium channels (Figure 3A). The FM1-43 destaining in the presence of GVIA was not significantly different from that due to photobleaching ($P>0.05$). In addition, we observed that the effect of low doses of propofol on synaptic vesicles exocytosis was independent on intracellular Ca^{2+} stores (Figure 3B). Our data suggest that FM1-43 destaining induced by propofol (10 μmol/L) was Ca^{2+} dependent and Na^+-independent.

Effects of high concentrations of propofol on exocytosis evoked by depolarizing stimuli

It has been shown that propofol at concentrations around 100 μmol/L inhibits skeletal muscle evoked contractions[15, 16]. We therefore tested in our system if this concentration of propofol could alter with 4AP-evoked FM1-43 destaining, which is dependent on extracellular Na^+. The incubation of nerve terminals with 4AP (1.0 mmol/L) during 30 min induced a significant FM1-43 destaining (Figure 4A). The destaining evoked by 4AP was reduced by TTX ($P<0.01$ compared to 4AP alone). Pre-incubation of FM1-43 stained nerve terminals with propofol (100 μmol/L) also reduced the 4AP-evoked exocytosis (Figure 4A; $P<0.01$ compared to 4AP alone). Moreover, the simultaneous pre-incubation with propofol (100 μmol/L) and TTX (1.0 μmol/L) produced a significant inhibition of 4AP evoked FM1-43 destaining without any additive effect (Figure 4A), suggesting that propofol reduces the 4AP-induced vesicle exocytosis by blocking Na^+ channels sensitive to TTX.

We next tested the effect of high doses of propofol on Na^+-independent exocytosis evoked by modified Ringer containing 60 mmol/L KCl. Nerve terminals were stained with FM1-43

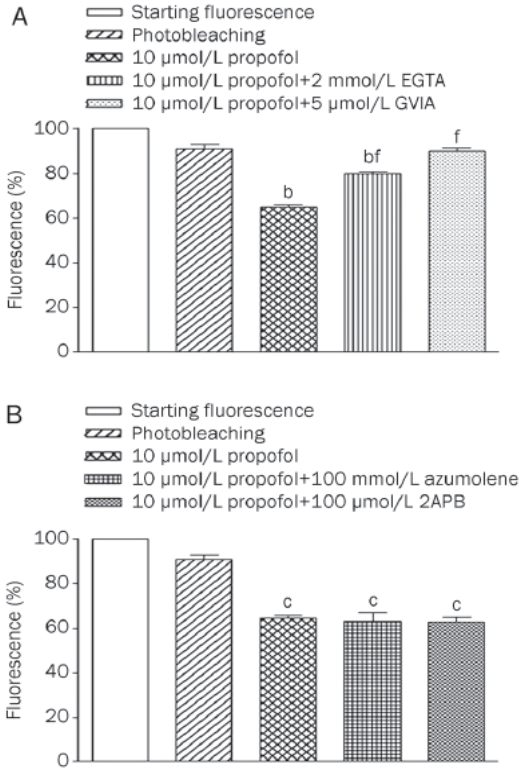

Figure 3. Low doses of propofol evoke synaptic vesicles exocytosis that is dependent on external calcium. (A) FM1-43 destaining evoked by photobleaching (second bar), propofol (10 μmol/L) (third bar), propofol (10 μmol/L)+EGTA (2 mmol/L) (fourth bar), propofol (10 μmol/L)+GVIA (5 μmol/L) (fifth bar). Note that even though EGTA was apparently slightly less effective than GVIA, both agents inhibited the propofol-evoked destaining. The results are mean±SEM of 192 fluorescent spots from 20 nerve terminals of 10 animals. $^bP<0.05$ compared to the second bar (photobleaching). $^fP<0.01$ compared to propofol (10 μmol/L). (B) FM1-43 destaining evoked by photobleaching (second bar), propofol (10 μmol/L) (third bar), propofol (10 μmol/L)+azumolene (100 μmol/L) (fourth bar), propofol (10 μmol/L)+2APB (100 μmol/L) (fifth bar). The results are mean±SEM of 237 fluorescent spots from 18 nerve terminals of 9 animals. $^cP<0.01$ compared to the second bar (photobleaching).

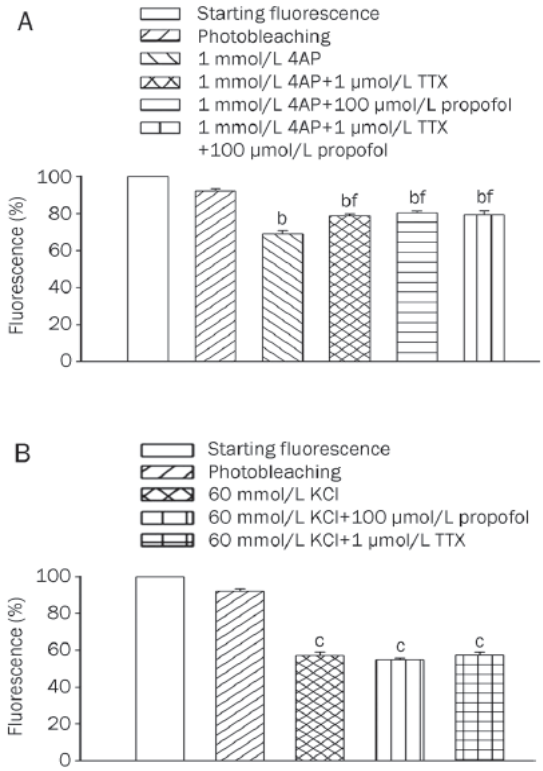

Figure 4. High doses of propofol inhibit synaptic vesicles exocytosis by a Na^+-dependent manner. (A) Graphic comparing FM1-43 destaining evoked by photobleaching (second bar), 4AP (1 mmol/L, third bar), 4AP (1 mmol/L)+TTX (1 μmol/L) (fourth bar), 4AP (1 mmol/L)+propofol (100 μmol/L) (fifth bar) and 4AP (1 mmol/L)+propofol (100 μmol/L)+TTX (1 μmol/L) (sixth bar). The results are mean±SEM of 114 fluorescent spots from 10 nerve terminals of 5 animals. $^bP<0.05$ compared to the second bar (photobleaching). $^fP<0.01$ compared to 4AP (1 mmol/L). (B) Quantification of exocytosis evoked by photobleaching (second bar), KCl (60 mmol/L) (third bar); KCl (60 mmol/L)+propofol (100 μmol/L) (fourth bar); KCl (60 mmol/L)+TTX (1 μmol/L) (fifth bar). The results are mean±SEM of 120 fluorescent spots from 10 nerve terminals of 5 animals. $^cP<0.01$ compared to the second bar (photobleaching).

and we observed a significant reduction on fluorescence after incubation with KCl for 30 min (Figure 4B). Pre-incubation of terminals with TTX had no effect on KCl-evoked reduction in fluorescence, confirming the data that depolarization induced by high concentration of K^+ is independent of extracellular Na^+ [29] (Figure 4B). In addition, pre-incubation with high doses of propofol did not inhibit KCl-evoked Na^+-independent exocytosis (Figure 4B). Taken together, these results suggest that high doses of propofol inhibit synaptic vesicles exocytosis on the neuromuscular junction by a Na^+-dependent manner.

Discussion

Propofol is widely used during general anesthesia, as well as for sedation in the intensive care unit. However, fatigue of the respiratory muscles, especially the diaphragm, may cause respiratory failure. Indeed, it has been demonstrated that volatile (halothane, enflurane, isoflurane, and sevoflurane) and intravenous (propofol and midazolam) anesthetics cause diaphragmatic contractile dysfunction which may probably contributes to acute respiratory failure[19–21, 30–32]. Studies *in vivo* suggested that several mechanisms such as reduction of blood flow, failure of neuromuscular transmission, and impairment of membrane excitation and excitation-contraction (E–C) coupling may be responsible for the neuromuscular effects of propofol. However, *in vivo* studies preclude any specification regarding the mechanism involved on the anesthetic effect and the use of the fluorescent probe FM1-43 enabled us to assess specifically a presynaptic effect of this agent on the neuromuscular junction. Hemmings *et al*[30] had already performed a pioneer study on cultured hippocampal neurons using this fluorescent dye to probe synaptic vesicles exocytosis in the presence of isoflurane and they showed that isoflurane depresses exocytosis evoked by multiple presynaptic targets.

In the present work, we examined the effect of propofol on spontaneous and evoked synaptic vesicle exocytosis at the neuromuscular junction, an experimental model that provides a direct way to investigate neurotransmitter release in an isolated synapse. We found that propofol, at low concentrations ranging from 10 to 25 μmol/L, induced synaptic vesicles exocytosis monitored by FM1-43 destaining on a Ca^{2+}-dependent and Na^+-independent manner. By contrast, high concentrations of propofol ranging from 50 to 200 μmol/L were ineffective to induce synaptic vesicle exocytosis.

It is well known that exocytosis depends on external Ca^{2+}[23] and we observed that in the absence of this ion, there was a significant reduction on FM1-43 destaining evoked by low doses of propofol, suggesting that synaptic vesicles exocytosis evoked by propofol is Ca^{2+}-dependent. In addition, we investigated which calcium channel subtype could be the target of low doses of propofol at the frog neuromuscular junction and we observed an inhibition of propofol evoked exocytosis in the presence of the *N*-type inhibitor omega-conotoxin GVIA. Because the FM1-43 destaining evoked by propofol in the presence of GVIA was similar to that due to photobleaching ($P>0.05$) , we suggest that propofol might act on N-type calcium channels promoting calcium influx that is coupled to synaptic vesicles exocytosis. Different from our data, previous works performed in CNS synapses have shown a predominant inhibition of calcium channels by propofol[5–7]. However, none of them have shown evidences that *N*-type calcium channels could be a target for propofol action. This discrepancy might be due to the fact that these studies were performed in brain slices that maintain intact neuronal circuitry whereas in the present work we were looking at nerve terminals without connection with motor neuron cell bodies. Therefore, we cannot rule out the possibility that propofol may exert an inhibitory effect on calcium channels located at motor neurons' cell bodies that are located at the spinal cord. Because we are looking at events that take place exclusively at the synaptic nerve terminal, such inhibition would not be detected in our experimental model. Nonetheless, our data provide direct evidences that low doses of propofol might act through *N*-type calcium channel that are directly coupled to synaptic vesicle exocytosis at motor nerve terminals. Moreover, we showed that propofol and KCl-evoked exocytosis were not affected by TTX suggesting that both conditions did not increase the synaptic vesicle exocytosis by interfering with Na^+ channels. Therefore, propofol and KCl can induce exocytosis in a Ca^{2+}-dependent and Na^+-independent fashion suggesting that this anesthetic may act directly on Ca^{2+} entry through *N*-type voltage-gated Ca^{2+} channels.

In agreement with our data, it has been observed that low concentrations of propofol increased the amplitude of the indirectly-elicited twitch and tetanic contractions in chick biventer cervices skeletal muscle, indicating that, in low concentrations, this anesthetic may stimulate skeletal muscle[14].

Previous work showed that propofol, at concentrations of 42 and 112 μmol/L, inhibited contraction of isolated rat diaphragm by decreasing ACh release on neuromuscular junction[16]. These authors also observed that this agent inhibited muscle contraction evoked by electrical field stimulation, suggesting that propofol, at this concentration range, may act by inhibiting Ca^{2+} entry through presynaptic voltage-gated Ca^{2+} channels. In the present work high doses of propofol inhibited Na^+-dependent exocytosis evoked by 4AP but did not have any significant effect on Na^+-independent exocytosis evoked by KCl. The decrease on vesicle exocytosis induced by 4AP in the presence of high doses of propofol is in correspondence with data showing a decreasing on the contractility of fatigued canine diaphragm with propofol in a dose-related fashion[21]. Previous studies in rat brain synaptosomes showed that propofol inhibits Ca^{2+}-dependent glutamate release evoked by veratridine and 4-AP with greater potency than Na^+ channel-independent release evoked by KCl[33–36]. In addition, it has been observed that high concentrations of propofol selectively inhibited 4AP-evoked but not KCl-evoked [^{3}H]norepinephrine release[37]. Considering that high doses of propofol inhibited 4AP-evoked synaptic vesicles exocytosis in a similar manner to TTX and did not interfere with KCl-evoked exocytosis, we could suggest that the effect of propofol on neuromuscular junction is thus caused primarily by inhibition of action potential-evoked synaptic vesicle exocytosis at a step upstream of

Ca^{2+} entry through voltage-gated Ca^{2+} channels, possibly as a result of Na^+ channel blockade. In addition, there are evidences in the literature suggesting that high doses of propofol might have a direct effect on Na^+ channels[10, 12, 13]. Finally, experiments in dogs show that administration of propofol decreases diaphragm contractility in a dose-dependent manner and that high dose of this anesthetic produces a progressive decrease in contractility[18]. Based on the data presented here, we could speculate that such diaphragmatic dysfunction might be due to a presynaptic effect of high doses of propofol. In addition, propofol and midazolam seems to cause diaphragm dysfunction through mechanisms other than E–C coupling failure[23]. However, the clinical importance of the present data requires further investigations and we are unable to extrapolate our *in vitro* findings to the clinical practice.

It is difficult to correlate the concentrations of anesthetics used *in vitro* experiments with those used during clinical anesthesia and it has been shown that the doses of intravenous anesthetics required in the case of experimental animals are 10-100 times higher than those used for humans[38]. Plasma concentrations of propofol during anesthesia in humans are estimated to range between 70 and 106 μmol/L[35, 39–41]. Because of the high protein binding (98%), the half-maximal effect free concentration of propofol is around 2.0 μmol/L[35, 42, 43]. It has been suggested that brain concentrations of propofol are about eight-fold higher than plasma free concentrations[44] but there is no estimative of the concentrations on neuromuscular junction. Moreover, the propofol concentration producing loss of righting reflex in Rana pipiens tadpoles ranged between 1 and 10 μmol/L[45] an end point that usually occurs at a lower concentration than surgical anesthesia. Finally, it has been argued that clinically relevant concentrations are difficult to estimate[1-4] and it is important to mention that clinically relevant concentrations of anesthetic are important to examine the integrated responses in the intact animal but their relevance to *in vitro* studies should be taken with care due to our lack of understanding of how to integrate *in vitro* systems into the anesthesia model[46].

In conclusion, we showed that propofol has a dual effect on the exocytosis of cholinergic synaptic vesicles from the neuromuscular transmission and the present results may contribute to understanding some of the clinical effects observed with this agent on neuromuscular function.

Acknowledgements

This work was supported by grants from CNPq, FAPEMIG and CAPES. We thank Dr Hugh C HEMMINGS Jr for valuable comments on this manuscript.

Author contribution

Luciana Ferreira LEITE and Matheus de Castro FONSECA performed research and analysed data; Renato Santiago GOMEZ designed research and wrote the paper; Marcus Vinicius GOMEZ wrote the paper; Cristina GUATIMOSIM design research and analysed data.

References

1 Franks NP, Lieb WR. Molecular and cellular mechanisms of general anaesthesia. Nature 1994; 367: 607–14.
2 Yamakura T, Bertaccini E, Trudell JR, Harris RA. Anesthetics and ion channels: molecular models and sites of action. Annu Rev Pharmacol Toxicol 2001; 41: 23–51.
3 Hemmings HC Jr, Akabas MH, Goldstein PA, Trudell JR, Orser BA, Harrison NL. Emerging molecular mechanisms of general anesthetic action. Trends Pharmacol Sci 2005; 26: 503–10.
4 Franks NP. Molecular targets underlying general anaesthesia. Br J Pharmacol 2006; 147: S72–81.
5 Inoue Y, Shibuya I, Kabashima N, Noguchi J, Harayama N, Ueta Y, *et al*. The mechanism of inhibitory actions of propofol on rat supraoptic neurons. Anesthesiology. 1999; 91: 167-78.
6 Shirasaka T, Yoshimura Y, Qiu DL, Takasaki M. The effects of propofol on hypothalamic paraventricular nucleus neurons in the rat. Anesth Analg 2004; 98: 1017–23.
7 Martella G, De Persis C, Bonsi P, Natoli S, Cuomo D, Bernardi G, *et al*. Inhibition of persistent sodium current fraction and voltage-gated *L*-type calcium current by propofol in cortical neurons: implications for its antiepileptic activity. Epilepsia 2005; 46: 624–35.
8 Ratnakumari L, Hemmings HC Jr. Effects of propofol on sodium channel-dependent sodium influx and glutamate release in rat cerebrocortical synaptosomes. Anesthesiology 1997; 86: 428–39.
9 Lingamaneni R, Birch ML Hemmings HC Jr. Widespread inhibition of sodium channel-dependent glutamate release from isolated nerve terminals by isoflurane and propofol. Anesthesiology 2001; 95: 1460–6.
10 Frenkel C, Urban BW. Human brain sodium channels as one of the molecular target sites for the new intravenous anaesthetic propofol (2,6-diisopropylphenol). Eur J Pharmacol 1991; 208: 75–9.
11 Frenkel C, Duch DS, Urban BW. Effects of iv anaesthetics on human brain sodium channels. Br J Anaesth 1993; 71: 15–24.
12 Lingamaneni R, Hemmings HC Jr. Differential interaction of anaesthetics and antiepileptic drugs with neuronal Na^+ channels, Ca^{2+} channels, and GABA(A) receptors. Br J Anaesth 2003; 90: 199–211.
13 Martella G, De Persis C, Bonsi P, Natoli S, Cuomo D, Bernardi G, *et al*. Inhibition of persistent sodium current fraction and voltage-gated *L*-type calcium current by propofol in cortical neurons: implications for its antiepileptic activity. Epilepsia 2005; 46: 624–35.
14 Wali FA. Effects of some intravenous anaesthetics on the contractile responses produced in the chick biventer cervicis skeletal muscle. Pharmacol Res Commun 1985; 17: 361–76.
15 Lebeda MD, Wegrzynowicz ES, Wachtel RE. Propofol potentiates both pre- and postsynaptic effects of vecuronium in the rat hemidiaphragm. Br J Anaesth 1992; 68: 282–5.
16 Abdel-Zaher AO, Askar FG. The myoneural effects of propofol emulsion (Diprivan) on the nerve-muscle preparations of rats. Pharmacol Res 1997; 36: 323–32.
17 Robertson EN, Fragen RJ, Booij LH, van Egmond J, Crul JF. Some effects of diisopropylphenol (ICI35868) on the pharmacodynamics of atracurium and vecuronium in anaesthetized man. Br J Anaesth 1983; 55: 723–8.
18 Fujii Y, Hoshi T, Takahashi S, Toyooka H. Propofol decreases diaphragmatic contractility in dogs. Anesth Analg 1999; 89: 1557–60.
19 Fujii Y, Hoshi T, Takahashi S, Toyooka H. The effect of sedative drugs on diaphragmatic contractility in dogs: propofol versus midazolam. Anesth Analg 2000; 91: 1035–7.
20 Fujii Y, Uemura A, Toyooka H. The dose-range effects of propofol on the contractility of fatigued diaphragm in dogs. Anesth Analg 2001;

93: 1194–8.
21 Fujii Y, Toyooka H. Midazolam versus propofol for reducing contractility of fatigued canine diaphragm. Br J Anaesth 2001; 86: 879–81.
22 Bouhemad B, Langeron O, Orliaguet G, Coriat P, Riou B. Effects of halothane and isoflurane on the contraction, relaxation and energetics of rat diaphragmatic muscle. Br J Anaesth 2002; 89: 479–85.
23 Nishina K, Mikawa K, Kodama S-I, Kagawa T, Uesugi T, Obara H. The effects of enflurane, isoflurane, and intravenous anesthetics on rat diaphragmatic function and fatigability. Anesth Analg 2003; 96: 1674–8.
24 Betz WJ, Bewick GS. Optical analysis of synaptic vesicle recycling at the frog neuromuscular junction. Science 1992; 255: 200–3.
25 Betz WJ, Mao F, Bewick GS. Activity-dependent fluorescent staining and destaining of living vertebrate motor nerve terminals. J Neurosci 1992; 12: 363–75.
26 Gaffield MA, Betz WJ. Imaging synaptic vesicle exocytosis and endocytosis with FM dyes. Nat Protoc 2006; 1: 2916–21.
27 Guatimosim C, Romano-Silva MA, Gomez MV, Prado MAM. Use of fluorescent probes to follow membrane traffic in nerve terminals. Braz J Med Biol Res 1998; 31: 1491–500.
28 Rizzoli SO, Richards DA, Betz WJ. Monitoring synaptic vesicle recycling in frog motor nerve terminals with FM dyes. J Neurocytol 2003; 32: 539–49.
29 Nicholls DG. The glutamatergic nerve terminal. Eur J Biochem 1993; 212: 613–31.
30 Hemmings HC Jr, Yan W, Westphalen RI, Ryan TA. The general anesthetic isoflurane depresses synaptic vesicle exocytosis. Mol Pharmacol 2005; 67: 1591–9.
31 Kochi T, Ide T, Isono S, Mizuguchi T, Nishino T. Different effects of halothane and enflurane on diaphragmatic contractility *in vivo*. Anesth Analg 1990; 70: 362–8.
32 Ide T, Kochi T, Isono S, Mizuguchi T. Diaphragmatic activity during isoflurane anaesthesia in dogs. Acta Anaesthesiol Scand 1993; 37: 253–7.
33 Kagawa T, Maekawa N, Mikawa K, Nishina K, Yaku H, Obara H. The effect of halothane and sevoflurane on fatigue-induced changes in hamster diaphragmatic contractility. Anesth Analg 1998; 86: 392–7.
34 Südhof TC. The synaptic vesicle cycle: a cascade of protein-protein interactions. Nature 1995; 375: 645–53.
35 Ratnakumari L, Hemmings HC Jr. Effects of propofol on sodium channel-dependent sodium influx and glutamate release in rat cerebrocortical synaptosomes. Anesthesiology 1997; 86: 428–39.
36 Lingamaneni R, Birch ML, Hemmings HC Jr. Widespread inhibition of sodium channel-dependent glutamate release from isolated nerve terminals by isoflurane and propofol. Anesthesiology 2001; 95: 1460–6.
37 Pashkov VN, Hemmings HC Jr. The effects of general anesthetics on norepinephrine release from isolated rat cortical nerve terminals. Anesth Analg 2002; 95: 1274–81.
38 Wakasugi M, Hirota K, Roth SH, Ito Y. The effects of general anesthetics on excitatory and inhibitory synaptic transmission in area CA1 of the rat hippocampus *in vitro*. Anesth Analg 1999; 88: 676–80.
39 Smith C, McEwan AI, Jhaveri R, Wilkinson M, Goodman D, Smith R, *et al*. The interaction of fentanyl on the CP50 of propofol for loss of consciousness and skin incision. Anesthesiology 1994; 81: 820–8.
40 Kazama T, Ikeda K, Morita K. The pharmacodynamic interaction between propofol and fentanyl with respect to the suppression of somatic or hemodynamic responses to skin incision, peritoneum incision, and abdominal wall retraction. Anesthesiology 1998; 89: 894–06.
41 Haeseler G, Störmer M, Bufler J, Dengler R, Hecker H, Piepenbrock S, *et al*. Propofol blocks human skeletal muscle sodium channels in a voltage-dependent manner. Anesth Analg 2001; 92: 1192–8.
42 Servin F, Desmonts JM, Haberer JP, Cockshott ID, Plummer GF, Farinotti R. Pharmacokinetics and protein binding of propofol in patients with cirrhosis. Anesthesiology 1988; 69: 887–91.
43 Rehberg B, Duch DS. Suppression of central nervous system sodium channels by propofol. Anesthesiology 1999; 91: 512–20.
44 Shyr MH, Tsai TH, Tan PP, Chen CF, Chan SH. Concentration and regional distribution of propofol in brain and spinal cord during propofol anesthesia in the rat. Neurosci Lett 1995; 184: 212–5.
45 Tonner PH, Poppers DM, Miller KW. The general anesthetic potency of propofol and its dependence on hydrostatic pressure. Anesthesiology 1992; 77: 926–31.
46 Eckenhoff RG, Johansson JS. On the relevance of "clinically relevant concentrations" of inhaled anesthetics in *in vitro* experiments. Anesthesiology 1999; 91: 856–60.

10. ANEXO 3: Artigo publicado durante o mestrado

EJN fens EUROPEAN JOURNAL OF NEUROSCIENCE

European Journal of Neuroscience, Vol. 38, pp. 2978–2987, 2013 doi:10.1111/ejn.12300

MOLECULAR AND SYNAPTIC MECHANISMS

Membrane cholesterol regulates different modes of synaptic vesicle release and retrieval at the frog neuromuscular junction

Hermann A. Rodrigues,[1] Ricardo F. Lima,[2,*] Matheus de C. Fonseca,[1] Ernani A. Amaral,[1,†] Patrícia M. Martinelli,[1] Lígia A. Naves,[2] Marcus V. Gomez,[3,4] Christopher Kushmerick,[2] Marco A. M. Prado[5] and Cristina Guatimosim[1]
[1]Departamento de Morfologia, Universidade Federal de Minas Gerais, Av. Antônio Carlos, 6627, Belo Horizonte, MG 31270-901, Brasil
[2]Departamento de Fisiologia e Biofísica, Universidade Federal de Minas Gerais, Belo Horizonte, Brasil
[3]Núcleo Santa Casa de Pós-Graduação, Universidade Federal de Minas Gerais, Belo Horizonte, Brasil
[4]INCT Molecular Medicine, Universidade Federal de Minas Gerais, Belo Horizonte, Brasil
[5]Robarts Research Institute and Department of Physiology and Pharmacology and Anatomy & Cell Biology, University of Western Ontario, London, ON, Canada

Keywords: cholesterol, fluorescence microscopy, FM1-43, neuromuscular junction, synaptic vesicle

Abstract

We investigated the effects of cholesterol removal on spontaneous and KCl-evoked synaptic vesicle recycling at the frog neuromuscular junction. Cholesterol removal by methyl-β-cyclodextrin (MβCD) induced an increase in the frequency of miniature end-plate potentials (MEPPs) and spontaneous destaining of synaptic vesicles labeled with the styryl dye FM1-43. Treatment with MβCD also increased the size of MEPPs without causing significant changes in nicotinic receptor clustering. At the ultrastructural level, synaptic vesicles from nerve terminals treated with MβCD were larger than those from control. In addition, treatment with MβCD reduced the fusion of synaptic vesicles that are mobilized during KCl-evoked stimulation, but induced recycling of those vesicles that fuse spontaneously. We therefore suggest that MβCD might favor the release of vesicles that belong to a pool that is different from that involved in the KCl-evoked release. These results reveal fundamental differences in the synaptic vesicle cycle for spontaneous and evoked release, and suggest that deregulation of cholesterol affects synaptic vesicle biogenesis and increases transmitter packing.

Introduction

Many studies in the last two decades have reported the presence of membrane microdomains with elevated proportions of cholesterol, sphingolipids and glycolipids (for a review see Lingwood *et al.*, 2009). These microdomains, named membrane rafts, are thought to allow the preferential association of many proteins (Simons & van Meer, 1988; Brown & Rose, 1992; Simons & Ikonen, 1997). More than 200 proteins have been localized to rafts (Foster *et al.*, 2003) including those related to control of the synaptic vesicle cycle, which is a key step for neurotransmitter release at the synapse (Yoshinaka *et al.*, 2004).

Synaptic vesicle exocytosis is regulated by a set of proteins, including the SNARE complex, which mediates the fusion of synaptic vesicles with the presynaptic membrane at active zones (reviewed by Murthy & De Camilli, 2003; Sudhof, 2004). In this context, it is noteworthy that changes in cholesterol content have a strong impact on synaptic transmission (Thiele *et al.*, 2000; Cho *et al.*, 2007). Zamir & Charlton (2006) reported that acute depletion of cholesterol with methyl-β-cyclodextrin (MβCD) blocked action potential conductance in the crayfish neuromuscular junction (NMJ) and increased miniature end-plate potential (MEPP) frequency. In hippocampal neurons, Wasser *et al.* (2007) observed that removal of synaptic vesicle cholesterol with MβCD resulted in an increase in the frequency of miniature excitatory postsynaptic current events and a decrease in evoked vesicle fusion. Taken together these findings suggested that the presence of cholesterol favors evoked synaptic vesicle fusion over spontaneous release, suggesting some fundamental difference in the vesicle pools that contribute to each form of release, or to intrinsic differences in the release mechanisms for evoked vs. spontaneous release, or both. Although vesicle pools in the vertebrate NMJ have been extensively characterized (Rizzoli & Betz, 2005), there is still no consensus of whether spontaneous release and evoked release come from the same pool (Alabi & Tsien, 2012), and if not what are the differences. Here we investigated the effects of MβCD on synaptic vesicle recycling at

Correspondence: Dr C. Guatimosim, as above.
E-mail: cguati@icb.ufmg.br

**Present address*: Departamento de Fisiologia e Farmacologia, Centro de Ciências da Saúde, Universidade Federal do Ceará, Fortaleza, Brasil.

†*Present address*: Instituto de Ciências e Tecnologia, Universidade Federal dos Vales do Jequitinhonha e Mucuri, Diamantina, Brasil.

Received 29 March 2013, revised 4 June 2013, accepted 9 June 2013

the frog NMJ using electrophysiology, optical and electron microscopy techniques to examine changes to evoked and spontaneous release and to the structure of the synapse during cholesterol depletion.

Material and methods

Drugs and chemicals

FM1-43, Vybrant Lipid Raft Kit and α-bungarotoxin-Alexa 594 were purchased from Invitrogen (Carlsbad, CA, USA); MβCD, hydroxypropyl-γ-cyclodextrin (HγCD) and D-tubocurarine were purchased from Sigma-Aldrich (St Louis, MO, USA). All other chemicals and reagents were of analytical grade.

Nerve-muscle preparations

All procedures were approved by the local animal care committee (CETEA-UFMG) and followed NIH guidelines for the care and use of laboratory animals. Experiments were performed on NMJs from frogs (*Rana catesbeiana)* weighing ~60 g. Frogs were killed by decapitation. The cutaneous pectoris muscle and a segment of its attached nerve were then dissected out and maintained in frog Ringer solution (115 mM NaCl, 2.5 mM KCl, 1.8 mM $CaCl_2$, 5 mM HEPES, pH adjusted to 7.2 with NaOH). Unless stated otherwise, all treatments and measurements were carried out in frog Ringer. During all imaging experiments, D-tubocurarine (16 μM) was included in the frog Ringer to prevent contractions. During electrophysiological experiments, tetrodotoxin (300 nM) was included in the frog Ringer to avoid action potentials.

Measuring exo- and endocytosis with FM1-43

Experiments with FM1-43 were done according to protocols described by Betz *et al.* (1992), Betz & Bewick (1992) and Guatimosim *et al.* (1998a,b). Cutaneous pectoris muscles were stained by incubating in high-K^+ (60 mM) frog Ringer containing FM1-43 (4 μM) for 10 min. After KCl (60 mM) stimulation, preparations were maintained in normal frog Ringer (+ FM1-43) for 15 min to allow FM1-43 uptake during the compensatory endocytosis that occurs after stimulation. Following labeling, muscles were washed for > 1 h in normal frog Ringer to remove extracellular FM1-43.

To investigate the effects of cholesterol removal on synaptic vesicle exocytosis, preparations labeled with FM1-43 were exposed to MβCD (1–10 mM) for 30 min at room temperature (25 °C). The same protocol was used for experiments using electron microscopy. As MβCD can bind FM dyes (Dason *et al.*, 2010), in experiments to assess the role of MβCD on endocytosis we used a modified protocol. The preparations were pre-incubated with MβCD (10 mM) for 30 min, washed for 15 min to remove the drug and then stimulated with KCl (60 mM) in the presence of FM1-43 as described above.

Staining of lipid rafts at frog NMJs

To stain lipid rafts at frog motor nerve terminals, we used the fluorescent subunit B from cholera toxin (CTxB-Alexa 488) available in the Vybrant Lipid Raft Kit (Invitrogen). Cutaneous pectoris muscles were incubated for 15 min in Ringer containing CTxB-Alexa 488 (1 μg/mL). Then, the muscles were incubated for 15 min with the antibody anti-CTxB and then fixed with paraformaldehyde (4%, in PBS) at 4 °C for 40 min. To investigate the effects of cholesterol removal on membrane rafts, muscles were pre-incubated with MβCD (10 mM) or HγCD (10 mM) for 30 min before labeling with CTxB-Alexa 488. Staining of nerve terminals in preparations treated with MβCD (10 mM) or HγCD (10 mM) was compared with that obtained in untreated controls.

Staining of nicotinic receptors at frog NMJs

Cutaneous pectoris muscles were incubated for 20 min with α-bungarotoxin-Alexa 594 (4 μg/mL). After labeling, muscles were washed and fixed with paraformaldehyde (4%, in PBS) at 4 °C. To investigate the effects of cholesterol sequestration on nicotinic acetylcholine receptor (nAChR) clusters, frog NMJs were pre-incubated with MβCD (10 mM) for 30 min before labeling with α-bungarotoxin.

Fluorescence microscopy and image analyses

Images of frog NMJs stained with FM1-43 were acquired using a fluorescence microscope (Leica DM2500) equipped with water-immersion objectives [63 ×, 0.95 NA and (or) 40 ×, 0.75 NA] and coupled to a CCD camera (12 bits, DFC345FX; Leica) and visualized on a computer screen using Leica Application Suite 4.0 software. Images of frog motor terminals labeled with CTxB-Alexa 488 and α-bungarotoxin-Alexa 594 were collected in a confocal microscope (Zeiss LSM 510 from CEMEL, ICB-UFMG) using a 40 × (1.30 NA) oil objective. An argon and helium–neon laser were used for excitation of terminals stained with CTxB-Alexa 488 and nAChR clusters marked with α-bungarotoxin, respectively.

Electrophysiological recordings

Standard intracellular recording techniques were used to record MEPPs with an Axoclamp-2A amplifier (Molecular Devices, Sunnyvale, CA, USA). The 10-times V_m output of the amplifier was band-pass filtered (0.1 Hz–10 KHz) and amplified a further 500-fold prior to digitization and acquisition on a computer running WinEDR (John Dempster, University of Strathclyde). Microelectrodes were fabricated from borosilicate glass and had resistances of 8–15 MΩ when filled with 3 M KCl. The membrane potential was also recorded and used to correct MEPP sizes to a standard resting potential of −80 mV using the method of Katz & Thesleff (1957). MβCD was added directly to the bath from a Ringer stock solution to the final concentrations given in the text.

Transmission electron microscopy

For ultrastructural analysis, preparations were incubated for 30 min with frog Ringer solution (control), or with frog Ringer containing MβCD (10 mM) or HγCD (10 mM). Following the incubation period, tissue was fixed in ice-cold modified Karnovsky fixative solution (4% paraformaldehyde and 2.5% glutaraldehyde in 0.1 M sodium cacodylate buffer at 4 °C) overnight, washed with cacodylate buffer (0.1 M), cut into four pieces, post-fixed in reduced osmium (2% osmium tetroxide containing 1.6% potassium ferrocyanide), contrasted *en bloc* with uranyl acetate (2%), dehydrated through an ascending series of ethanol solutions and embedded in EPON. The blocks were then sectioned (50 nm) and collected on 200-mesh copper grids and contrasted with lead citrate. The sections were viewed with a 120-kV electron microscope (Tecnai-G2-Spirit-FEI/Quanta microscope; Philips, Eindhoven, The Netherlands). Experiments and analyses involving electron microscopy were performed in the Center of Microscopy at the Universidade Federal de Minas Gerais, Belo Horizonte, MG, Brazil (http://www.microscopia.ufmg.br).

EM image analysis

NMJs were identified based on the presence of junctional folds in the postsynaptic membrane. Single sections through the NMJ were traced and the terminal areas and synaptic vesicle number were determined. Synaptic vesicle distribution was evaluated by quantification of the vesicles located at different distances from the active zone within the selected area, as described by Becherer *et al.* (2001) and Hua *et al.* (2011) and the vesicles counted were marked to prevent their recounting. We counted the number of vesicles located within 10–50 nm of the presynaptic membrane. Vesicle circumference was calculated as $C = 2\pi[(d_1^2 + d_2^2)/2]^{0.5}$ considering the longest diameter (d_1) and the diameter at right angles (d_2) according to Van der Kloot *et al.* (2002). Synaptic vesicle shape was quantified using the shape factor described by Croft *et al.* (2005): shape factor = $(4 \times \pi \times \text{area})/(\text{perimeter})^2$. This parameter reaches a maximum of 1 for a circular object. All image analysis in this study was performed 'blind' in the sense that the person performing the analysis did not know what treatment the sample had received.

Statistical analysis

Image analysis was performed using the program ImageJ (Wayne Rasband, National Institutes of Health, Bethesda, MD, USA). Data were analysed in Microsoft Excel and plotted using the program SigmaPlot 10.0 (SyStat Software) or GraphPad Prism 4 or Igor (Wavemetrics). Statistical significance was evaluated using the paired or un-paired Student's *t*-test or the Kolmogorov–Smirnov test, as described in the text. Values of $P < 0.05$ were considered significant.

Results

To investigate the effects of cholesterol on exo- and endocytosis at the frog NMJ we used MβCD, a cyclic dextrin with a hydrophobic core that extracts cholesterol from the cellular membrane (Kilsdonk *et al.*, 1995). Figure 1A shows representative images of nerve terminals previously labeled with FM1-43 before (upper panels) or after (lower panels) treatment with KCl (60 mM), MβCD (10 mM) or HγCD (10 mM). As expected, KCl (60 mM) caused strong destaining of the nerve terminal that reflects loss of FM dye due to exocytosis of labeled synaptic vesicles (Betz *et al.*, 1992). Treatment with MβCD (10 mM) also caused strong FM destaining whereas HγCD [a cyclic dextrin with a much lower affinity for cholesterol (Ohtani *et al.*, 1989)] had no effect, suggesting that cholesterol removal stimulates exocytosis. Figure 1B shows destaining curves for MβCD (1, 5 and 10 mM), photobleaching (control) and KCl (60 mM). Results from independent experiments are summarized in Fig. 1C. Destaining by MβCD was significantly greater than photobleaching controls for concentrations of 5 mM ($t_4 = 5.45$, $P = 0.006$, unpaired Student's *t*-test) and 10 mM ($t_4 = 7.95$, $P = 0.001$, unpaired Student's *t*-test). Destaining by HγCD (10 mM) was not different from photobleaching control ($t_2 = 0.10$, $P = 0.93$, unpaired Student's *t*-test).

To confirm membrane raft disruption by MβCD (10 mM), we used the fluorescent subunit B from cholera toxin (CTxB-Alexa 488), which has affinity for the ganglioside GM1 located at membrane rafts (Harder *et al.*, 1998). Pre-incubation of neuromuscular preparations with HγCD (10 mM for 30 min) did not cause any significant change in CTxB labeling of motor terminals ($t_4 = 1.7$, $P = 0.17$; unpaired Student's *t*-test; Fig. 1D and E). On the other hand, pre-incubation with MβCD (10 mM for 30 min) significantly inhibited staining with fluorescent CTxB ($t_4 = 9$, $P = 0.0008$; unpaired Student's *t*-test; 45 nerve terminals per experimental condition; Fig. 1D and E, for quantification). The results obtained based on fluorescently labeled CTxB binding to membrane surface GM1 provided a visual confirmation that rafts were successfully disrupted by the treatment with MβCD.

We next investigated whether MβCD-induced FM1-43 destaining at frog NMJs was due to an increase in spontaneous synaptic vesicle fusion with the plasma membrane. To test this, we measured MEPPs in the same fiber before and during treatment with MβCD or HγCD. Treatment with MβCD (10 mM) induced a time- and dose-dependent increase in MEPP frequency that was not observed with HγCD (10 mM). Figure 1F shows a single representative experiment in which the increase in MEPP frequency is visible in the membrane potential traces or as a leftward shift in the distribution of MEPP intervals. For statistical analysis, MEPP frequency for each experiment was normalized to its own control before averaging, and we tested whether the average normalized frequency was greater than 1 (Fig. 1G). These data showed that MβCD caused a dose- and time-dependent increase in MEPP frequency that was not observed in preparations treated with HγCD. Application of MβCD (10 mM, 5 min) increased MEPP frequency by 18 ± 1.6-fold (mean ± SEM; $t_3 = 10.6$, $P = 0.0018$, single sample *t*-test, $n = 4$) whereas in preparations treated with HγCD (10 mM, 5 min) MEPP frequency was 0.95 ± 0.12 of control ($t_3 = 0.42$, $P = 0.70$, single sample *t*-test, $n = 4$).

In addition to the increase in MEPP frequency described above, treatment with MβCD also increased the size of MEPPs (Fig. 2). In experiments in which MEPPs were recorded from the same fiber before and during treatment with MβCD (2.5 mM, 10 min), MEPP amplitudes were increased by 25 ± 12% (mean ± SEM; $P < 0.05$, $n = 3$, Kolmogorov–Smirnov test). We also observed that the half-width of MEPPs was increased after treatment with MβCD, as can be observed in Fig. 2A in which the broken line represents the control MEPP scaled to peak amplitude of the MEPP recorded after MβCD. To quantify the effect of MβCD on the MEPP time course, we measured the area under the MEPP by calculating its time integral. MβCD (2.5 mM, 10 min) increased MEPP integrals by 60 ± 25% (mean ± SEM; $P < 0.05$; Kolmogorov–Smirnov test; $n = 3$; compare Fig. 2B).

The slowing of the MEPP decay, reflected in a larger time integral, could result from an inhibitory action of MβCD on acetylcholinesterase. To test this, we measured the effect of MβCD after pre-treatment with neostigmine (10 μM, 30 min). As expected, neostigmine increased MEPP areas (Fig. 2C). In the presence of neostigmine, MβCD (2.5 mM, 10 min) further increased MEPP integrals by 60 ± 10% (mean ± SEM; $P < 0.05$; Kolmogorov–Smirnov test; $n = 3$), indicating an effect that was additive to the effect of neostigmine (compare Fig. 2B and C). Hence, the effect of MβCD was not due to inhibition of acetylcholinesterase.

A second possible explanation for the increase in MEPP size after MβCD may be related to changes on proper clustering of nAChRs at the NMJ as the stability of these receptors is extremely important to the correct functioning of cholinergic synapses. To test this possibility, we stained nAChR clusters with α-bungarotoxin-Alexa 594 after pre-incubation with MβCD (10 mM). These experiments revealed no morphological alterations in comparison with that obtained in control condition (Fig. 2D). Although treatment with MβCD revealed a small tendency to increase the intensity of labeling with fluorescent bungarotoxin, this might be a consequence of a better accessibility of the toxin to the nAChR clusters after cholesterol sequestration. Thus,

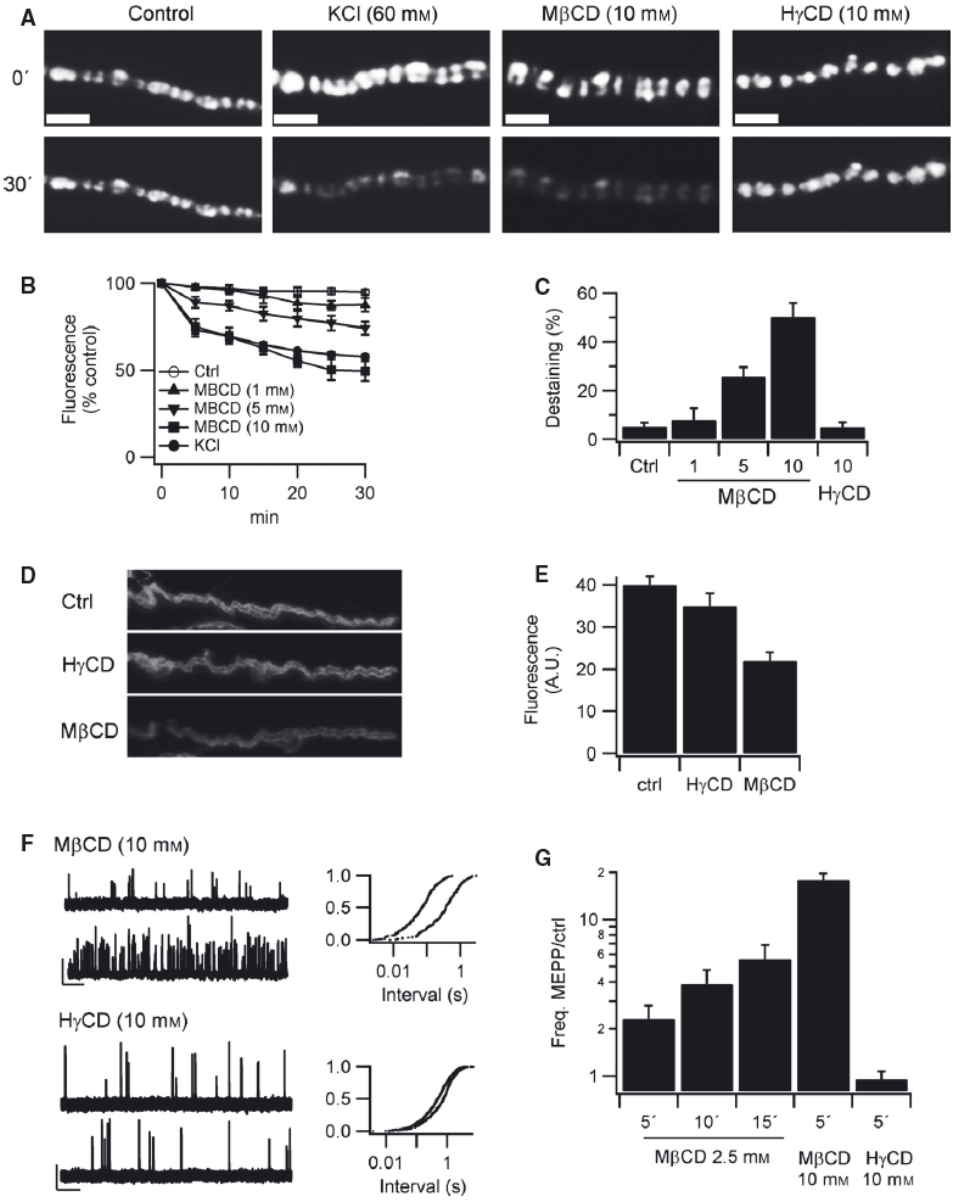

FIG. 1. MβCD evokes exocytosis at the frog NMJ and disrupts membrane rafts. (A) Fluorescence images of nerve terminals after labeling the recycling vesicle pool with the fluorescent dye FM1-43 by stimulation followed by extensive washing. Upper panels show initial staining and lower panels show remaining fluorescence after 30 min in the indicated treatments (control, 60 mM KCl, 10 mM MβCD or 10 mM HγCD, a negative control for non-specific effects of cyclodextrins). (B) Dose and time dependence of destaining evoked by MβCD. Traces from top to bottom are control, MβCD (1, 5 and 10 mM) and KCl (60 mM) averaged from three independent experiments. (C) Destaining quantification after 30 min treatment with cyclodextrins at the concentrations shown (in mM) (n = 3 animals per experimental condition. *P < 0.05). (D) Images of nerve terminals stained with Alexa-488-labeled cholera toxin B in control or cyclodextrin-treated preparations. (E) Quantification of cholera toxin staining from three independent experiments (*P < 0.05). (F) MEPPs recorded with an intracellular electrode. Upper panels of each pair show a 10-s portion of the recording immediately before addition of cyclodextrin (10 mM MβCD or 10 mM HγCD as indicated) and lower panels show recording from the same junction after 5 min treatment. Scale bars are 0.5 mV and 1 s. Panels to the right give the cumulative frequency distribution of intervals between successive MEPPs from the same recordings. Black traces are in control and grey traces after treatment with cyclodextrin. Note logarithmic scale on the ordinate. (G) Time- and concentration-dependence of cyclodextrins on the frequency of MEPPs. At each junction, MEPPs were recorded in control and after treatment with cyclodextrin at the concentration and for the times indicated. For each junction tested, effects were measured as the frequency of MEPP measured after treatment divided by the frequency in control in the same end plate (n = 4 animals per experimental condition; *P < 0.05).

treatment with MβCD does not appear to generate any gross disruptions to postsynaptic AChR receptors in our model.

We next examined NMJs at the ultrastructural level to determine if MβCD causes changes to the structure of the synaptic terminals. Preparations treated with MβCD (10 mM) or HγCD (10 mM) showed no difference regarding surface area [Fig. 3A–D; Control: 3.4 ± 0.25 μm^2 (mean ± SEM) (15 nerve terminal profiles); HγCD: 3.7 ± 0.18 μm^2 (15 nerve terminal profiles); MβCD: 3.1 ± 0.31 μm^2 (18 nerve terminal profiles); t_2 = 1.04, P = 0.36 for control vs. HγCD; t_2 = 0.71, P = 0.52 for control vs. MβCD; unpaired Student's t-test]. The same was observed for the total number of synaptic vesicles [Fig. 3A–C and E; Control: 110 ± 8.0 (mean ± SEM) (15 nerve terminal profiles); HγCD: 127 ± 5.0 (15 nerve terminal profiles); MβCD: 123 ± 2.0 (18 nerve terminal profiles); t_2 = 1.626, P = 0.1793 for control vs. HγCD; t_2 = 1.439, P = 0.2236 for control vs. MβCD; unpaired Student's t-test].

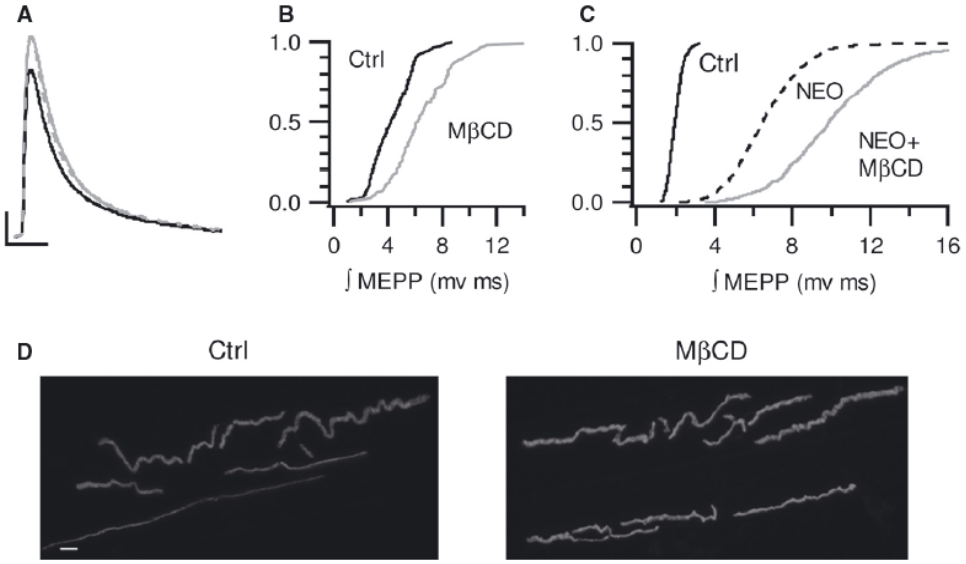

FIG. 2. MβCD increases quantal size. (A) Representative MEPP recorded before (ctrl) and after treatment with MβCD (2.5 mM, 10 min), as indicated. The broken line represents the control MEPP scaled to the peak amplitude of the MβCD-treated MEPP. Scale bars are 5 ms and 0.2 mV. (B) Distribution of MEPP voltage–time integrals recorded from an end-plate before (ctrl) and after MβCD (2.5 mM, 10 min), as indicated (n = 4 animals per experimental condition). (C) Distribution of MEPP voltage–time integrals from a muscle end-plate before (ctrl) and after 30 min treatment with neostigmine (10 μM, NEO), an inhibitor of the acetylcholine esterase and after further treatment with NEO + MβCD (2.5 mM, 10 min) (n = 4 animals per experimental condition). (D) Images of nAChR labeled with α-bungarotoxin conjugated to Alexa-594 from two different neuromuscular preparations in control condition or after 30 min incubation with MβCD (10 mM). Scale bar: 10 μm (n = 3 animals per experimental condition).

We compared the circumference (Van der Kloot *et al.*, 2002) and shape (Croft *et al.*, 2005) of synaptic vesicles of motor terminals from control and those treated with HγCD and MβCD. We observed an increase in the circumference of synaptic vesicles in terminals treated with MβCD (10 mM) when compared with untreated terminals or terminals treated with HγCD (10 mM) [Fig. 3F: control = 239 ± 1.5 nm (mean ± SEM); HγCD = 240 ± 1.5 nm; MβCD = 249 ± 1.6 nm; $P > 0.05$ for HγCD vs. control and $P < 0.01$ for MβCD vs. control and HγCD; Kolmogorov–Smirnov test; 322 synaptic vesicles from 15 nerve terminal profiles for control and HγCD and 18 nerve terminal profiles for MβCD]. In contrast, we observed no change in the shape factor (SF) in any of the experimental groups (Fig. 3G – untreated control: SF = 0.923 ± 0.002; HγCD: SF = 0.921 ± 0.0018; MβCD: SF = 0.924 ± 0.0019; $P > 0.05$; Kolmogorov–Smirnov test; 322 synaptic vesicles from 15 nerve terminal profiles for control and HγCD and 18 nerve terminal profiles for MβCD).

We next investigated the effects of MβCD (10 mM) on KCl (60 mM)-evoked synaptic vesicle release measured as FM dye destaining evoked by KCl (60 mM). Control preparations labeled with FM 1-43 were readily destained with KCl (60 mM) [Fig. 3H second bar; 43.64 ± 1.898% (mean ± SEM); $t_2 = 14.92$, $P = 0.0001$; unpaired Student's t-test; 15 fluorescent spots from three terminals for each condition]. In contrast, when preparations were first partially destaining by MβCD (10 mM, 30 min), no further destaining was observed when KCl was applied [Fig. 3H, third and fourth bar, respectively; KCl + MβCD = 34.67 ± 2.219% (mean ± SEM); MβCD = 30.07 ± 1.067%; $t_2 = 1.871$, $P = 0.1347$; unpaired Student's t-test; 15 fluorescent spots from three terminals for each condition]. We thus suggest that after treatment with MβCD (10 mM), the remaining labeled synaptic vesicles cannot be released by KCl.

Exocytosis and FM dye destaining evoked by KCl depend on Ca^{2+} influx through the voltage-gated calcium channel (VGCC; Guatimosim *et al.*, 1997). To investigate if MβCD treatment inhibits exocytosis through inhibition of the VGCC, we compared the amount of destaining by the calcium ionophore ionomycin (10 μM) in untreated preparations and in preparations pre-treated with MβCD (10 mM, 30 min), then washed to avoid possible sequestration of ionomycin by MβCD. We observed a statistically significant inhibition of exocytosis evoked by ionomycin after treatment with MβCD [Fig. 3H compare fifth and sixth bars; ionomycin = 42.80 ± 2.041% (mean ± SEM); ionomycin + MβCD = 33.92 ± 2.386%; $t_2 = 2.828$, $P < 0.05$; unpaired Student's t-test; 15 fluorescent spots from three nerve terminals for each condition]. These results indicate that treatment with MβCD inhibits Ca^{2+}-dependent exocytosis.

After evoked exocytosis, synaptic vesicle pools are replenished by compensatory endocytosis (Ceccarelli *et al.*, 1973; Heuser & Reese, 1973; Richards *et al.*, 2001; reviewed by Royle & Lagnado, 2003). Endocytosis can be studied by observing the uptake of FM1-43 in response to stimulation (Ribchester *et al.*, 1994). To investigate the effect of cholesterol removal on endocytosis, preparations of frog NMJs were pre-incubated with MβCD (10 mM) or HγCD (10 mM) before staining with FM1-43 under KCl stimulation (see Methods). Pre-incubation with MβCD significantly reduced FM1-43 uptake induced by KCl (60 mM) (compare Fig. 4A and C). When we measured the fluorescence intensity from several spots, we observed that the NMJ pre-incubated with MβCD showed a lower intensity fluorescent signal (91.49 ± 7.036 arbitrary units (AU); mean ± SEM) than those incubated with KCl alone (138.3 ± 6.788 AU) and pre-incubated with HγCD (147.7 ± 6.112 AU). Furthermore, when MβCD (10 mM) was used as the secretagogue we did not observe FM1-43 uptake in nerve terminals ($t_2 = 4.792$, $P = 0.0001$ for MβCD pre-incubated vs. KCl alone; unpaired Student's t-test; $t_2 = 6.035$, $P < 0.0001$ for MβCD pre-incubated vs. HγCD; unpaired Student's t-test; 45 fluorescent spots from three nerve terminals for each condition; Fig. 4D and E).

Previous studies have suggested that spontaneously released vesicles do not belong to the readily releasable pool (RRP, vesicles immediately available for evoked release) (Sara *et al.*, 2005).

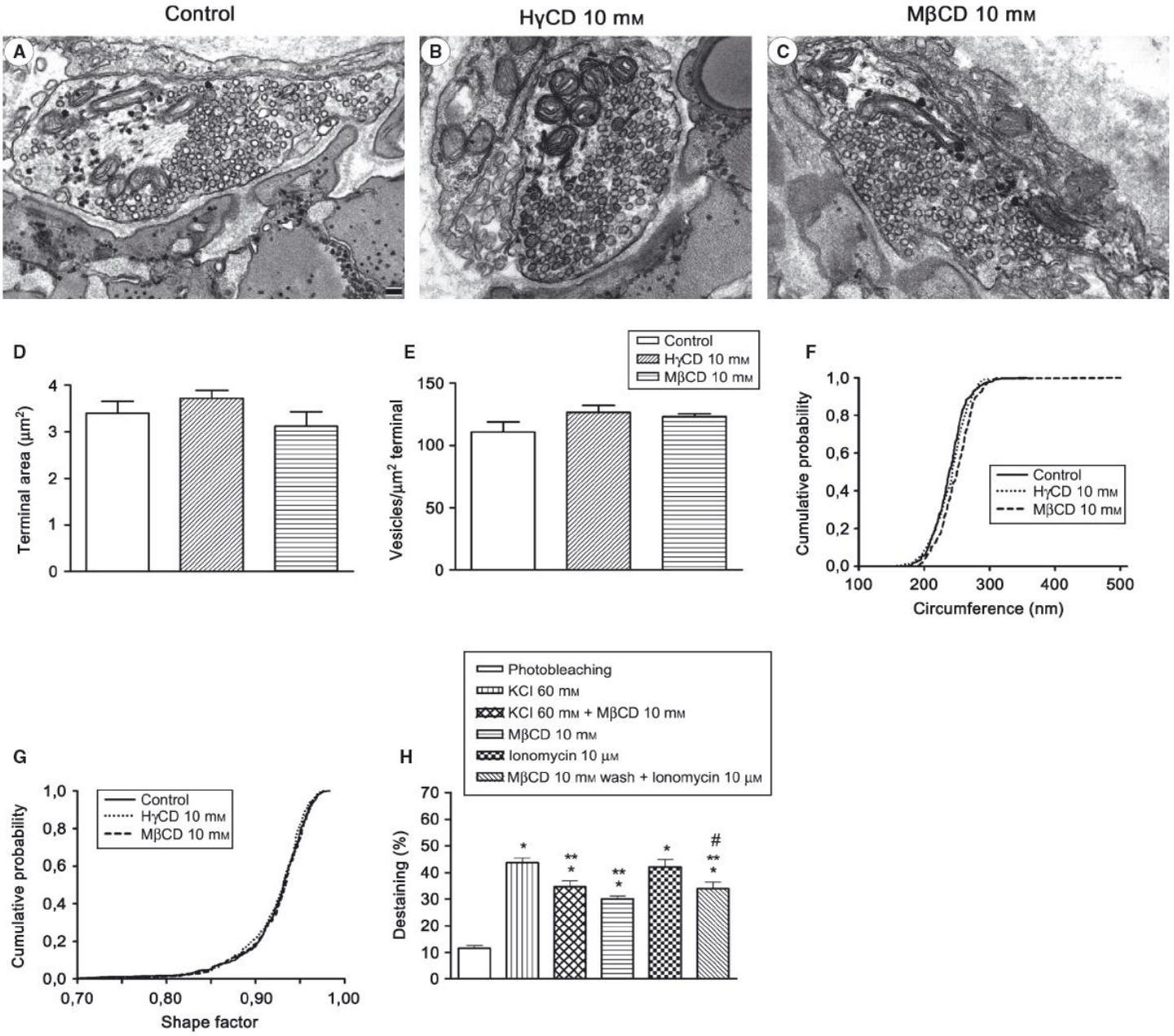

FIG. 3. Optical and ultrastructural analysis of synaptic vesicle exocytosis in nerve terminals treated with MβCD. (A–C) Representative electron micrographs from frog motor nerve terminals in control condition (A) or after 30 min of incubation with HγCD (10 mM) (B) or MβCD (10 mM) (C). Scale bar: 100 nm, magnification: 23 000× . (D) Average area of the presynaptic terminals. (E) Average total number of synaptic vesicles per nerve terminal. (F) Cumulative probability of synaptic vesicle circumference measured from EM sections of NMJs in control, HγCD and MβCD condition. (G) Cumulative probability of synaptic vesicle shape measured from EM sections of NMJs in control, HγCD and MβCD condition (n = 3 animals per experimental condition). (H) Graph representing FM1-43 destaining induced by KCl (60 mM), KCl (60 mM) + MβCD (10 mM), MβCD (10 mM), ionomycin (10 μM) and MβCD (10 mM) wash + ionomycin (10 μM) [n = 3 animals per experimental condition; $^{*}P < 0.05$ compared with photobleaching; $^{**}P < 0.05$ compared with KCl alone; $^{\#}P < 0.05$ comparing ionomycin 10 μM and ionomycin 10 μM + MβCD (10 mM)].

Reinforcing this hypothesis, recent work in central synapses showed that vesicles that recycle spontaneously and under depolarizing stimuli do not mix and are segregated in different vesicular pools (Fredj & Burrone, 2009; Chung *et al.*, 2010). Because our data show that MβCD induces spontaneous vesicle release without stimulating FM1-43 uptake, we looked at ultrathin sections of neuromuscular preparations in control conditions or in muscle exposed to MβCD (10 mM) to visualize the distribution of synaptic vesicles in nerve terminals, especially in the vicinity of the active zones which is the location of the RRP. We did not detect any difference concerning the distribution of synaptic vesicles in control and MβCD-treated nerve terminals, despite the increase in exocytosis induced by cholesterol depletion (Fig. 1). In addition, the number of synaptic vesicles that were close to the active zone were the same, suggesting that at least for the NMJ, the RRP seems to be intact [Fig. 4F: 10 nm – MβCD: 3.0 ± 1.0 synaptic vesicles (mean ± SEM), Control: 4.0 ± 1.0; 20 nm – MβCD: 5.0 ± 1.0, Control: 4.0 ± 1.0; 30 nm – MβCD: 5.0 ± 1.0, Control: 5.0 ± 0.0; 40 nm – MβCD: 5.0 ± 1.0, Control: 6.0 ± 0.0; 50 nm – MβCD: 7.0 ± 1.0, Control: 6.0 ± 0.0; $P > 0.05$, unpaired Student's t-test; 15 nerve terminal profiles for control and 18 nerve terminal profiles for MβCD].

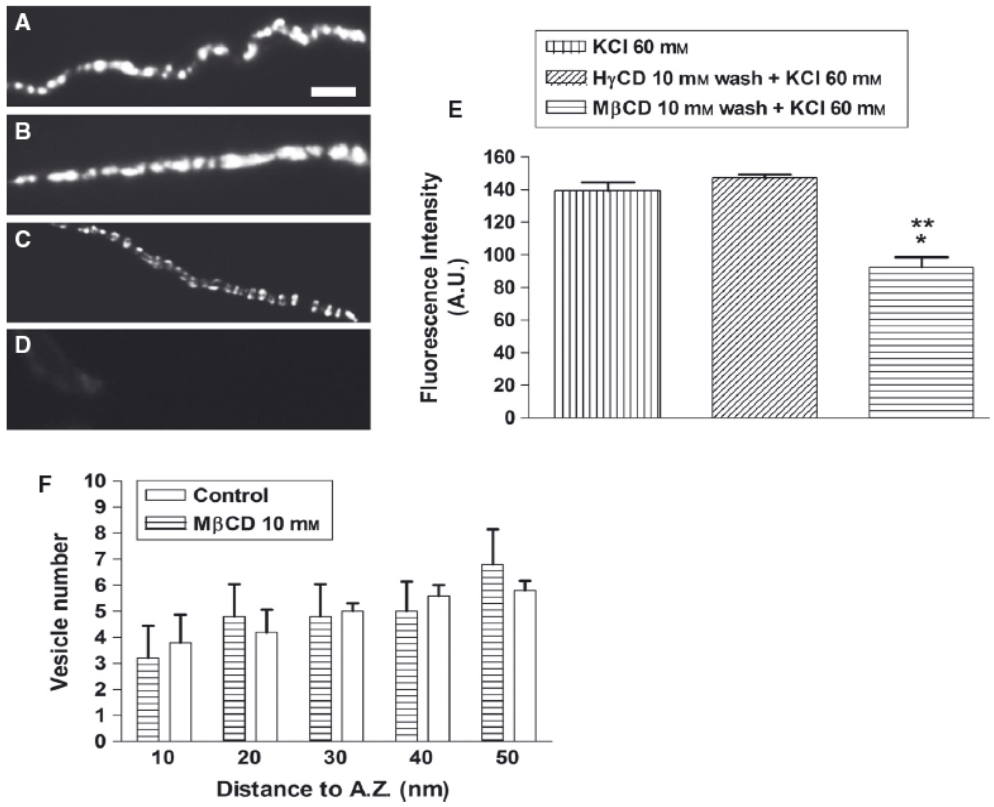

FIG. 4. MβCD and synaptic vesicle endocytosis in frog motor nerve terminals. (A) Nerve terminal labeled with FM1-43 during a high KCl stimulus for 10 min. Note the typical fluorescent spots of FM1-43 labeling. (B) Motor terminal pre-incubated with HγCD (10 mM, 30 min), followed by a washing time of 15 min and subsequent staining with FM1-43 in a high KCl medium. (C) Terminal pre-incubated with MβCD (10 mM, 30 min) followed by a washing time of 15 min and subsequent staining with FM1-43 in a high KCl medium. Note the reduced FM1-43 uptake. (D) Terminal pre-incubated with MβCD (10 mM, 30 min) followed by a washing time of 15 min and subsequent staining with FM1-43. There was no detectable FM1-43 uptake when MβCD was used as stimuli. Scale bars: 10 μm for each image. (E) Graph comparing the fluorescence intensity of nerve terminals stained with FM1-43 in the conditions described in A–D [$n = 3$ animals per experimental condition; $^{*}P < 0.05$ compared with KCl (60 mM) alone; $^{**}P < 0.05$ compared with pre-incubation with HγCD (10 mM)]. (F) Histogram representing the average number of vesicles located at different distances from the active zone ($n = 7$ and $n = 5$ active zones for MβCD and Control, respectively, from three animals per experimental condition). For this quantification we used electron micrographs obtained individually under control and MβCD conditions. All active zone profiles fully visualized were used for quantification.

Discussion

Here we have investigated the effect of cholesterol removal by MβCD in synaptic vesicle recycling at motor nerve terminals of the frog NMJ. We confirmed that MβCD treatment increased MEPP frequency, but we also found an increase in MEPP amplitude that may be due to an increase in the size of synaptic vesicles resulting in increased capacity for neurotransmitter release. Hence, membrane cholesterol regulates both the size of synaptic vesicles and quantal size defined as the post-synaptic membrane potential change induced by release of a single quantum of neurotransmitter. We also showed that after cholesterol removal by MβCD, KCl-evoked synaptic vesicle exocytosis is impaired, suggesting that normal levels of membrane cholesterol are important to maintain a balance between populations of synaptic vesicles that belong to a pool responsible for spontaneous release and a pool responsible for evoked release of neurotransmitter. Our data suggest that MβCD-treated preparations continue to release FM1-43 dye from labeled vesicles during exocytosis, but are unable to internalize dye during compensatory endocytosis. This remarkable characteristic suggests that lack of cholesterol changes the way vesicles undergo exo-endocytosis, perhaps facilitating a mechanism of kiss-and-run that allows for dye diffusion out of vesicles, but that limits lateral diffusion of FM1-43.

Using FM1-43 imaging and electrophysiology techniques, we showed that acute cholesterol removal induces FM1-43 destaining of labeled synaptic vesicles and increases the frequency of MEPPs. Although Zamir & Charlton (2006) reported no MβCD-induced effects on MEPP amplitude or kinetics at the crayfish NMJ, we observed an increase in MEPP amplitude that could not be explained by effects of MβCD on acetylcholinesterase (Fig. 2B and C). As MβCD has been reported to disperse nAChRs in myoblast cultures (Stetzkowski-Marden *et al.*, 2006), we examined AChR receptor density and distribution with fluorescent bungarotoxin and observed no difference in untreated and treated preparations (Fig. 2B and C).

To further investigate changes that could generate large MEPPs, we looked at MβCD-treated and untreated nerve terminals at the ultrastructural level. Considering that our ultrastructure data show no difference regarding the terminal area or the total number of synaptic vesicles in control or MβCD (10 mM)-treated terminals (Fig. 3D and E), this result could not be explained by endocytosis inhibition. We therefore suggest that synaptic vesicles that fuse spontaneously under MβCD treatment endocytose differently from those that are released under KCl-evoked stimulation and may not be able to internalize FM1-43. This result is in agreement with previous work from Zefirov *et al.* (2004), showing a weak FM1-43 staining when frog NMJs were soaked in hyperosmotic solution compared with high-potassium medium, suggesting two modes of recycling depending on the stimuli paradigm.

Recent studies have shed additional light on the mechanism that cholesterol removal interferes with synaptic vesicle exocytosis.

Smith *et al.* (2010) showed that activity of presynaptic protein kinases such as PKA and PKC is sensitive to changes of membrane cholesterol content at cerebellar synapses, suggesting that cholesterol might restrain the access of the aforementioned active kinases to the exocytotic release apparatus. Data obtained from our research group also showed that cholesterol removal facilitates protein kinase activation that favors spontaneous synaptic vesicles and glutamate release in cortical synaptosomes (Teixeira *et al.*, 2012). Therefore, it would be interesting to test in future experiments at the NMJ if the massive increase in spontaneous release observed after cholesterol removal is also sensitive to protein kinase inhibitors. Mailman *et al.* (2011) also showed that cholesterol biosynthesis inhibitors of the statin family, such as lovastatin, are able to impair synaptic vesicle exocytosis in hippocampal neurons, proposing that these neurons need a certain level of endogenous cholesterol biosynthesis for the maturation and maintenance of fully functional synapses and that chronic exposures to these drugs may affect synaptic transmission. These findings raise the question of whether those drugs might also affect peripheral neurotransmission.

Most synaptic systems seem to rely on several pools of vesicles to maintain effective neurotransmission. At the frog NMJ, the main characteristics of vesicle pools can be described as follows: (i) readily releasable pools, which comprises ~10 000 vesicles (0.4% total); (ii) recycling pool corresponding to ~75 000 vesicles (14–19% total); and (iii) reserve pool with ~400 000 vesicles (80% total) (data extracted from a review by Rizzoli & Betz, 2005). The precise location of synaptic pools and the molecular components that distinguish members of the pools have been under intense debate and investigation (Rizzoli & Betz, 2005). More recently, an attempt has been made to relate those vesicle pools to modes of release (Sara *et al.*, 2005; Wasser *et al.*, 2007; Fredj & Burrone, 2009; Wasser & Kavalali, 2009; Hua *et al.*, 2011). Our data show that preparations that are cholesterol-depleted failed to internalize FM1-43 after a depolarizing stimulus (Fig. 4C). Moreover, MβCD increases destaining of vesicles and augments the frequency of MEPPs, suggesting that it can increase exocytosis. Considering that kinetics of partitioning/departitioning of FM1-43 into membranes is not affected by cholesterol levels on the double layer of phospholipids (Wu *et al.*, 2009), the effects of MβCD over exo-/endocytosis should result from alterations on membrane traffic but not on FM affinity for membranes. Sara *et al.* (2005) have proposed that the functional segregation of vesicles that belong to the spontaneous and evoked release pool may be mediated by differences in the protein and/or lipid composition of the synaptic vesicles that make up the two pools. This raised the question of whether those vesicles that fuse spontaneously under MβCD treatment belong to a distinct pool of vesicles, which is not part of the recycling pool of synaptic vesicles. Those vesicles might be unable to internalize FM1-43 because they are not recruited during an evoked stimulus. Indeed, Fredj & Burrone (2009) performed studies in cultured hippocampal neurons showing that calcium-dependent evoked and spontaneous vesicle fusion recruits distinct pools of synaptic vesicles. They also showed evidence that spontaneously released vesicles are mobilized from a resting pool, which was originally described as an activity-independent set of vesicles that do not participate in vesicle cycling. More recently, two elegant studies provided additional evidence that vesicles from the resting pool are more prompt to recycle spontaneously and this might involve different proteins other than the canonic SNARES (Hua *et al.*, 2011; Ramirez & Kavalali, 2012). In agreement with this hypothesis, we showed that under MβCD treatment there an enlargement of synaptic vesicles and modest FM1-43 uptake, suggesting that at least for the frog NMJ, synaptic vesicles recycle differently after cholesterol removal.

It is interesting, however, that MβCD impairs FM1-43 but at the same time increases its release from vesicles. It is possible that removal of cholesterol leads vesicles to undergo a kiss-and-run type of exocytosis. In this framework, FM1-43 inside vesicles would be able to diffuse down its gradient concentration when a fusion pore is formed, that would also allow for the release of neurotransmitter. However, during the endocytic process, dye embedded in the plasma membrane may not diffuse laterally and enter the synaptic vesicle lumen, perhaps due to limits imposed by a fusion pore, which would explain the lack of internalization of the dye upon MβCD treatment. This interpretation is also consistent with the fact that the synaptic vesicle population determined by electron microscopy is not changed in MβCD-treated nerve endings, despite increased exocytosis. Therefore, this result lends additional support to the idea that release of spontaneous and evoked synaptic vesicles might be regulated independently, requiring distinct synaptic vesicle recycling machinery and pools (Ramirez & Kavalali, 2011).

However, we noted that synaptic vesicles were larger in MβCD-treated nerve terminals than in control terminals (Fig. 3F). Van der Kloot *et al.* (2002) showed that at the frog NMJ the synaptic vesicle content of acetylcholine can change without any notable alteration in synaptic vesicle size. However, whether an enlarged synaptic vesicle may store a higher quantity of neurotransmitter was not determined. The mechanisms responsible for the regulation of how much neurotransmitter a synaptic vesicle can stock are not well-established. At least for dopaminergic secretory cells, there is a correlation between the size of the synaptic vesicle and the amount of transmitter it can store (Sulzer & Pothos, 2000). In addition, Colliver *et al.* (2000) showed that the amount of transmitter stored in a vesicle by the vesicular monoamine transporter (VMAT) can regulate its volume in PC12 cells. Additional evidence came from experiments performed in *Drosophila* larval NMJ by Zhang *et al.* (1998). These researchers have shown that mutants for a clathrin adaptor protein required for endocytosis (AP180) present an increased quantal size (Zhang *et al.*, 1998) due to larger vesicles. Lastly, Rodal *et al.* (1999) showed that extraction of plasma membrane cholesterol from HEp-2 and other cell lines with MβCD perturbs formation of clathrin-coated endocytic vesicles, revealing an intimate interaction between this sterol and formation of clathrin-coated vesicles. Our data are consistent with the possibility that in cholinergic nerve terminals the amount of transmitter stored may change with the size of the vesicle. However, because we do not know if the decreased level of cholesterol can change the H^+-ATPase activity or the activity of the vesicular ACh transporter in our model, it is impossible to conclude if an increase in vesicle diameter increased ACh storage or vice versa. Some authors have investigated the H^+-pumping and ATPase activity of vacuolar ATPase, which was reconstituted into phospholipid vesicles, and showed that the omission of cholesterol inhibited the development of ΔpH without much effect on ATPase activity (Perez-Castiñeira & Apps, 1990). The interrelationship between the cholesterol content in synaptic vesicle membrane and the ability of vesicles to accumulate protons was directly confirmed in experiments with isolated synaptic vesicles (Tarasenko *et al.*, 2010). As has been revealed, MβCD (3 mM) added to synaptic vesicles caused dissipation of the proton gradient, whereas MβCD complexed with cholesterol induced additional acidification of vesicles.

Nonetheless, the increase in synaptic vesicle circumference and amplitude of MEPPs are consistent. MβCD increased synaptic vesicle circumference by $4.3 \pm 1.3\%$, which corresponds to a $13.5 \pm 3.9\%$ increase in vesicle volume assuming spherical vesicles.

If enlarged synaptic vesicles contained more ACh, then at least part of the observed increase in quantal size could be explained by the effect of MβCD on synaptic vesicle size. Other possible causes of increased quantal size include changes in AChR sensitivity to ACh, changes in AChR single-channel conductance, reduced desensitization of AChR or an increased input resistance of the muscle fiber.

In conclusion, this work has provided new data showing that membrane cholesterol acts on the modulation of synaptic vesicle cycle and seems to be essential for the balance between KCl-evoked and spontaneous release at the frog NMJ. Moreover, our results reinforce the hypothesis of coexistence of a synaptic vesicle pool mobilized during activity and another pool that is more ready to be released spontaneously that have distinct sensitivity to cholesterol removal.

Acknowledgements

We acknowledge the Center of Microscopy at the Universidade Federal de Minas Gerais for providing the equipment and technical support for experiments involving electron microscopy. This work was supported by grants from CNPq, FAPEMIG and CAPES, Millennium Institute and FINEP. The authors have no conflict of interest to declare.

Abbreviations

ACh, acetylcholine; CTxB, subunit B from cholera toxin; HγCD, hydroxypropyl-γ-cyclodextrin; MβCD, methyl-β-cyclodextrin; MEPP, miniature end plate potential; nAChR, nicotinic acetylcholine receptor; NMJ, neuromuscular junction; RRP, readily releasable pool; SF, shape factor; VGCC, voltage-gated calcium channel.

References

Alabi, A.A. & Tsien, R.W. (2012) Synaptic vesicle pools and dynamics. *Cold Spring Harb. Perspect. Biol.*, **4**, a013680.

Becherer, U., Guatimosim, C. & Betz, W. (2001) Effects of staurosporine on exocytosis and endocytosis at frog motor nerve terminals. *J. Neurosci.*, **21**, 782–787.

Betz, W.J. & Bewick, G.S. (1992) Optical analysis of synaptic vesicle recycling at the frog neuromuscular junction. *Science*, **255**, 200–203.

Betz, W.J., Mao, F. & Bewick, G.S. (1992) Activity-dependent fluorescent staining and destaining of living vertebrate motor nerve terminals. *J. Neurosci.*, **12**, 363–375.

Brown, D.A. & Rose, K.J. (1992) Sorting of GPI-anchored proteins to glycolipid enriched membrane subdomains during transport to the apical cell surface. *Cell*, **68**, 533–544.

Ceccarelli, B., Hurlbut, W.P. & Mauro, A. (1973) Turnover of transmitter and synaptic vesicles at the frog neuromuscular junction. *J. Cell Biol.*, **57**, 499–524.

Cho, W.J., Jeremic, A., Jin, H., Ren, G. & Jena, B.P. (2007) Neuronal fusion pore assembly requires membrane cholesterol. *Cell Biol. Int.*, **31**, 1301–1308.

Chung, C., Barylko, B., Leitz, J., Liu, X. & Kavalali, E.T. (2010) Acute dynamin inhibition dissects synaptic vesicle recycling pathways that drive spontaneous and evoked neurotransmission. *J. Neurosci.*, **30**, 1363–1376.

Colliver, T.L., Pyott, S.J., Achalabun, M. & Ewing, A.G. (2000) VMAT-mediated changes in quantal size and vesicular volume. *J. Neurosci.*, **20**, 5267–5282.

Croft, B.G., Fortin, G.D., Corera, A.T., Edwards, R.H., Beaudet, A., Trudeau, L.E. & Fon, E.A. (2005) Normal biogenesis and cycling of empty synaptic vesicles in dopamine neurons of vesicular monoamine transporter 2 knockout mice. *Mol. Biol. Cell*, **16**, 306–315.

Dason, J.S., Smith, A.J., Marin, L. & Charlton, M.P. (2010) Vesicular sterols are essential for vesicle cycling. *J. Neurosci.*, **30**, 15856–15865.

Foster, L.J., De Hoog, C.L. & Mann, M. (2003) Unbiased quantitative proteomics of lipid rafts reveals high specificity for signaling factors. *Proc. Natl. Acad. Sci. USA*, **100**, 5813–5818.

Fredj, N.B. & Burrone, J. (2009) A resting pool of vesicles is responsible for spontaneous vesicle fusion at the synapse. *Nat. Neurosci.*, **12**, 751–758.

Guatimosim, C., Romano-Silva, M.A., Cruz, J.S., Beirão, P.S., Kalapothakis, E., Moraes-Santos, T., Cordeiro, M.N., Diniz, C.R., Gomez, M.V. & Prado, M.A. (1997) A toxin from the spider *Phoneutria nigriventer* that blocks calcium channels coupled to exocytosis. *Brit. J. Pharmacol.*, **122**, 591–597.

Guatimosim, C., Romano-Silva, M.A., Gomez, M.V. & Prado, M.A. (1998a) Use of fluorescent probes to follow membrane traffic in nerve terminals. *Braz. J. Med. Biol. Res.*, **31**, 1491–1500.

Guatimosim, C., Romano-Silva, M.A., Gomez, M.V. & Prado, M.A. (1998b) Recycling of synaptic vesicles at the frog neuromuscular junction in the presence of strontium. *J. Neurochem.*, **70**, 2477–2483.

Harder, T., Scheiffele, P., Verkade, P. & Simons, K. (1998) Lipid domain structure of the plasma membrane revealed by patching of membrane components. *J. Cell Biol.*, **141**, 929–942.

Heuser, J.E. & Reese, T.S. (1973) Evidence for recycling of synaptic vesicle membrane during transmitter release at the frog neuromuscular junction. *J. Cell Biol.*, **57**, 315–344.

Hua, Z., Leal-Ortiz, S., Foss, S.M., Waites, C.L., Garner, C.C., Voglmaier, S.M. & Edwards, R.H. (2011) v-SNARE composition distinguishes synaptic vesicle pools. *Neuron*, **17**, 474–487.

Katz, B. & Thesleff, S. (1957) On the factors which determine the amplitude of the miniature end-plate potential. *J. Physiol.*, **137**, 267–278.

Kilsdonk, E.P., Yancey, P.G., Stoudt, G.W., Bangerter, F.W., Johnson, W.J., Phillips, M.C. & Rothblat, G.H. (1995) Cellular cholesterol efflux mediated by cyclodextrins. *J. Biol. Chem.*, **270**, 17250–17256.

Lingwood, D., Kaiser, H.J., Levental, I. & Simons, K. (2009) Lipid rafts as functional heterogeneity in cell membranes. *Biochem. Soc. T.*, **37**, 955–960.

Mailman, T., Hariharan, M. & Karten, B. (2011) Inhibition of neuronal cholesterol biosynthesis with lovastatin leads to impaired synaptic vesicle release even in the presence of lipoproteins or geranylgeraniol. *J. Neurochem.*, **119**, 1002–1015.

Murthy, V.N. & De Camilli, P. (2003) Cell biology of the presynaptic terminal. *Annu. Rev. Neurosci.*, **26**, 701–728.

Ohtani, Y., Irie, T., Uekama, K., Fukunaga, K. & Pitha, J. (1989) Differential effects of alpha-, beta- and gamma-cyclodextrins on human erythrocytes. *Eur. J. Biochem.*, **186**, 17–22.

Perez-Castiñeira, J.R. & Apps, D.K. (1990) Vacuolar H^+-ATPase of adrenal secretory granules Rapid partial purification and reconstitution into proteoliposomes. *Biochem. J.*, **271**, 127–131.

Ramirez, D.M. & Kavalali, E.T. (2011) Differential regulation of spontaneous and evoked neurotransmitter release at central synapses. *Curr. Opin. Neurobiol.*, **21**, 275–282.

Ramirez, D.M. & Kavalali, E.T. (2012) The role of non-canonical SNAREs in synaptic vesicle recycling. *Cell Logist.*, **2**, 20–27.

Ribchester, R.R., Mao, F. & Betz, W.J. (1994) Optical measurements of activity-dependent membrane recycling in motor nerve terminals of mammalian skeletal muscle. *Proc. Biol. Sci.*, **255**, 61–66.

Richards, D.A., Guatimosim, C. & Betz, W.J. (2001) Two endocytic recycling routes selectively fill two vesicle pools in frog motor nerve terminals. *Neuron*, **27**, 551–559.

Rizzoli, S.O. & Betz, W.J. (2005) Synaptic vesicle pools. *Nat. Rev. Neurosci.*, **6**, 57–69.

Rodal, S.K., Skretting, G., Garred, O., Vilhardt, F., van Deurs, B. & Sandvig, K. (1999) Extraction of cholesterol with methyl-beta-cyclodextrin perturbs formation of clathrin-coated endocytic vesicles. *Mol. Biol. Cell*, **10**, 961–974.

Royle, S.J. & Lagnado, L. (2003) Endocytosis at the synaptic terminal. *J. Physiol.*, **553**, 345–355.

Sara, Y., Virmani, T., Deák, F., Liu, X. & Kavalali, E.T. (2005) An isolated pool of vesicles recycles at rest and drives spontaneous neurotransmission. *Neuron*, **45**, 563–573.

Simons, K. & Ikonen, E. (1997) Functional rafts in cell membranes. *Nature*, **387**, 569–572.

Simons, K. & van Meer, G. (1988) Lipid sorting in epithelial cells. *Biochemistry*, **27**, 6197–6202.

Smith, A.J., Sugita, S. & Charlton, M.P. (2010) Cholesterol-dependent kinase activity regulates transmitter release from cerebellar synapses. *J. Neurosci.*, **30**, 6116–6121.

Stetzkowski-Marden, F., Gaus, K., Recouvreur, M., Cartaud, A. & Cartaud, J. (2006) Agrin elicits membrane lipid condensation at sites of acetylcholine receptor clusters in C2C12 myotubes. *J. Lipid Res.*, **47**, 2121–2133.

Sudhof, T.C. (2004) The synaptic vesicle cycle. *Annu. Rev. Neurosci.*, **27**, 509–547.

Sulzer, D. & Pothos, E.N. (2000) Regulation of quantal size by presynaptic mechanisms. *Rev. Neuroscience.*, **11**, 159–212.

Tarasenko, A.S., Sivko, R.V., Krisanova, N.V., Himmelreich, N.H. & Borisova, T.A. (2010) Cholesterol depletion from the plasma membrane impairs proton and glutamate storage in synaptic vesicles of nerve terminals. *J. Mol. Neurosci.*, **41**, 358–367.

Teixeira, G., Vieira, L.B., Gomez, M.V. & Guatimosim, C. (2012) Cholesterol as a key player in the balance of evoked and spontaneous glutamate release in rat brain cortical synaptosomes. *Neurochem. Int.*, **61**, 1151–1159.

Thiele, C., Hannah, M.J., Fahrenholz, F. & Huttner, W.B. (2000) Cholesterol binds to synaptophysin and is required for biogenesis of synaptic vesicles. *Nat. Cell Biol.*, **2**, 42–49.

Van der Kloot, W., Molgo, J., Cameron, R. & Colasante, C. (2002) Vesicle size and transmitter release at the frog neuromuscular junction when quantal acetylcholine content is increased or decreased. *J. Physiol.*, **541**, 385–393.

Wasser, C.R. & Kavalali, E.T. (2009) Leaky synapses: regulation of spontaneous neurotransmission in central synapses. *Neuroscience*, **158**, 177–188.

Wasser, C.R., Ertunc, M., Liu, X. & Kavalali, E.T. (2007) Cholesterol-dependent balance between evoked and spontaneous synaptic vesicle recycling. *J. Physiol.*, **579**, 413–429.

Wu, Y., Yeh, F.L., Mao, F. & Chapman, E.R. (2009) Biophysical characterization of styryl dye-membrane interactions. *Biophys. J.*, **97**, 101–109.

Yoshinaka, K., Kumanogoh, H., Nakamura, S. & Maekawa, S. (2004) Identification of V-ATPase as a major component in the raft fraction prepared from the synaptic plasma membrane and the synaptic vesicle of rat brain. *Neurosci. Lett.*, **363**, 168–172.

Zamir, O. & Charlton, M.P. (2006) Cholesterol and synaptic transmitter release at crayfish neuromuscular junctions. *J. Physiol.*, **571**, 83–99.

Zefirov, A.L., Abdrakhmanov, M.M. & Grigor'ev, P.N. (2004) Kiss-and-run quantal secretion in frog nerve-muscle synapse. *B. Exp. Biol. Med.*, **137**, 107–110.

Zhang, B., Koh, Y.H., Beckstead, R.B., Budnik, V., Ganetzky, B. & Bellen, H.J. (1998) Synaptic vesicle size and number are regulated by a chlatrin adaptor protein required for endocytosis. *Neuron*, **21**, 1466–1475.

11. ANEXO 4: Artigo publicado durante o mestrado

OPEN ACCESS Freely available online

PLOS | ONE

Reduced Expression of the Vesicular Acetylcholine Transporter and Neurotransmitter Content Affects Synaptic Vesicle Distribution and Shape in Mouse Neuromuscular Junction

Hermann A. Rodrigues[1], Matheus de C. Fonseca[1], Wallace L. Camargo[2], Patrícia M. A. Lima[3], Patrícia M. Martinelli[1], Lígia A. Naves[2], Vânia F. Prado[4], Marco A. M. Prado[4], Cristina Guatimosim[1]*

1 Departamento de Morfologia, ICB, Universidade Federal de Minas Gerais, Belo Horizonte, Brasil, **2** Departamento de Fisiologia e Biofísica, ICB, Universidade Federal de Minas Gerais, Belo Horizonte, Brasil, **3** Departamento de Engenharia de Biossistemas, Universidade Federal de São João Del Rei, São João Del Rei, Brasil, **4** Robarts Research Institute and Department of Physiology and Pharmacology and Anatomy & Cell Biology, University of Western Ontario, London, ON, Canada

Abstract

In vertebrates, nerve muscle communication is mediated by the release of the neurotransmitter acetylcholine packed inside synaptic vesicles by a specific vesicular acetylcholine transporter (VAChT). Here we used a mouse model (VAChT KD^{HOM}) with 70% reduction in the expression of VAChT to investigate the morphological and functional consequences of a decreased acetylcholine uptake and release in neuromuscular synapses. Upon hypertonic stimulation, VAChT KD^{HOM} mice presented a reduction in the amplitude and frequency of miniature endplate potentials, FM 1–43 staining intensity, total number of synaptic vesicles and altered distribution of vesicles within the synaptic terminal. In contrast, under electrical stimulation or no stimulation, VAChT KD^{HOM} neuromuscular junctions did not differ from WT on total number of vesicles but showed altered distribution. Additionally, motor nerve terminals in VAChT KD^{HOM} exhibited small and flattened synaptic vesicles similar to that observed in WT mice treated with vesamicol that blocks acetylcholine uptake. Based on these results, we propose that decreased VAChT levels affect synaptic vesicle biogenesis and distribution whereas a lower ACh content affects vesicles shape.

Citation: Rodrigues HA, Fonseca MdC, Camargo WL, Lima PMA, Martinelli PM, et al. (2013) Reduced Expression of the Vesicular Acetylcholine Transporter and Neurotransmitter Content Affects Synaptic Vesicle Distribution and Shape in Mouse Neuromuscular Junction. PLoS ONE 8(11): e78342. doi:10.1371/journal.pone.0078342

Editor: William Phillips, University of Sydney, Australia

Received July 16, 2013; **Accepted** September 18, 2013; **Published** November 8, 2013

Funding: This work was supported by funds from CNPq (472286/2009-9 and 306483/2010-6) and FAPEMIG. The funders had no role in study design, data collection and analysis, decision to publish, or preparation of the manuscript.

Competing Interests: The authors have declared that no competing interests exist.

* E-mail: cguati@icb.ufmg.br

Introduction

Acetylcholine (ACh) plays an important role during nervous system development [1,2,3]. In mammalian neuromuscular junction (NMJ), ACh is synthesized in presynaptic terminals of cholinergic neurons from choline and acetyl-coenzyme A (acetyl-CoA) by choline acetyltransferase (ChAT) and then transported into synaptic vesicles (SVs) by the vesicular acetylcholine transporter (VAChT) [4]. After depolarization, ACh is released into the synaptic cleft and binds to nicotinic receptors present on the postsynaptic muscle membrane, transmitting the signal for muscular contraction [4,5].

The release of neurotransmitters depends on its storage into SVs [6,7,8], and VAChT expression represents a key point in the regulation of cholinergic transmission [9,10]. VAChT knockout ($VAChT^{del/del}$) mice appear to have normal SV recycling, but they are unable to store or release sufficient ACh in response to neural activity. As a consequence, they do not survive more than few minutes after birth [3]. In contrast, mice with 70% reduced VAChT expression (VAChT KD^{HOM}) reach adulthood, but these animals show cardiac dysfunction and cognitive alterations [3,9,11]. In addition, VAChT KD^{HOM} mice present a pronounced deficit in neuromuscular transmission characterized by a reduction in quantal content and size, reduced miniature end-plate potentials frequency, impairment of motor performance and severe deficit in muscle strength [9,10]. Understanding how synaptic terminals respond to reduced expression of this transporter is relevant, as decreased levels of VAChT have been reported in response to drug treatments [12,13], as well as in distinct neurodegenerative diseases [14,15]. To investigate whether decreased levels of VAChT, and consequently reduced ACh storage, can regulate any aspect of the SV cycle, studies using the NMJ are ideal, due to the homogenous cholinergic nature of this synapse and its accessibility to imaging and electron microscopy.

Although studies using the fluorescent dye FM1-43 suggested that VAChT KD^{HOM} mice appear to have normal SV cycle [9], a detailed ultrastructural investigation of the NMJ in these mice was not performed. In the present study we characterized, at the ultrastructure level, the morphology of synaptic nerve terminals from diaphragm muscles of VAChT KD^{HOM} mice. Our data show that reduced expression of VAChT does not interfere with the overall morphology of the NMJ, but changes the distribution

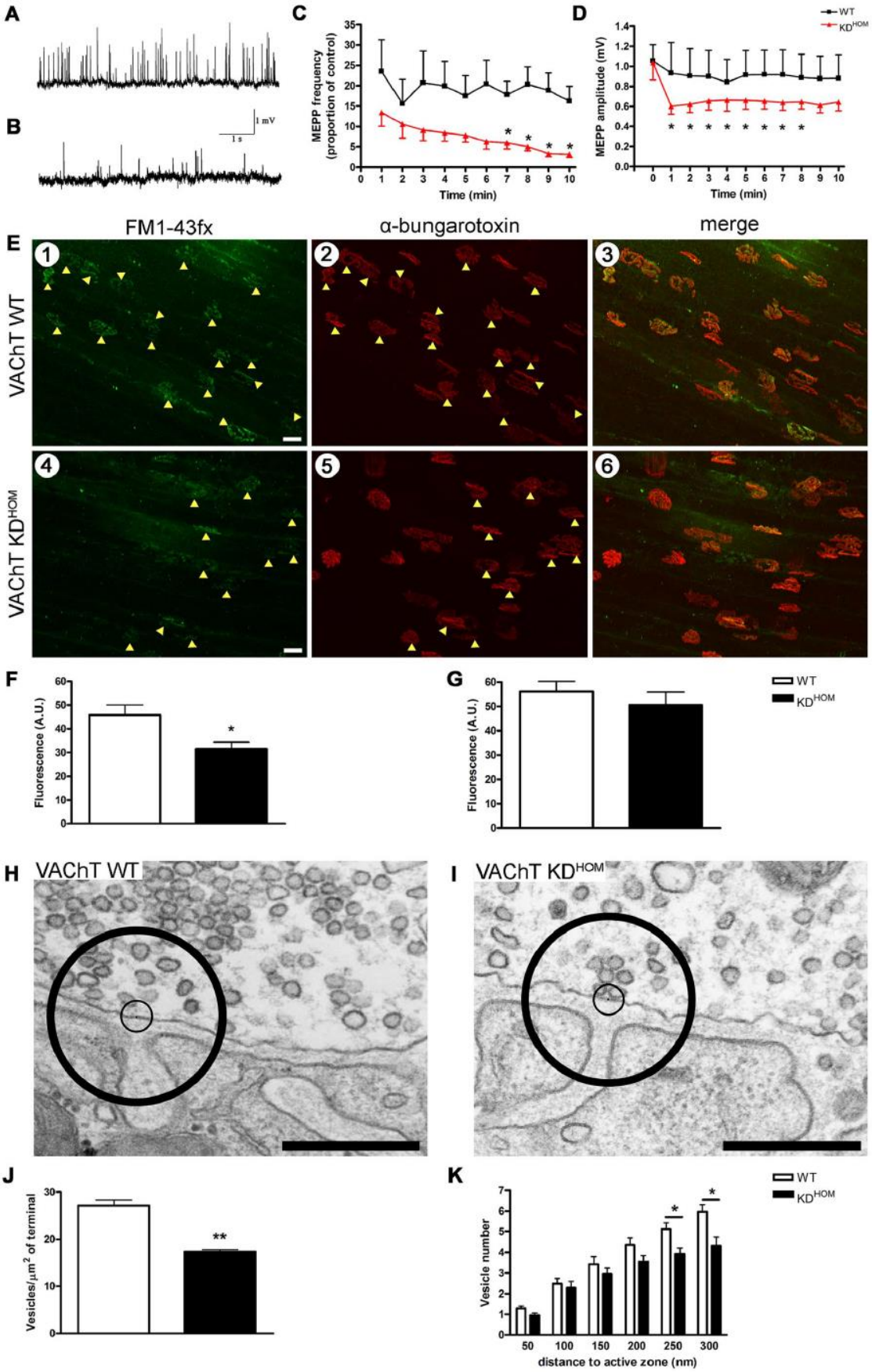
A
B
1 mV
1 s
C
MEPP frequency (proportion of control)
Time (min)
D
WT
KD^HOM
MEPP amplitude (mV)
Time (min)
E
FM1-43fx
α-bungarotoxin
merge
VAChT WT
VAChT KD^HOM
F
Fluorescence (A.U.)
G
Fluorescence (A.U.)
WT
KD^HOM
H
VAChT WT
I
VAChT KD^HOM
J
Vesicles/μm² of terminal
K
Vesicle number
distance to active zone (nm)
WT
KD^HOM

Figure 1. Alteration in SVs recycling and distribution after hypertonic sucrose stimulation in VAChT KD^{HOM} NMJs. A and B – Representative records of MEPPs obtained from the diaphragm muscle of VAChT WT and VAChT KD^{HOM} mice, respectively, measured in the presence of hypertonic sucrose solution (500 mM) at the end of 10 minutes. C -Graph comparing the mean values of normalized MEPPs frequency measured in the presence of hypertonic sucrose during 10 minutes. The results were normalized using the basal MEPPs values for each genotype. D – Graph showing the mean values of MEPP amplitude before (time zero) and during 10 minutes in hypertonic solution. In C and D all results are expressed as mean ± SEM. * $p<0.05$; n = 4 animals per genotype E– Confocal representative images of NMJs from the diaphragm muscle of VAChT WT (E1–E3) and VAChT KD^{HOM} mice (E4–E6): E1 and E4– presynaptic terminals stained with FM1-43 fx after hypertonic stimulation for 10 min; E2 and E5– postsynaptic nAChR clusters stained with α-bungarotoxin-Alexa 594; E3 and E6– colocalization of synaptic elements. Scale bar = 10 μm. F– Graph showing the fluorescence intensity of the presynaptic terminal in arbitrary units (A.U.) (* $p<0.05$). G– Graph comparing the fluorescence intensity of the postsynaptic nAChR clusters in arbitrary units (A.U.). (n = 3 animals of each genotype). H and I– Representative electron-micrographs of two diaphragm NMJs profiles of VAChT WT and VAChT KD^{HOM} mice after hypertonic stimulation for 10 min, showing altered distribution and reduced number of SVs inside the areas labeled within the circles: 50 and 300 nm from the membrane, small and big circles respectively. Scale bar = 500 nm. Magnification 50.000x. J– Graph comparing the relationship of SVs/μm^2 of presynaptic terminal. (** $p<0.01$). K– Graph showing the average number of SVs located at different distances from the presynaptic active zones. (n = 3 individual animals per genotype; * $p<0.05$).
doi:10.1371/journal.pone.0078342.g001

of SV within the nerve terminal. In addition, reduced expression of VAChT changes the shape of SVs suggesting that neurotransmitter content may play a key role in maintaining their structure. Our results demonstrate a link between ACh storage and regulation of SV recycling.

Materials and Methods

Drugs and chemicals

FM1-43fx and ProLong® Gold antifade were purchased from Invitrogen™; d-tubocurarine, ADVASEP-7, (±)-Vesamicol hydrochloride were purchased from Sigma-Aldrich and μ-conotoxin was obtained from Alomone Labs. All other chemical and reagents were of analytical grade.

Ethics Statement

All experimental procedures were carried out in accordance with protocol approved by the local animal care committee (CETEA-UFMG – protocol 40/2009) and followed NIH guidelines for the Care and Use of Animals in Research and Teaching.

Nerve-muscle preparation

Generation of VAChT KD^{HOM} mice has been previously described in detail [9]. The experiments were performed using adult 3 month-old VAChT WT and VAChT KD^{HOM} mice. The diaphragm muscle associated with the corresponding nerve were dissected out, split in two hemidiaphragms and bathed in mouse Ringer solution (135 mM NaCl, 5 mM KCl, 2 mM $CaCl_2$, 1 mM $MgCl_2$, 12 mM $NaHCO_3$, 1 mM NaH_2PO_4, 11 mM D-glucose, pH 7.4) and bubbled with a mixture of 5%CO2/95%O2. In transmission electron microscopy experiments, diaphragm muscles were fixed in ice-cold modified Karnovsky solution fixative (4.0% paraformaldehyde and 2.5% glutaraldehyde in 0.1 M sodium cacodylate buffer).

Monitoring endocytosis with FM1–43fx

Experiments with FM1-43 were performed according to the protocol previously described [16,17] except that a fixable (fx) FM1-43 analog was used. Diaphragm muscles were stimulated with hypertonic sucrose solution (500 mM) containing FM1-43fx (8 μM) for 10 min. After stimulation, the preparation was maintained at rest in normal Ringer solution with FM1-43fx for 10 min to guarantee maximal FM1-43fx uptake during compensatory endocytosis. Following labeling, muscles were washed for 1 hour in normal mouse Ringer containing Advasep-7 (1 mM) to remove extracellular FM1-43fx. For labeling of nicotinic acetylcholine receptor (nAChR) clusters, the preparations were exposed to α-bungarotoxin-Alexa 594 (12 μM) during 20 minutes and then washed [16]. Diaphragms were post-fixed with paraformaldehyde 4% in PBS for 40 min and mounted onto glass slide using ProLong® Gold antifade reagent.

Confocal microscopy and image analysis

Images of NMJs stained with FM1-43fx and α-bungarotoxin were acquired using a 40x oil immersion (NA 1.30) objective attached to a laser-scanning confocal microscope (Zeiss 510 META) located at Center of Acquisition and Processing of Images (CAPI) – ICB – UFMG. An argon (488 nm) and helium-neon (543 nm) laser were used for excitation of terminals stained with FM 1–43fx and nAChR cluster marked with α-bungarotoxin, respectively. Z series optical sections were collected at 2.0 μm intervals and the whole hemidiaphragms were scanned. The nerve terminals were indentified considering their colocalization with nAChR clusters. Images were converted to gray scale format (8 bits) and each synaptic element was individually evaluated and the mean fluorescence intensity was considered for comparison between genotypes.

Electrophysiological recordings

Standard intracellular recording techniques were used to record miniature endplate potentials (MEPPs) with an Axopatch-200 amplifier (Molecular Devices). Recordings were low-pass filtered at 5 KHz and amplified 50X prior to digitization and acquisition on a computer running WinEDR (John Dempster, University of Strathclyde). Microelectrodes were fabricated from borosilicate glass and had resistances of 8–15 MΩ when filled with 3 M KCl. MEPPs were recorded during 10 min in presence of normal Ringer and during exposure to sucrose hypertonic solution (500 mM). μ-Conotoxin GIIIB (0.37 μM) was added to avoid muscle contraction. MEPP amplitudes were recorded and scaled for differences in resting potential using −70 mV as the standard. MEPPs were recorded in the same fiber for 10 min before and during application of hypertonic sucrose.

Transmission Electron Microscopy (TEM)

For ultrastructural characterization, VAChT WT and VAChT KD^{HOM} mice were anesthetized with ketamine/xilazine (70/10 mg/kg) i.p. and transcardially perfused with ice-cold PBS for 10 min, followed by ice-cold fixative modified Karnovsky solution for 10 min. Perfused diaphragm muscles were maintained in fixative solution overnight at 4°C. For experiments with stimulation, nerve muscle preparations were electrically stimulated (20 Hz/5 min) through the phrenic nerve (calcium-dependent stimuli) and immediately fixed or stimulated with hypertonic sucrose solution (500 mM) for 10 min (calcium-independent stimuli). After stimulation, the preparation was maintained at rest for 10 minutes in mouse Ringer solution without sucrose and fixed in ice-cold modified Karnovsky solution overnight at 4°C.

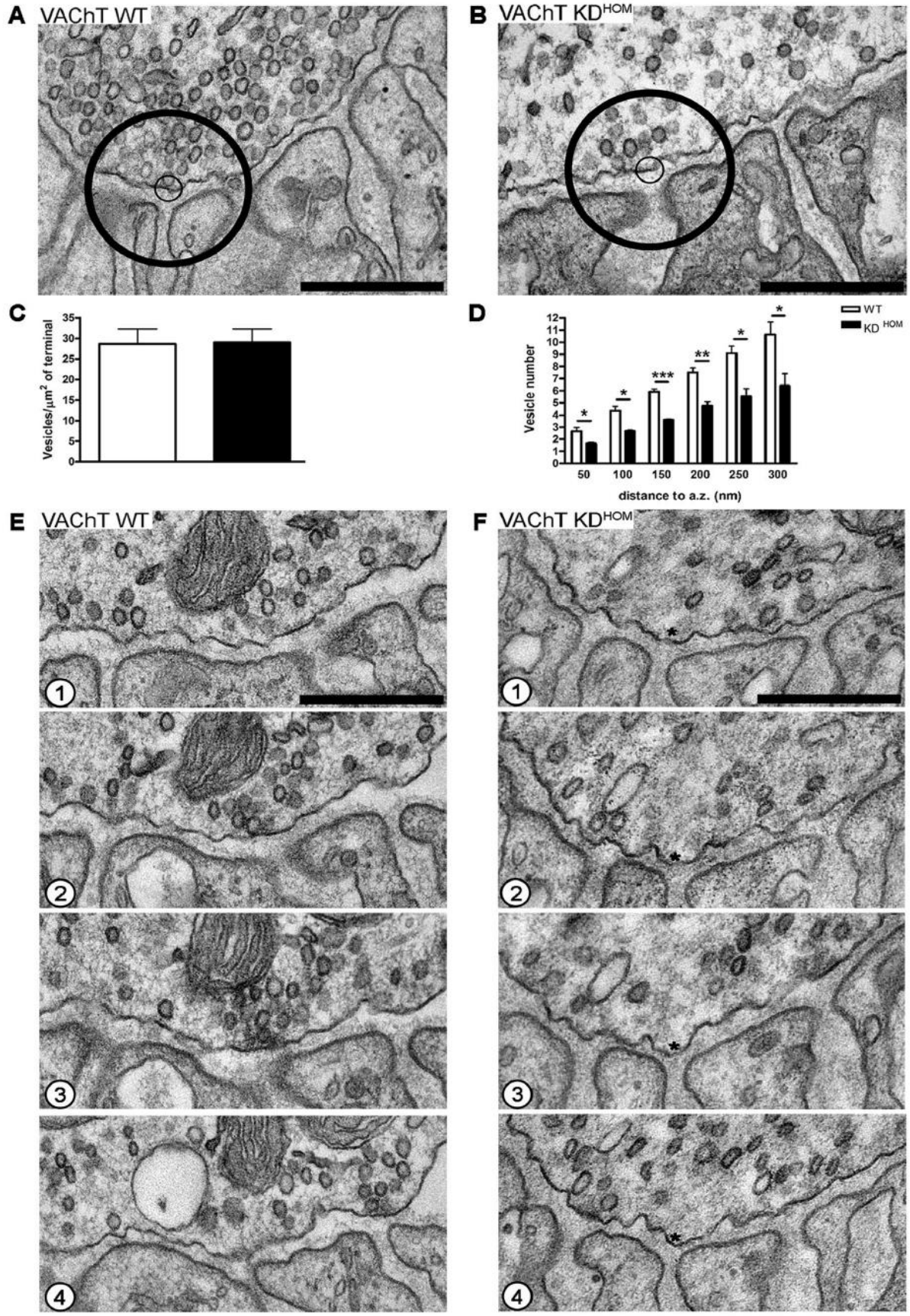

Figure 2. The reduced expression of VAChT alters SVs distribution involved in eletrically stimulated NMJs. A and B – Representative images of two NMJs from diaphragm muscle of VAChT WT and VAChT KD^{HOM} mice after electrical stimulation (20 Hz for 5 minutes) showing an altered SVs distribution from the active zone within the circles: 50 and 300 nm from the membrane, small and big circles respectively. Scale bar

= 500 nm. Magnification 50.000x. C– Graph of the ratio SVs/area of presynaptic terminal in μm^2. D – Graph showing the average number of SVs located at different distances from the presynaptic active zones. E and F– Four serial sections of NMJs from VAChT WT (E1–E4) and VAChT KD^{HOM} (F1–F4) diaphragm showing the altered SVs distribution in the active zone (* represent areas depleted of SVs touching the membrane) of motor terminals of VAChT KD^{HOM} after electrical stimulation. Scale bar = 500 nm. Magnification 50.000x. (n = 3 individual animals per genotype. * $p<0.05$, ** $p = 0.005$; *** $p = 0.0006$).
doi:10.1371/journal.pone.0078342.g002

To investigate the effects of reduced ACh storage in SVs morphology, the diaphragm muscle from C57BL/6 mice was electrically stimulated (3 Hz/20 min) through the phrenic nerve in the presence of (±)-vesamicol (4 μM), a VAChT inhibitor [18] and immediately fixed overnight at 4°C.

After fixation, samples were washed with cacodylate buffer (0.1 M), cut into several pieces, post-fixed in reduced osmium (1% osmium tetroxide containing 1,6% potassium ferrocyanide), contrasted *en bloc* with uranyl acetate (2% uranyl acetate in deionized water), dehydrated through an ascending series of ethanol solutions and embedded in EPON. Blocks were sectioned (50 nm) and collected on 200 or 300 mesh copper grids and contrasted with lead citrate. Serial ultrathin sections (50 nm) were collected and mounted on formvar-coated slot cooper grids and contrasted with lead citrate. Sections were viewed with a Tecnai-G2-Spirit-FEI/Quanta electron microscope (120 kV Philips) located at Microscopy Center – UFMG or with an EM 10 Zeiss electron microscope (80 Kv) located at CAPI (ICB – UFMG).

TEM image analysis

NMJs of interest were selected based on the presence of junctional folds in the postsynaptic membrane. Single sections through NMJs of interest were traced and the terminal areas (cross section area of each nerve terminal), postsynaptic junctional folds length and SV number were determined. SV distribution was evaluated by quantification of the vesicles located at different distances from the active zone within the selected area (small and big circle), as previously described [19,20] and vesicles counted were marked to prevent their recounting. Vesicles within 50 to 300 nm of the presynaptic membrane were counted in 50 nm bins. We have defined active zone as presynaptic regions immediately opposed to postsynaptic fold within 300 nms from the plasma membrane. Vesicle circumference was measured using the equation $2\pi\ [(d_1^2+d_2^2)/2]^{0.5}$ considering the longest diameter ($d1$) and the diameter at right angles ($d2$) [8]. SVs shape was determined using the equation: shape factor = $(4\times\pi\times \text{area})/(\text{perimeter})^2$. This parameter reaches a maximum of 1 for a circular object [21]. All image analysis in this study was performed "blind" in the sense that the person performing the analysis did not know what genotype or treatment the sample had received.

Statistical Analysis

Image analysis was performed using the program Image J (Wayne Rasband, National Institutes of Health, USA) or Image-Pro Plus® 4.0 (4.5 (Media Cybernetics, Silver Spring, MD, EUA) or AxioVision 4.8 (Carl Zeiss). Data were analyzed in Microsoft Excel and plotted using the program SigmaPlot 10.0 (SyStat Software) or GraphPad Prism 4 or Igor (Wavemetrics). The averages ± standard error of the mean (SEM) from each group were calculated and compared. Statistical significance was evaluated using the paired or un-paired Student's *t*-test or the Komogorov-Smirnov test, as described in the text. Values of $P<0.05$ were considered significant.

Results

Previous studies from our research group showed that internalization of FM1-43 by motor terminals of VAChT KD^{HOM} mice and WT controls in response to electrical stimulation is very similar, suggesting that endocytosis is not affected in VAChT KD^{HOM} mice [9]. Likewise, internalization of FM1-43 by NMJs of $VAChT^{del/del}$ mice indicates the existence of bulk SV recycling even in the absence of this transporter [3]. To further investigate the recycling and distribution of SV from the readily releasable pool (RRP) in nerve terminals from diaphragm muscle of VAChT KD^{HOM} mice we used hypertonic sucrose (500 mM) as a stimulus [22]. Hypertonic extracellular solution has been shown to increase the frequency of MEPPs at the frog and rat NMJs [23,24,25,26]. The mechanism behind this increase is still unknown, however, it has been described that hypertonicity does not require Ca^{2+} influx or release from internal stores and may facilitate fusion of docked vesicles [22,27]. Figures 1A and 1B show two representative traces of MEPPs measured from diaphragm neuromuscular preparations of VAChT WT and KD^{HOM}, respectively, at the end of 10 minutes in the presence of hypertonic sucrose solution (500 mM). Before hypertonic solution, MEPPs frequencies were: VAChT WT ($0.4\pm0.1\ s^{-1}$) and VAChT KD^{HOM} ($0.7\pm0.1\ s^{-1}$) (mean ± SEM). Application of hypertonic solution increased MEPPs frequency in both WT and VAChT KD^{HOM} preparations. In WT, the increased frequency was sustained for ten minutes. In contrast, MEPPs frequency in VAChT KD^{HOM} decreased steadily from the peak. After 10 minutes of hypertonic stimulation, the MEPPs frequency in VAChT WT was $16.\pm3.7$ times the pre-stimulation frequency whereas in VAChT KD^{HOM} frequency was only 3.1 ± 0.8 times the pre-stimulation value (Figure 1C – $p<0.05$; unpaired Student's *t*-test; 4 muscle fiber for each genotype). Before hypertonic solution, MEPP amplitude was: VAChT WT (1.1 ± 0.2 mV) VAChT KD^{HOM} (1.0 ± 0.2 mV) (mean ± SEM). Application of hypertonic solution decreased MEPP amplitude in the mutants but not in WT. The decrease in amplitude in VAChT KD^{HOM} was seen as soon as the first minute, where MEPP amplitude was 0.6 ± 0.1 mV (Figure 1D – $p<0.05$; paired Student's *t*-test; 4 muscle fiber for each genotype). These data suggest that during hypertonic stimulation, vesicle filling cannot keep up with release and VAChT KD^{HOM} mutants release partially filled vesicles. The decrease in frequency, which occurs later, may reflect either reduced release or release of empty vesicles. If the latter, it suggests that vesicles filling occurs in at least two stages.

One potential mechanism to explain these results is that some synaptic vesicles in the RRP of VAChT KD^{HOM} mice have low levels of neurotransmitter that make them invisible for electrophysiology recordings. A second potential mechanism is that in the absence of VAChT, a population of SVs in the RRP is impaired. To determine which of these two potential mechanisms are involved with reduced MEPP frequency in VAChT KD^{HOM} mice in response to hypertonic stimulation, we initially measured internalization of FM1-43fx to evaluate endocytosis under this condition. Figures 1E1 and E4 show representative images of diaphragm nerve terminals labeled with FM1-43 fx from VAChT WT and VAChT KD^{HOM} mice, respectively. When we measured fluorescence intensity, we observed that the presynaptic terminals

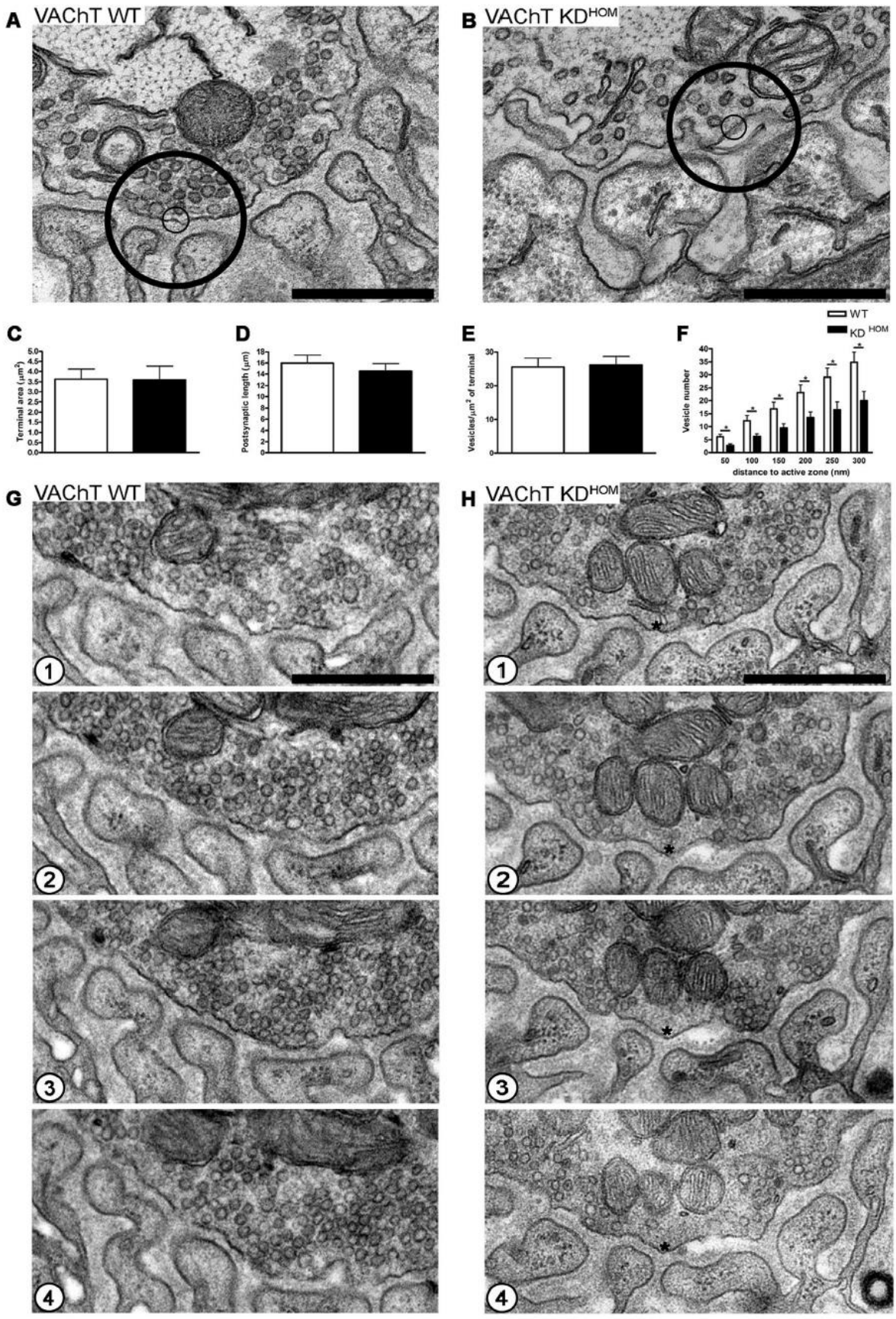

Figure 3. VAChT KD^{HOM} NMJs have normal morphology but altered SVs distribution in the absence of stimulus. A and B– Representative images of nerve terminal profile from VAChT WT and VAChT KD^{HOM} mice in the absence of stimulation showed a altered SVs distribution from the active zone within the circles: 50 and 300 nm from the membrane, small and big circles respectively. Scale bar = 500 nm. Magnification 50.000x. C– Graph showing the area of the presynaptic terminals in µm^2. D– Graph comparing the total postsynaptic membrane lenght

(μm). E – Graph of the ratio SVs/area of presynaptic terminal in μm^2. F– Graph showing the average number of SVs located at different distances from the presynaptic active zones. G and H– Four serial sections of the profile of NMJs of VAChT WT (G1–G4) and VAChT KD^{HOM} (H1–H4) mice showing the altered SVs distribution in the active zone (* represent depletion areas of SVs) of motor terminals of VAChT KD^{HOM} in the absence of stimulus. Scale bar = 500 nm. Magnification 50.000x. (n = 5 individual animals per genotype. * $p<0.05$).
doi:10.1371/journal.pone.0078342.g003

of VAChT KD^{HOM} showed decreased fluorescent signal when compared to terminals from VAChT WT mice [WT = 45.87± 4.190 A.U. (mean ± SEM); KD^{HOM} = 31.60±2.809 A.U.; $p<0.05$; unpaired Student's *t*-test], suggesting that recycling of SVs of the RRP in VAChT KD^{HOM} might be reduced (Figure 1F – quantification of 1248 and 572 presynaptic nerve terminal in WT and KD^{HOM}, respectively; n = 3 mice per genotype). Because hypertonic stimuli recruit a small number of SVs, FM1-43 fx internalization and fluorescence levels of presynaptic terminals are reduced in both genotypes. So to ensure that the measurement of fluorescent signal was really occurring at the nerve terminals level we performed the labeling of postsynaptic nAChR clusters with α-bungarotoxin to identify the precise location of the presynaptic terminals. Figures 1E2 and E5 show representative images of diaphragm postsynaptic nAChR clusters labeled with α-bungarotoxin-Alexa 594 from VAChT WT and VAChT KD^{HOM} mice, respectively. We observed that fluorescence intensity of postsynaptic elements was similar between genotypes [WT = 56.21± 4.088 A.U. (mean ± SEM); KD^{HOM} = 50.67±5.285 A.U.; $p = 0.4535$; unpaired Student's *t*-test] (Figure 1G –quantification of 1814 and 1609 postsynaptic nAChR clusters in WT and KD^{HOM}, respectively; n = 3 mice per genotype). Figures 1E3 and E6 show the colocalization of pre and postsynaptic elements in diaphragm muscle from VAChT WT and VAChT KD^{HOM} mice, respectively.

To precisely determine whether the NMJ of VAChT KD^{HOM} mice show reduction in the number of SVs from RRP when submitted to hypertonic stimulation, we used transmission electron microscopy. Ultrastructural analysis showed a reduction in the total number and altered distribution of SVs in presynaptic nerve terminals from VAChT KD^{HOM} animals compared to WT (Figure 1H and 1I – small and big circles standing for synaptic vesicles located within 50 and 300 nm from the plasma membrane respectively). Morphometric analysis confirmed that the total number of SVs/μm^2 was significantly reduced in VAChT KD^{HOM} mice (17.0±0.0 SVs) when compared to WT controls (27.0±1.0 SVs) (Figure 1J – $p<0.01$, unpaired Student's *t*-test). Additionally, we analyzed the distribution of SVs in motor nerve terminals of VAChT KD^{HOM} mice after sucrose stimulation and found a altered distribution of SVs located near the presynaptic active zones when compared with VAChT WT mice (Figure 1K – 250 nm: WT = 5.0 SVs (mean), KD^{HOM} = 4.0 SVs; 300 nm: WT = 6.0 SVs, KD^{HOM} = 4.0 SVs; $p<0.05$, unpaired Student's *t*-test; 15 nerve terminal profiles per genotype; n = 3 mice per condition).

We next investigated at the EM level, the distribution and recycling of SVs in diaphragm nerve terminals of VAChT KD^{HOM} mice after electrical stimulation (20 Hz/5 min). We observed an altered distribution of SVs near the presynaptic active zones from NMJs of VAChT KD^{HOM} (Figure 2A and 2B – small and big circles standing for synaptic vesicles located within 50 and 300 nm from the plasma membrane respectively). However, we did not observe any difference in the total number of SVs/μm^2 of terminal between genotypes (Figure 2C – WT = 29.0±4.0 SVs [mean ± SEM]; KD^{HOM} = 29.0±3.0 SVs; $p>0.05$; unpaired Student's *t*-test; 15 nerve terminals profile per genotype; n = 3 mice per genotype), confirming our previous observation that SV recycling evoked by electrical stimulation is normal in VAChT KD^{HOM} nerve terminals [9]. Quantitative analysis confirmed that the NMJs of VAChT KD^{HOM} mice exhibited an altered distribution of SVs located at different distances from presynaptic active zone after electrical stimulation when compared with the VAChT WT mice [Figure 2D – 50 nm: WT = 3.0 SVs (mean), KD^{HOM} = 2.0 SVs; 100 nm: WT = 4.0 SVs, KD^{HOM} = 3.0 SVs; 150 nm: WT = 6.0 SVs, KD^{HOM} = 4.0 SVs; 200 nm: WT = 8.0 SVs, KD^{HOM} = 5.0 SVs; 250 nm: WT = 9.0 SVs, KD^{HOM} = 6.0 SVs; 300 nm: WT = 11.0 SVs, KD^{HOM} = 6.0 SVs; $p<0.05$, unpaired Student's *t*-test; we analyzed 15 nerve terminals profiles per genotype; n = 3 mice per genotype]. Figures 2E and 2F show four serial sections (50 nm thick) of NMJs of VAChT WT (E1–E4) and VAChT KD^{HOM} (F1–F4) mice after electrical stimulation (20 Hz/5 min), respectively. These serial sections of NMJs of VAChT KD^{HOM} animals illustrate the altered distribution of SVs in the presynaptic terminals of the diaphragm muscle after electrical stimulation (Figure 2– F1–F4 – asterisks represent areas depleted of SVs near the plasma membrane).

We also looked at the ultrastructure of motor endplates from the diaphragm of VAChT KD^{HOM} and WT mice in absence of stimulation. We found that the NMJs of VAChT KD^{HOM} and WT mice presented a very similar morphology, regarding terminal area, postsynaptic length and total number of SVs (Figure 3A and 3B- small and big circles standing for synaptic vesicles located 50 and 300 nm from the plasma membrane respectively). Morphometric analysis showed that there was no difference in the surface area of nerve endings (cross section area of nerve terminals) comparing VAChT WT (3.635±0.4854 μm^2) and VAChT KD^{HOM} mice (3.601±0.6639 μm^2) (Figure 3C – $p>0.05$; unpaired Student's *t*-test; 25 nerve terminals per genotype; n = 5 mice per condition). We also measured the length of the postsynaptic junctional folds considering possible compensatory changes in muscle cell due to the cholinergic deficit, but no differences were observed between genotypes (Figure 3D – WT = 15.96±1.458 μm [mean ± SEM]; KD^{HOM} = 14.51±1.377 μm; $p>0.05$; unpaired Student's *t*-test; 25 nerve terminals profile per genotype; n = 5 mice per genotype).

Considering that VGLUT1 KO mice exhibit a reduction in the number of SVs in non-stimulated glutamatergic nerve terminals [28], we asked whether the decreased VAChT levels could have a similar effect in the number of SVs in cholinergic motor terminals. However, we observed no difference in the total number of SVs/μm^2 of terminal between VAChT WT (25.0±3.0 SVs [mean ± SEM]) and VAChT KD^{HOM} (26.0±2.0 SVs) in the absence of stimulation (Figure 3E – $p>0.05$; unpaired Student's *t*-test; 25 nerve terminal profiles per genotype; n = 5 mice per genotype).

However, quantitative analysis showed an altered distribution of SVs located at different distances from the presynaptic active zone in VAChT KD^{HOM} when compared to VAChT WT mice in the absence of stimulation [Figure 3F –50 nm: WT = 6.0 SVs (mean), KD^{HOM} = 3.0 SVs; 100 nm: WT = 12.0 SVs, KD^{HOM} = 6.0 SVs; 150 nm: WT = 17.0 SVs, KD^{HOM} = 9.0 SVs; 200 nm: WT = 23.0 SVs, KD^{HOM} = 14.0 SVs; 250 nm: WT = 29.0 SVs, KD^{HOM} = 17.0 SVs; 300 nm: WT = 35.0 SVs, KD^{HOM} = 20.0 SVs; $p<0.05$, unpaired Student's *t*-test; (25 nerve terminals profiles per genotype; n = 5 mice per genotype)]. Figures 3G and 3H show four serial sections (50 nm thick) of unstimulated NMJs of VAChT WT (G1 – G4) and VAChT KD^{HOM} (H1–H4) mice, respectively,

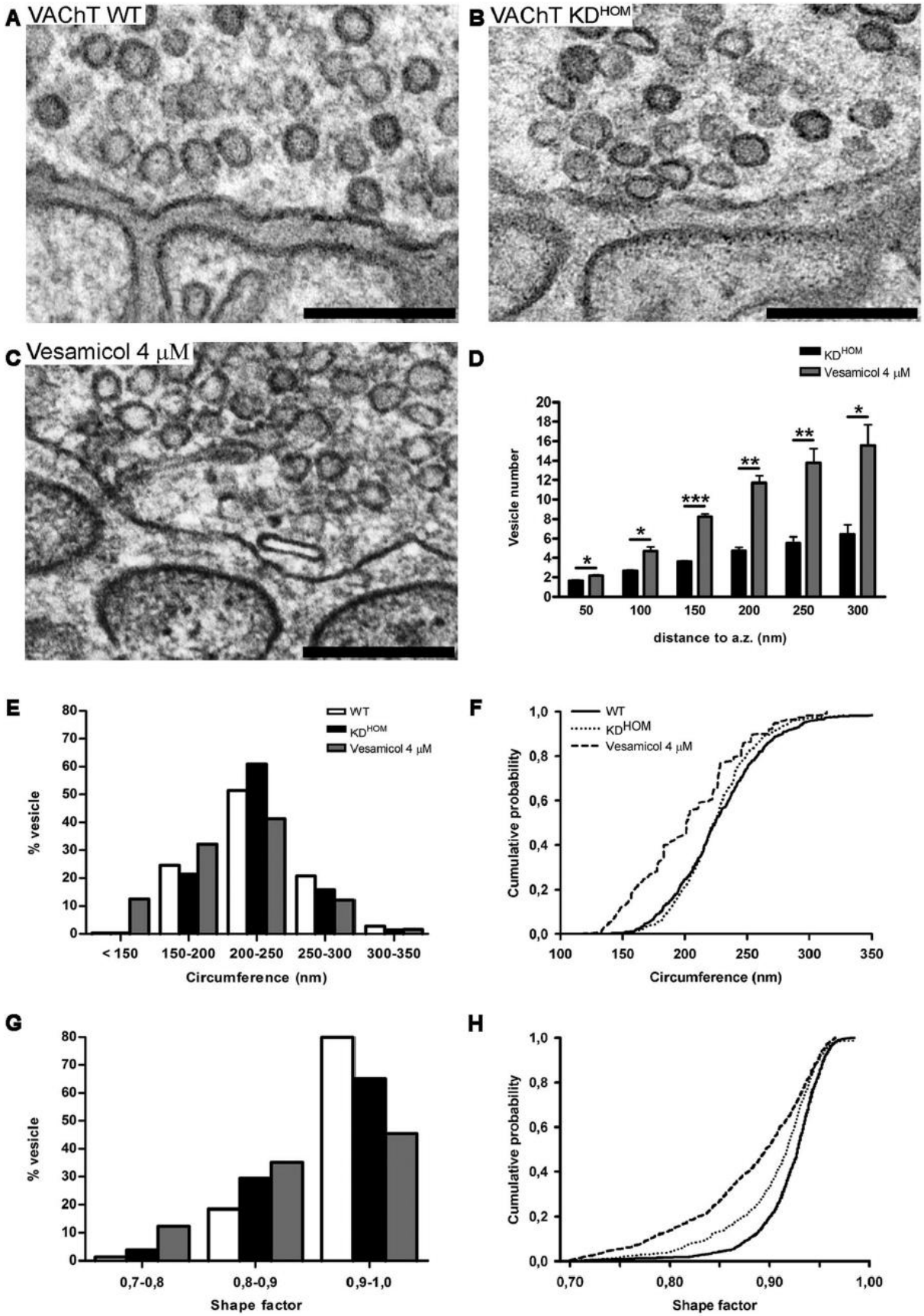

Figure 4. SVs morphology in nerve terminal from VAChT KD^{HOM} mice is influenced by neurotransmitter content. A and B – Representative images of nerve terminal profile from VAChT WT and VAChT KD^{HOM} mice after electrical stimulation (20 Hz for 5 minutes). Scale bar = 500 nm. Magnification 50.000x. C– Representative image of nerve terminal profile from diaphragm muscle of WT mice after treatment with (±)-vesamicol (4 μM) during electrical stimulation (3Hz/20 min). Scale bar = 500 nm. Magnification 50.000x. D– Graph showing the average number of

SVs located at different distances from the presynaptic active zones (n = 3 individual animals for condition. * $p<0.05$, ** $p<0.01$; *** $p<0.0001$). E– Frequency histogram of SVs circumference measured from sections of NMJs from diaphragm of VAChT WT and VAChT KD^{HOM} mice after electrical stimulation and WT mice after treatment with (±)-vesamicol. F– Cumulative probability plot of the data in (E). (n = 3 individual animals per experimental condition). G– Frequency histogram of SVs shape VAChT WT and VAChT KD^{HOM} mice after electrical stimulation and WT mice after treatment with (±)-vesamicol. H– Cumulative probability plot of the data in (G). (n = 3 individual animals per experimental condition).
doi:10.1371/journal.pone.0078342.g004

which allows a more accurate monitoring of the distribution of SVs in motor terminals. Altered distribution of SVs near active zones in nerve terminals of VAChT KD^{HOM} does not account for a change in the total number of vesicles (Figure 1E), probably because the SVs near active zones represent only a small fraction of the total number (about 500,000) of vesicles present in motor terminals of vertebrates [29].

The size and shape of SVs and specialized secretory granules can be influenced by changes in neurotransmitter transporter expression or by the amount of transmitter stored. For instance, overexpression or reduced expression of VGLUT in *Drosophila* NMJs determine an increase or decrease in the diameter of SVs, respectively [30,31]. Increased vesicular loading is coupled with an increase in specialized secretory vesicle volume [32,33]. Additionally, the morphology of SVs also seem to correlate with neurotransmitter filling [8,34]. Consistent with these findings, in the present work we observed that NMJs of VAChT KD^{HOM} mice show numerous vesicles with irregular morphology (flattened and elliptical) (Figure 4). To test whether the change in shape of SVs in motor terminals of VAChT KD^{HOM} mice occurs due to a reduction in ACh quantal content, we compared the circumference and shape of SVs of motor terminals from VAChT WT (Figure 4A), VAChT KD^{HOM} mice (Figure 4B) and WT mice treated with (±)-vesamicol (Figure 4C), a VAChT blocker [35,36,37]. Quantitative analysis show a similar total number of SVs in nerve terminals of VAChT KD^{HOM}, VAChT WT (non-treated) and WT treated with (±)-vesamicol (not shown).

Additionally, we analyzed the distribution of SVs in motor terminals of VAChT KD^{HOM} (non-treated) and found a altered distribution of SVs located at different distances from presynaptic active zone when compared with the WT treated with (±)-vesamicol [Figure 4D – 50 nm: KD^{HOM} = 1.0 SVs (mean), Vesamicol = 2.0 SVs; 100 nm: KD^{HOM} = 3.0 SVs, Vesamicol = 5.0 SVs; 150 nm: KD^{HOM} = 4.0 SVs, Vesamicol = 8.0 SVs; 200 nm: KD^{HOM} = 5.0 SVs, Vesamicol = 12.0 SVs; 250 nm: KD^{HOM} = 6.0 SVs, Vesamicol = 14.0 SVs; 300 : KD^{HOM} = 6.0 SVs, Vesamicol = 16.0 SVs; $p<0.05$, unpaired Student's *t*-test; we analyzed 15 nerve terminals profiles per genotype; n = 3 mice per condition]. However, we observed that nerve terminals from VAChT KD^{HOM} exhibited SVs slightly smaller (224.0±1.0 nm) than those from VAChT WT (226.0±1.0 nm) ($p<0.05$; Kolmogorov-Smirnov test). We also observed that nerve terminals from WT treated with (±)-vesamicol presented even smaller SVs (203±2.0 nm) compared to VAChT KD^{HOM} and VAChT WT mice ($p<0.0001$; Kolmogorov-Smirnov test. Figure 4E and 4F – 712 vesicles for WT and KD^{HOM} and 724 vesicles for vesamicol from 15 nerve terminal profiles for each experimental condition; n = 3 mice per condition). Furthermore, NMJs from both VAChT KD^{HOM} non-treated and WT mice treated with (±)-vesamicol showed a reduced number of SVs with spherical shape when compared with VAChT WT (non-treated) ($p<0.0001$; Kolmogorov-Smirnov test. Figure 4G and H –1104 vesicles for WT and KD^{HOM} and 1193 vesicles for vesamicol from 15 nerve terminal profiles for each experimental condition; n = 3 mice per experimental condition). These results suggest that the distribution and morphology of SVs in motor terminals from diaphragm NMJ of VAChT KD^{HOM} mice may be related to level of VAChT expression and ACh storage, respectively.

Discussion

In this study, we investigated the impact of reduced expression of VAChT on the morphology of NMJs from the diaphragm muscle of VAChT KD^{HOM} adult mice. Using transmission electron microscopy we found that the synaptic elements of NMJs exhibited normal overall morphology concerning presynaptic terminals size, total number of SVs per terminal and postsynaptic membrane length, when compared with VAChT WT. Considering that ACh coordinates synaptic maturation [1,3,38,39], our results suggest that reduced expression of VAChT ensures a minimal level of ACh release which is sufficient to maintain the development and normal formation of neuromuscular synapses in VAChT KD^{HOM} mice. Differently, VAChT$^{del/del}$ or ChAT KO mice exhibit abnormal development of NMJs, showing increase in motoneurons and nerve terminals number, dilated motor end-plates, profusion of ACh receptors in the proximity of nerve terminals, multiple synaptic sites on individual myotubes; hyper-innervation of individual synaptic sites and decreased number of junctional folds in the postsynaptic membrane [1,2,3].

A new finding of this study relates to our results using hypertonic sucrose to stimulate SV recycling from the RRP in motor nerve terminals from diaphragm of mice with cholinergic deficit. We found that VAChT KD^{HOM} mice exhibit reduced MEEP frequency and amplitude during hypertonic stimulation. Furthermore, we observed a reduction in FM1-43fx staining in these mice, compatible with the reduction in the total number of SVs revealed by ultrastructural analysis when compared to WT. Hypertonic extracellular solution increases MEPP frequency at the vertebrate NMJ [23,24,25,26]. Although the mechanism for such enhancement is unknown, there are evidences suggesting that this stimulus does not require Ca^{2+} influx or release from internal stores and consists of a calcium-independent neurotransmitter release that mobilizes specifically the RRP [22,27]. Therefore, our results suggest that, at least to hypertonic stimulation, the reduction in the MEPPs frequency does not occur only by competition between empty and filled vesicles [10], but also by considerable defect of SVs recycling from RRP.

The NMJ of vertebrates has a total vesicle pool of about 500,000 vesicles [29], which are divided into three pools showing distinct functional properties: the readily releasable pool (RRP), the recycling pool (RP) and the resting pool (R_tP), according to the proposal for unifying terminology [40]. Aside from differences in spatial location, no other ultrastructural features clearly distinguish the SVs pools within a presynaptic terminal [29,40]. Thus, subtle changes of SV distribution in motor terminals of VAChT KD^{HOM} would not be perceived during FM1-43 staining when considering the existence of such a large total pool. However, our ultrastructural data show altered SV distribution near active zones in hypertonically stimulated (Figure 1), electrically stimulated (Figure 2) and non-stimulated nerve terminals (Figure 3), suggesting a defect in vesicle mobilization in VAChT KD^{HOM} mice compared to WT. An elegant study performed in primary cultures of neonatal rat hippocampal neurons [41] suggested that SVs undergo alterations, or maturation processes that result in the

reduction of their mobility and in their clustering into a preexisting pool. Interestingly, our data shows that synaptic vesicle distribution near the active zone in vesamicol treated WT mice differs from VAChT KD^{HOM} (Figures 4D). Based on this and the afore mentioned work in hippocampal neurons [41], we suggest that a change in the number of copies of VAChT per synaptic vesicle in VAChT KD^{HOM}, may signal an immature state of cholinergic SVs and make them less mobile early, resulting in reduction in the clustering of SVs in individual pools and reduced interconversion of vesicles between pools [29,40,42].

Another possibility to explain the change in the SVs distribution in motor nerve terminals of VAChT KD^{HOM} mice could lie in the fact that changes in VAChT expression may impair the expression of proteins that regulate vesicle mobility and thereby impair the formation of vesicular pools or result in dispersion of vesicles. Some studies have shown a correlated expression between proteins involved with SVs mobility and vesicular neurotransmitter transporter from the central nervous system, especially to VGLUT-1, VGLUT-2 and VGAT [28,43], but not VAChT [43]. However, it would be reasonable that presynaptic proteins could regulate the mobility of SVs in motor terminals of VAChT KD^{HOM}, through the interaction with the VAChT. Future studies could focus on the mechanisms of interaction between VAChT and other presynaptic protein and the consequences of reduced expression of this transporter for the formation of SVs pools.

Another important finding of this work relates to the observed alteration in morphology of SVs from NMJ of VAChT KD^{HOM} mice. Considering that VAChT KD^{HOM} animals have a reduction in the number of copies of the transporter in the SVs membrane and that they exhibit reduced quantal ACh content [10], we hypothesized that the change in morphology of SVs is a consequence of the reduced filling with ACh. To test this hypothesis we compared circumference and shape of SVs from NMJ of VAChT KD^{HOM} mice and WT treated with vesamicol, a VAChT blocker [35,36,37]. Ultrastructural analysis revealed that the pharmacological inhibition of VAChT also changes the morphology of SVs.

The relationship between SVs size and changes in quantal acethylcholine content has been investigated specially at cholinergic nerve terminal from the frog NMJ [8]. At the NMJ cholinergic SV recycling continued to occur in nerve terminals stimulated in the presence of vesamicol, showing that transport of ACh into recycled vesicles is not a requisite for repeated SV cycle [44]. Experiments using hypertonic gluconate and aspartate solution to increase quantal size showed an increase in the size of MEPPs that was not accompanied by changes in SV size [8]. In addition, vesicle size was not substantially decreased when the quantal content was reduced by treatment with hemicholinium (inhibitor of choline uptake) or NH_4^+ (which diminishes the proton gradient for ACh uptake into the vesicles). However, treatment with vesamicol induced a decrease in vesicle size [8], which agrees with our findings from mice with reduced VAChT expression and treated with vesamicol described in Figure 4. Interestingly, previous work suggested that vesamicol may be altering vesicle size by a mechanism other than inhibiting VAChT [8], but our data showing changes in circumference and shape in VAChT KD^{HOM} and vesamicol treated nerve terminals indicate that this might not be the case at least in the mice NMJ.

VAChT is a transmembrane protein that uses the electrochemical gradient generated by a V-type proton ATPase to accumulate ACh in SVs [4,7,45,46]. Therefore, a change in the VAChT activity could impact on proton exchange, changing tonicity and inducing morphological changes in SVs. Indeed, it has been recently reported [47] that aldehyde fixation induces flattening of SVs in hippocampal synapses of VGLUT1$^{-/-}$ mice due to an alteration in the tonicity of excitatory SVs. We therefore suggest that in cholinergic vesicles the normal expression and activity of VAChT are also important for maintaining tonicity and morphology of SVs in nerve terminals from diaphragm NMJ.

Even though our results suggest that ACh content interferes with the morphology of SVs we cannot rule out the possibility that the reduced VAChT protein levels or activity in our experimental model may also affect vesicle shape. Removal of plasma membrane components, such as cholesterol, does not alter the SVs shape, although considerably alters circumference in frog NMJ [48]. Furthermore, overexpression or reduced expression of VGLUT in *Drosophila* NMJ induces an increase or decrease in the diameter of SVs, respectively [30,31]. Additionally, morphological aspect of SVs may also be defined after clathrin-mediated endocytosis [49,50,51]. Considering that VAChT interacts with clathrin adaptors [52,53,54], reduced expression of this transporter could compromise the number of sites necessary for proper connection between them. Therefore, it is possible that changes in shape of SVs from motor nerve terminals of VAChT KD^{HOM} mice may also be related to a defect in modeling during endocytosis. One intriguing possibility is that these changes in SVs circumference and shape that we detect in the absence of VAChT may be the reason for the altered recycling of SVs in the RRP that we observed in these mutant mice.

In conclusion, our data show that decreased VAChT expression play a role in recycling and mobilization of specific pools of SV in NMJ. We suggest that quantal ACh content and reduced VAChT protein levels or activity are important to define the morphology and distribution of SVs and the recycling of the RRP. Our results also suggest that functional alterations caused by VAChT deficiency [9,55,56] may involve multiple mechanisms, including a decreased in neurotransmitter storage in addition to deficits in the recycling and mobilization of the RRP. Future studies will be needed to clarify the relation between expression of VAChT and regulation of SVs mobility in neuromuscular synapses.

Acknowledgments

The authors would like to acknowledge the Center of Acquisition and Processing of Images (CAPI) – ICB – Universidade Federal de Minas Gerais and Microscopy Center at Universidade Federal de Minas Gerais for providing the equipment and technical support for experiments involving electron microscopy and also the Prado laboratory.

Author Contributions

Conceived and designed the experiments: HAR LAN VFP MAMP CG. Performed the experiments: HAR PMAL PMM WLC LAN. Analyzed the data: HAR MCF WLC LAN CG. Contributed reagents/materials/analysis tools: PMM LAN VFP MAMP CG. Wrote the paper: HAR MAMP CG.

References

1. Misgeld T, Burgess RW, Lewis RM, Cunningham JM, Lichtman JW, et al (2002) Roles of neurotransmitter in synapse formation: development of neuromuscular junctions lacking choline acetyltransferase. Neuron 36: 635–648.

2. Brandon EP, Lin W, D'amour KA, Pizzo DP, Dominguez B, et al. (2003) Aberrant patterning of neuromuscular synapses in choline acetyltransferase-deficient mice. J Neurosci 23: 539–549.

3. de Castro BM, De Jaeger X, Martins-Silva C, Lima RD, Amaral E, et al. (2009) The vesicular acetylcholine transporter is required for neuromuscular development and function. Mol Cell Biol, 29: 5238–5250.
4. Prado VF, Roy A, Kolisnyk B, Gros R, Prado MA (2013) Regulation of cholinergic activity by the vesicular acetylcholine transporter. Biochem J 450: 265–274.
5. Birks RI, MacIntosh FC (1961) Acetylcholine metabolism of a sympathetic ganglion. Can J Biochem Physiol 39: 787–827.
6. Katz B (1971) Quantal Mechanism of Neural Transmitter Release. Science 173: 123–126.
7. Parsons SM (2000) Transport mechanisms in acetylcholine and monoamine storage. FASEB J 14: 2423–2434.
8. Van der Kloot W, Molgó J, Cameron R, Colasante C (2002) Vesicle size and transmitter release at the frog neuromuscular junction when quantal acetylcholine content is increased or decreased. J Physiol 541: 385–393.
9. Prado VF, Martins-Silva C, de Castro BM, Lima RF, Barros DM, et al. (2006) Mice deficient for the vesicular acetylcholine transporter are myasthenic and have déficits in object and social recognition. Neuron 51: 601–612.
10. Lima RF, Prado VF, Prado MA, Kushmerick C (2010) Quantal Release of Acetylcholine in Mice with Reduced Levels of the Vesicular Acetylcholine Transporter. J Neurochem 113: 943–951.
11. Lara A, Damasceno DD, Pires R, Gros R, Gomes ER, et al. (2010) Dysautonomia due to reduced cholinergic neurotransmission causes cardiac remodeling and heart failure. Mol Cell Biol 30: 1746–1756.
12. Terry AVJr, Parikh V, Gearhart DA, Pillai A, Hohnadel E, et al. (2006) Time-dependent effects of haloperidol and ziprasidone on nerve growth factor, cholinergic neurons, and spatial learning in rats. J Pharmacol Exp Ther 318: 709–724.
13. Terry JrAV, Gearhart DA, Warner S, Hohnadel EJ, Middlemore ML, et al. (2007) Protracted effects of chronic oral haloperidol and risperidone on on nerve growth factor, cholinergic neurons, and spatial reference learning in rats. Neuroscience 150: 413–424.
14. Smith R, Chung H, Rundquist S, Maat-Schieman ML, Colgan L, et al. (2006) Cholinergic neuronal defect without cell loss in Huntington's disease. Hum Mol Genet 15: 3119–3131.
15. Chen KH, Reese EA, Kim HW, Rapoport SI, Rao JS (2011) Disturbed neurotransmitter transporter expression in Alzheimer's disease brain. J Alzheimers Dis 26: 755–766.
16. Betz WJ, Mao F, Bewick GS (1992) Activity dependent fluorescent staining and destaining of living vertebrate motor nerve terminals. J Neurosci 12: 363–375.
17. Gaffield MA, Betz WJ (2006) Imaging synaptic vesicle exocytosis and endocytosis with FM dyes. Nat Protoc 1: 2916–2921.
18. Whitton PS, Marshall IG, Parsons SM (1986) Reduction of quantal size by vesamicol (AH 5183), an inhibitor of vesicular acetylcholine storage. Brain Res 385: 189–192.
19. Becherer U, Guatimosim C, Betz WJ (2001) Effects of staurosporine on exocytosis and endocytosis at frog motor nerve terminals. J Neurosci 21: 782–787.
20. Han Y, Kaeser PS, Südhof TC, Schneggenburger R (2011) RIM determines Ca^{2+} channel density and vesicle docking at the presynaptic active zone. Neuron 69: 304–316.
21. Croft BG, Fortin GD, Corera AT, Edwards RH, Beaudet A, et al. (2005) Normal biogenesis and cycling of empty synaptic vesicles in dopamine neurons of vesicular monoamine transporter 2 knockout mice. Mol Biol Cell 16: 306–315.
22. Rosenmund C, Stevens CF (1996) Definition of the readily releasable pool of vesicles at hippocampal synapses. Neuron 16: 1197–1207.
23. Fatt P, Katz B (1952) Spontaneous subthreshold activity at motor nerve endings. J Physiol 117: 109–128.
24. Hubbard JI, Jones SF, Landau EM (1968) An examination of the effects of osmotic pressure changes upon transmitter release from mammalian motor nerve terminals. J Physiol 197: 639–657.
25. Kita H, Van der Kloot W (1977) Time course and magnitude of effects of changes in tonicity on acetylcholine release at frog neuromuscular junction. J Neurophysiol 40: 212–224.
26. Cheng H, Miyamoto MD (1999) Effect of hypertonicity on augmentation and potentiation and on corresponding quantal parameters of transmitter release. J Neurophysiol 81: 1428–1431.
27. Sara Y, Mozhayeva MG, Liu X, Kavalali ET (2002) Fast vesicle recycling supports neurotransmission during sustained stimulation at hippocampal synapses. J Neurosci 22: 1608–1617.
28. Fremeau JrRT, Kam K, Qureshi T, Johnson J, Copenhagen DR, et al. (2004) Vesicular glutamate transporter 1 e 2 target to functionally distinct synaptic release sites. Science 304: 1815–1819.
29. Rizzoli SO, Betz WJ (2005) Synaptic vesicle pools. Nat Rev Neurosci 6: 57–69.
30. Daniels RW, Collins CA, Gelfand MV, Dant J, Brooks ES, et al. (2004) Increased expression of the *Drosophila* vesicular glutamate transporter leads to excess glutamate release and a compensatory decrease in quantal content. J Neurosci 24: 10466–10474.
31. Daniels RW, Collins CA, Chen K, Gelfand MV, Featherstone DE, et al. (2006) A Single Vesicular Glutamate Transporter Is Sufficient to Fill a Synaptic Vesicle. Neuron 49: 11–16.
32. Colliver TL, Pyott SJ, Achalabun M, Ewing AG (2000) VMAT-Mediated changes in quantal size and vesicular volume. J Neurosci 20: 5276–5282.
33. Pothos EN, Larsen KE, Krantz DE, Liu Y, Haycock JW, et al. (2000). Synaptic vesicle transporter expression regulates vesicle phenotype and quantal size. J Neurosci 20: 7297–7306.
34. Budzinski KL, Allen RW, Fujimoto BS, Kensel-Hammes P, Belnap DM, et al. (2009) Large structural change in isolated synaptic vesicles upon loading with neurotransmitter. Biophys J 97: 2577–2584.
35. Marshall IG (1970) Studies on the blocking actions of 2-(4-phenylpiperidino) cyclohexanol (AH5183). Br J Pharmacol 38: 503–516.
36. Anderson DC, King SC, Parsons S M (1983) Pharmacological characterization of the acetylcholine transport system in purified *Torpedo* electric organ synaptic vesicles. Mol Pharmacol 24: 48–54.
37. Prado MA, Gomez MV, Collier B (1993) Mobilization of a vesamicol-insensitive pool of acetylcholine from a sympathetic ganglion by ouabain. J Neurochem. 61: 45–56.
38. Witzemann V (2006) Development of the neuromuscular junction. Cell Tissue Res 326: 263–271.
39. Katz B (1969) The Release of Neural Transmitter Substances (Liverpool University Press, Liverpool, UK).
40. Alabi AA, Tsien RW (2012) Synaptic vesicle pools and dynamics. Cold Spring Harb Perspect Biol 4: 1–18.
41. Kamin D, Lauterbach MA, Westphal V, Keller J, Schönle A, et al. (2010) High- and low-mobility stages in the synaptic vesicle cycle. Biophys J 99: 675–684.
42. Südhof TC (2000) The synaptic vesicle cycle revisited. Neuron 28: 317–320.
43. Bogen IL, Haug KH, Roberg B, Fonnum F, Walaas SI (2009) The importance of synapsin I and II for neurotransmitter levels and vesicular storage in cholinergic, glutamatergic and GABAergic nerve terminals. Neurochem Int 55: 13–21.
44. Parsons RL, Calupca MA, Merriam LA, Prior C (1999) Empty synaptic vesicles recycle and undergo exocytosis at vesamicol-treated motor nerve terminals. J Neurophysiol 81: 2696–2700.
45. Nguyen ML, Cox GD, Parsons SM (1998) Kinetic parameters of the vesicular acetylcholine transporter: two protons are exchanged for one acetylcholine. Biochemistry 37: 13400–13410.
46. Prado VF, Prado MA (2002) Signals involved in targeting membrane proteins to synaptic vesicles. Cell Mol Neurobiol 22: 565–577.
47. Siksou L, Silm K, Biesemann C, Nehring RB, Wojcik SM, et al. (2013) A role for vesicular glutamate tranporter 1 in synaptic vesicle clustering and mobility. Eur J Neurosci. 37: 1631–1642.
48. Rodrigues HA, Lima RF, Fonseca MC, Amaral E, Martinelli PM, et al. (2013) Membrane cholesterol regulates different modes of synaptic vesicle release and retrieval at the frog neuromuscular junction. Eur J Neurosci "In press".
49. Zhang B, Koh YH, Beckstead RB, Budnik V, Ganetzky B, et al. (1998) Synaptic vesicle size and number are regulated by a clathrin adaptor protein required for endocytosis. Neuron 21: 1465–1475.
50. Nonet ML, Holgado AM, Brewer F, Serpe CJ, Norbeck BA, et al. (1999) UNC-11, a *Caenorhabditis elegans* AP180 homologue, regulates the size and protein composition of synaptic vesicles. Mol Biol Cell 10: 2343–2360.
51. Petralia RS, Wang YX, Indig FE, Bushlin I, Wu F, et al. (2013) Reduction of AP180 and CALM produces defects in synaptic vesicle size and density. NeuroMolecular Med 15: 49–60.
52. Barbosa JJr, Ferreira LT, Martins-Silva C, Santos MS, Torres GE, et al. (2002) Trafficking of the vesicular acetylcholine transporter in SN56 cells: a dynamin-sensitive step and interaction with the AP-2 adaptor complex. J Neurochem 82: 1221–1228.
53. Ferreira LT, Santos MS, Kolmakova NG, Koenen J, Barbosa JJr, et al. (2005) Structural requirements for steady-state localization of the vesicular acetylcholine transporter. J Neurochem 94: 957–69.
54. Kim MH, Hersh LB (2004) The vesicular acetylcholine transporter interacts with clathrin-associated adaptor complexes AP-1 and AP-2. J Biol Chem 279: 12580–12587.
55. Guzman MS, De Jaeger X, Raulic S, Souza IA, Li AX, et al. (2011) Elimination of the vesicular acetylcholine transporter in the striatum reveals regulation of behaviour by cholinergic-glutamatergic co-transmission. PLoS Biol 9: e1001194. doi: 10.1371/journal.pbio.1001194. Epub 2011.
56. Martyn AC, De Jaeger X, Magalhães AC, Kesarwani R, Gonçalves DF, et al. (2012) Elimination of the vesicular acetylcholine transporter in the forebrain causes hyperactivity and deficits in spatial memory and long-term potentiation. Proc Natl Acad Sci USA 109: 17651–17656.